AN ANALYTICAL AND EXPERIMENTAL INVESTIGATION OF A FREQUENCY-SHIFT-KEYED SIGNAL GENERATED BY A PHASE-LOCKED-LOOP WITH APPLICATION TO NARROWBAND FSK

by

Thomas Hunter Gee

Thesis submitted to the Graduate Faculty of the
Virginia Polytechnic Institute
in partial fulfillment for the degree of

DOCTOR OF PHILOSOPHY

in

Electrical Engineering

APPROVED:

Chairman Dr. W. W. Cannon

Dr. W. A. Blackwell

Dr. H. K. Ebert

Dr. R. H. Bond

Dr. M. Y. Rhee

June 1968

Blacksburg, Virginia

ACKNOWLEDGMENTS

The author wishes to express his sincere appreciation to Dr. Walton W. Cannon, Advisor and Chairman of the graduate committee, for his guidance throughout this work. The author is grateful to the members of his committee, Drs. W. A. Blackwell, R. H. Bond, H. K. Ebert and M. Y. Rhee, for the assistance rendered during the graduate program. The consideration and interest shown by Dr. R. H. Bond, and exhibited through many stimulating discussions with the author, is expecially appreciated.

The author wishes to acknowledge the assistance of Mr. R. R. Stone and T. H. Gattis of the U. S. Naval Research Laboratory. To his wife, Nancy, the author is deeply grateful for her help and understanding during his entire graduate program.

TABLE OF CONTENTS

INDEX OF FIGURES

I. INTRODUCTION

A major consideration in the design of narrowband, binary, frequency-shift-keyed carrier* communications systems is transient response. The transient response of a system is defined here to be any response which differs from the final pattern of behavior called the steady state. Such transient behavior can appear as an amplitude transient, a frequency transient, or both. The transients that are incurred may be the result of discontinuous waveforms or discontinuities in the waveform derivatives, as produced by frequency modulation. Transients generated by carrier frequency shifts in narrowband networks affect system operation from several viewpoints. Distortion caused by finite transient decay time, excessive transient current and voltage and adjacent channel interference are of particular interest. Binary frequency-shift-keyed (FSK) carrier systems are normally operated in conjunction with teletype printing equipment; hence, the transient decay time must be sufficiently shorter than one bit of the teletype code to allow satisfactory detection by the receiver. In applications where very high power transmitters are frequency-shift-keyed, it is necessary to limit transient currents and voltages to a level that is compatible with transmitter operation. Further, abrupt

---

*Frequency-shift-keying (FSK) is accomplished by shifting the frequency between two oscillator frequencies designated as mark and space. Many authors use the terminology "rectangular wave frequency modulation." The frequency source may be a single source whose frequency of oscillation is shifted or two distinct signal frequencies.

changes in frequency may produce sideband components at frequencies that are widely spaced from the carrier frequency. These frequency components are the source of adjacent channel interference.

Just as in the case where the FSK frequency transition is assumed to be instantaneous (a frequency step), the characteristics and effects of a finite frequency transition interval are of considerable importance. The finite frequency transition interval is exemplified by the oscillator frequency of a frequency-shifted phase-locked-loop (FS-PLL), the phase-locked-loop (PLL) being common to many frequency synthesis techniques. Depending on the particular application, this transition may vary from an almost instantaneous transition to one taking place over a time interval that is significant when compared to the time constant of a circuit excited by such a frequency shift. The finite frequency transition interval, frequency-shifted carrier excitation is of interest because of its direct application to system design, or as a basis for assuming instantaneous frequency transitions.

It has been shown that high order frequency components resulting from rapid changes in frequency, as found in FSK, can be reduced by shaping the frequency transition [1]*. Normally, the rectangular wave keying signal is shaped by passing it through a filter which removes the abrupt leading and lagging edges. The PLL can accomplish

---

*Numbers in brackets refer to Bibliography.

the same effect by proper choice of loop parameters, gain and bandwidth. The loop reference frequency is frequency modulated by the rectangular keying wave, and the PLL's oscillator output (hereafter referred to as the PLL output) frequency transition interval is finite. That is, the PLL operates on the keying wave as a low pass filter.

The investigation undertaken here is partially concerned with the characterization of a typical PLL employed as a frequency-shifted source, with application to FSK. The PLL consists of a voltage controlled oscillator (VCO), a phase comparator which produces a VCO control voltage proportional to the phase difference between the VCO and reference signals, and a low pass filter which provides attenuation to all frequencies except the relatively slowly varying VCO control signal. Linearity of PLL operation is normally dependent upon the phase comparator's characteristics. A phase comparator that is often used is the sinusoidal or multiplier type, which has a small linear operating range. A second device, the sawtooth phase comparator, offers linear transfer characteristics over a wide range of phase error. A linear model of the PLL is analysed, assuming that the loop's reference signal takes the form of a continuous phase frequency step. Mathematical expressions are developed which describe the PLL output signal, including phase and frequency time functions. A spectral analysis is made of the output of a repetitively keyed PLL.

The results are compared with the spectrum of the more conventional square wave frequency modulated carrier.

When using the FS-PLL source in a linear network, various methods are available for obtaining the network response. Unfortunately, a straightforward closed form solution to the response of elementary networks is complicated by the necessity to evaluate complex integrals. Besides direct solution of the network differential equations, the convolution integral, quasi-stationary method or state variable approach readily give results in the form of integral equations. Appropriate references are made in Chapter II. Evaluation of the integrals involved can be accomplished by utilizing series or numerical techniques. The Fourier series method is available when the network is excited by a periodically keyed carrier. Another series, consisting of a carrier term plus damped sinusoidal terms, is developed in this work which describes a single frequency shift. Truncation of this series is discussed; and it is shown that in the limit the series can be identified with the Bessel-Fourier series for sinusoidal frequency modulation. Laplace transform techniques are employed in conjunction with the series of damped sinusoids to determine the response of a narrowband series tuned circuit. This response is compared with that of a series tuned circuit excited by a frequency step.

In order to verify the theory presented, an experiment is devised to provide data on the FS-PLL, including phase and frequency

as a function of time and also output spectrum. Likewise, experimental data are obtained on the FS-PLL excited tuned circuit response.

The narrowband series tuned circuit is selected for consideration here because of its application to very low frequency (VLF) FSK communications systems. This narrowband circuit is an acceptable circuit equivalent for the VLF transmitting antenna, which is inherently a high Q device [2]. The FS-PLL provides the controllable frequency transition interval and signal coherence necessary in some modes of VLF-FSK operation. Such a VLF-FSK communications network is operated by the U. S. Navy [3].

II. BACKGROUND INFORMATION

Information pertinent to this investigation is found in the literature in three areas. First is transient response of networks excited by means of frequency modulated carriers. Of particular interest are forms of frequency-shift modulated carriers. The second area concerns the spectral analysis of frequency modulated carriers, with application to FSK. The third interest area is the literature on phase-locked-loops and their application to frequency synthesis.

Transient Response to Frequency Modulated Carriers. Many investigators have contributed to the literature in the area of transient response of networks to frequency modulated signals. Among the methods available, the convolution integral can be employed to obtain the response of networks to a general form of frequency modulation, whereby the response is expressed in terms of integral equations [4]. This result is extended in the quasi-stationary approach, first reported by Carson and Fry [5]. Van der Pol [6] and Stumpers [7] also expanded the response into a quasi-stationary term plus an infinite series which is utilized to make corrections to the quasi-stationary results. Others [8-9] have refined and extended this method. A more recent publication by Weiner and Leon [10] provides further insight into the physical significance of the terms involved in the quasi-stationary method. The instantaneous frequency of the composite (transient plus steady

state) signal is of primary interest in the work of Weiner and Leon, and an extensive bibliography is presented. The major objection to the quasi-stationary method is the number of corrections necessary. Johnson [11] compares the use of the Fourier series method with the quasi-stationary approach, from the viewpoint of a computerized analysis, for a limited number of modulation waveforms. Unfortunately, the response of networks to arbitrary frequency modulated carriers cannot be expressed in closed form.

Investigations which are restricted to frequency step excitation include the work of Hartley [12] who presented an approximate method for obtaining the response of one- and two-pole narrowband networks excited by means of a symmetrical frequency shift. This analysis employs Laplace transform techniques and provides good results for the high Q circuits so common to very low frequency FSK systems. Keying conditions which minimize the transient response of a series tuned circuit are considered by this author [13] for the case of a frequency step excitation. It is shown that a zero transient response condition exists for this particular circuit configuration.

Systems analysts have shown great interest in recent years in the state variable method, applied to computerized analysis of networks as well as complete systems. This approach is presented by DeRusso, Roy and Close [14] and others.

Spectral Analysis of FSK Carriers. The frequency spectrum for square-wave frequency-modulated carriers can readily be determined by conventional mathematical methods, as has been shown by van der Pol [15], Corrington [16] and others. Davey and Matte [1] established that an FSK carrier bandwidth can be reduced by shaping the keying wave. This amounts to rounding-off the sharp corners of a rectangular wave. Experimental results of a keying wave with half-sinusoidal build-up were obtained by Cawthra and Thomson [17]. Allnatt and Jones [18] considered, theoretically and experimentally, a straight line build-up or trapezoidal wave shape. Watt, Zurich and Coon [19] investigated the effect of low pass filtering on the shape of a keying wave, and the subsequent effects on FSK spectra, by approximate time varying frequency analysis. Furthermore, the primary factors to be considered in the proper choice of the keying wave shape are discussed from the viewpoint of adjacent channel interference.

Bennett and Rice [20] studied the power spectrum associated with rectangular-wave frequency-modulated carriers. Various keying conditions were considered, such as continuous and discontinuous phase and the effect of differing carrier to keying rate ratios. The conditions necessary for the presence of discrete spectral lines in FSK carrier spectra were developed.

Phase-locked-loops. The phase-locked-loop (PLL) has found wide applications in the fields of communications and control. Chaffee [21] is credited with the original idea. The first applications appearing in

the literature were concerned with synchronizing circuits for television [22-23]. Further applications have included frequency synthesis [24], tracking filters in communications receivers [25-26] and various instrumentation applications. Viterbi [27] and others [28-30] have presented phase plane analyses of a PLL which employs a sinusoidal phase comparator. This type of analysis is primarily concerned with the loop's pull-in range and pull-in time as functions of the initial phase and frequency. The literature normally treats the case where a phase lag filter is employed in the PLL. This is primarily due to the fact that this type of filter gives a loop which is described by a second order differential equation; and a more general loop filter would result in higher order equations. The optimum loop filter was derived by Jaffe and Rechtin [31] for three types of excitation: (1) a phase step, (2) a frequency step and (3) a frequency ramp. The filters are optimized from the standpoint of minimum phase error. Based on the optimum filter functions, Jaffe and Rechtin discussed physically realizable alternatives where applicable. Gardner [32] has summarized the theory and application of phase-locked techniques, along with an extensive bibliography.

In addition to the sinusoidal phase comparator, other comparators are discussed in the literature [33-34]. A comparator possessing linear characteristics over a wide dynamic range is the sawtooth phase comparator treated by Goldstein [35]. This paper provides a theoretical description of the in-lock and out-of-lock operation of the loop. In a

companion paper, Byrne [36] presents an experimental study, and discusses engineering aspects of the sawtooth comparator. The sawtooth comparator is comprised of a bistable flip-flop, and operates as a sample data device. Byrne cites unpublished work whereby E. C. Kimme of Bell Telephone Laboratories has proven that the sawtooth comparator is a continuous approximation to the discrete sample data system, provided the comparator's input frequency is large compared to the natural frequency of the PLL. Splitt [27] has compared the sinusoidal and sawtooth comparators.

III. THE PHASE-LOCKED-LOOP AS A FREQUENCY-SHIFTED CARRIER SOURCE

The phase-locked-loop is a device which is often used to generate a signal whose frequency and phase are controlled by an input reference signal. Hence, the PLL can be considered as a filter which locks onto the strongest frequency component available at the input, which is within the pull-in frequency range of the loop. The loop (in general non-linear) differs from linear passive filters in that it automatically tunes itself, over a limited band, and can provide gain between the reference input and voltage controlled oscillator (VCO) output.

3.1 Functional Description of the Phase-locked-loop

The PLL consists of three major components: (1) a phase comparator, (2) a low pass filter and (3) a voltage controlled oscillator (VCO). Figure 3.1 is a block diagram representation of the PLL. In-lock operation of the loop can be described as follows. Assume initially that the VCO is oscillating at its natural frequency; hence, the VCO control voltage is zero. Now, let a reference frequency be applied which differs from the VCO natural frequency. The phase comparator produces a dc voltage that is proportional to the phase difference between the VCO and reference signals. Any high frequency components out of the comparator are attenuated by the low pass filter.

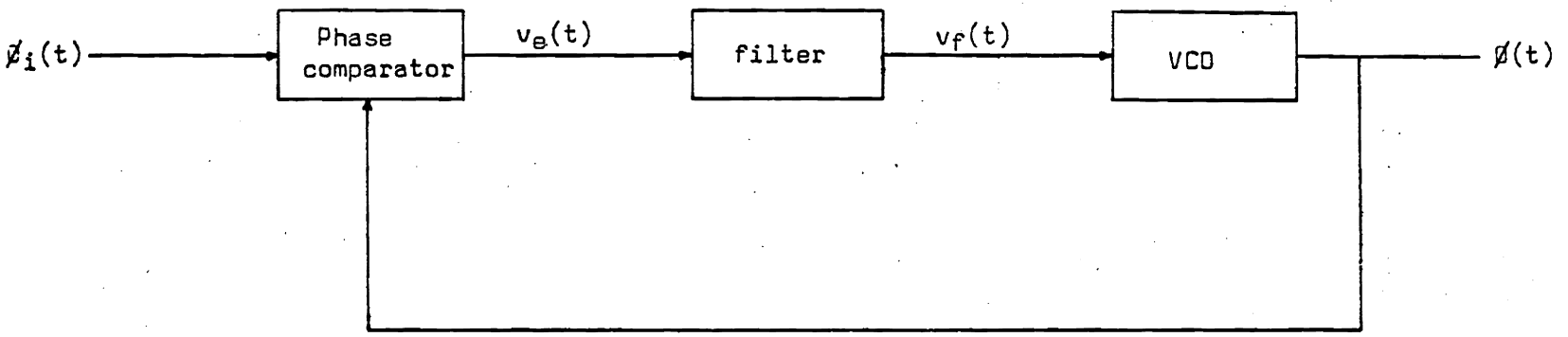

Figure 3.1. Phase-locked-loop block diagram.

The dc error voltage, resulting from the phase error, is passed through the filter and acts to pull the VCO into lock with the reference signal frequency and phase. When the reference frequency differs from the VCO natural frequency, a steady state phase error must exist to hold the VCO off its natural frequency.

If the reference frequency experiences a large change, the relative phase may become so large that it exceeds the in-lock operating range of the comparator. In such a case, the loop is considered to be out-of-lock, and one of two situations exists. First, if the reference is within the PLL pull-in range, the loop will re-acquire lock. If the reference is outside the pull-in range, the VCO will be frequency modulated at the difference frequency of the VCO and reference, and lock will not occur. The out-of-lock conditions are discussed in the literature [27], and will not be pursued further here, since this investigation concerns in-lock operation of the PLL.

Phase Comparators. The analysis undertaken in this investigation assumes a linear PLL model. In order to establish the linear operating conditions, the phase comparator characteristics must be considered.

An often used comparator is the sinusoidal, or multiplier type. The output (error signal) of such a comparator is

$$v_e(t) = v_i(t) \times v(t) ,$$

where $v_i(t)$ is the loop's reference and $v(t)$ is the VCO output signal. With this type comparator, the error voltage is zero when the inputs to

the comparator are in quadrature. This can be seen by initially assuming $v_i(t)$ and $v(t)$ such that

$$v_e(t) = - k_c V_i V \sin \left[\omega_c t + \phi_i(t)\right] \cos \left[\omega_c t + \phi(t)\right] .$$

The carrier frequency is ω_c, and the phase time-function, $\phi_i(t)$, represents carrier modulation of the loop's reference signal. By means of trigonometric identities,

$$v_e(t) = \frac{k_c V_i V}{2} \left\{ \sin \left[\phi_i(t) - \phi(t)\right] - \sin \left[2\omega_c t + \phi_i(t) + \phi(t)\right] \right\},$$

where k_c is the gain of the comparator. Since the loop's low pass filter suppresses the double frequency component, it is unnecessary to consider this component further. In the range

$$\left|\phi_e(t)\right| = \left|\phi_i(t) - \phi(t)\right| \ll \pi/2 \text{ radians} , \tag{3.1}$$

the error voltage becomes

$$v_e(t) = \frac{k_c V_i V}{2} \left[\phi_i(t) - \phi(t)\right] . \tag{3.2}$$

The small phase error assumption of (3.1) obviously restricts the use of (3.2) to in-lock PLL operation.

A second type of phase comparator, the sawtooth comparator, is of primary interest in this investigation, for reasons which will become apparent. The sawtooth phase comparator is exemplified by a

bistable flip-flop, where $v_i(t)$ sets the flip-flop in one state and $v(t)$ resets the circuit. Figure 3.2 depicts in an exaggerated manner, the operation of this comparator as a function of the phase error. The waveform out of the flip-flop can be expressed by means of a Fourier series. The loop's low pass filter attenuates the high frequency components, passing the low frequency component to the VCO as the control voltage. It is assumed that the error voltage is zero when the reference and VCO frequencies are identical and equal to the VCO natural frequency. This means that the VCO output is 180° out of phase with the reference signal, or

$$v(t) = V \sin [\omega_c t + \phi(t)] \tag{3.3}$$

when

$$v_i(t) = - V_i \sin [\omega_c t + \phi_i(t)] \tag{3.4}$$

and the phase error is given by

$$\phi_e(t) = \phi_i(t) - \phi(t) \ . \tag{3.5}$$

It can be seen from Figure 3.2 that the gain of the comparator is

$$k_c = V_c/\pi \quad \text{volts per radian} \ . \tag{3.6}$$

Thus the comparator's output voltage is expressed by

$$v_e(t) = k_c [\phi_i(t) - \phi(t)] \ . \tag{3.7}$$

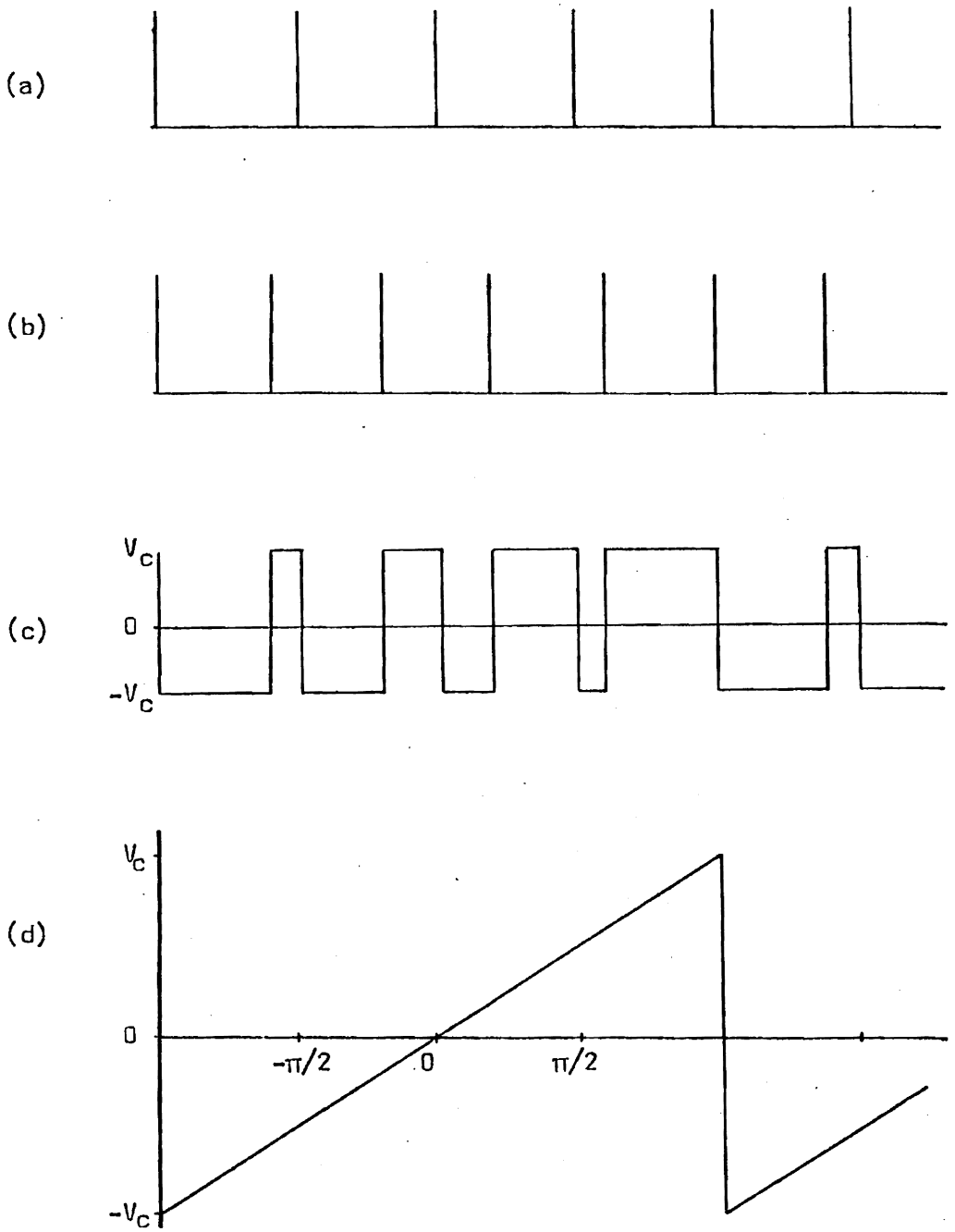

Figure 3.2. Sawtooth phase comparator characteristics, (a) reference phase input, (b) controlled phase input, (c) phase comparator output and (d) ideal low pass filtered phase comparator output.

The sawtooth comparator is a continuous approximation to a sample data device, provided the comparator's input frequency is large compared to the natural frequency of the PLL [36]. The linear model of the PLL is applicable when the continuous time system condition is satisfied, and

$$\left|\phi_e(t)\right| < \pi \text{ radians} . \tag{3.8}$$

Comparing (3.1) and (3.8) it is seen that the sawtooth comparator has a much larger linear range than that of the sinusoidal comparator. In addition, the gain of the sawtooth comparator is independent of the amplitude of its input signals, which is not true for the ideal sinusoidal comparator.

Filter. Low pass filters commonly employed in phase-locked-loops attenuate the high frequency components of the comparator's output signal, and reduce the effects of noise. The filter also acts to shape the PLL's response to the error signal. Figure 3.3 shows the filter which is commonly employed in the PLL. Sometimes R_2 is made zero to result in the simplest form of RC filter. Either of these two filters lead to a second order loop characterized by a second order differential equation, while more general filters produce higher order systems.

The filter's impulse response, h(t), can be obtained from the filter transfer function,

$$H(S) = \frac{t_b S + 1}{t_a S + 1} , \tag{3.9}$$

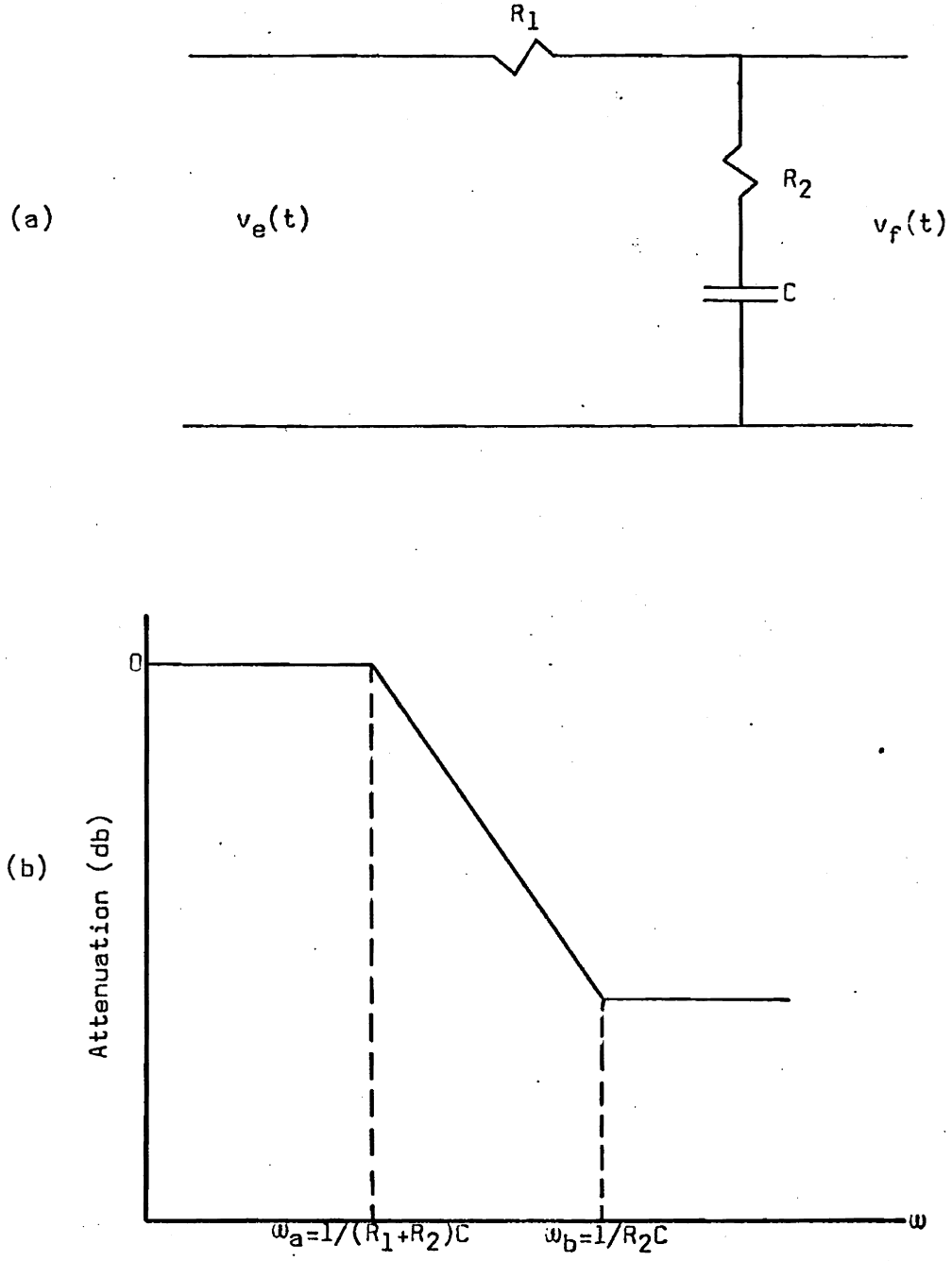

Figure 3.3. Phase lag filter, (a) circuit and (b) frequency response.

where

$$t_a = (R_1 + R_2)C$$

and

$$t_b = R_2C \cdot$$

The down-break frequency (ω_a) and the up-break frequency (ω_b) are equal to $1/t_a$ and $1/t_b$, respectively. The output of the loop filter can then be expressed in terms of the convolution integral as

$$v_f(t) = \int_{-\infty}^{t} v_e(t - x)\, h\,(x)\, dx \cdot \qquad (3.10)$$

Voltage Controlled Oscillator. The voltage controlled oscillator produces the output signal. The frequency of this oscillator may be controlled by means of a voltage sensitive component in the VCO's frequency selective circuitry. In most situations the voltage control can be assumed to be a linear process. The necessary conditions for linearity depend on the particular oscillator design. Generally, a small frequency change compared with the natural frequency of the VCO and a corresponding small change in the component value is the primary requirement for linearity. Under such conditions, the change in the VCO frequency from its natural frequency is proportional to the applied control voltage. Since phase is the integral of frequency, the VCO acts as an integrator and

$$\phi(t) = \int_{-\infty}^{t} k_o v_f(t)dt \ , \qquad (3.11)$$

where k_o is the gain constant of the VCO.

3.2. Analysis of the Phase-locked-loop

The purpose of this paper is to treat the PLL as a frequency-shifted carrier source. The VCO output signal, or simply PLL output, is described by its phase-time function. Such a function is developed here, along with the output frequency-time function, for a step change of input frequency. The model utilized for analysis is shown in Figure 3.1. Major components of the model have been described above.

Application of the PLL here involves binary frequency-shifting the loop's reference signal, by instantaneously switching between two frequency sources. The switching instant is restricted to occur at such a time that the phases of the two sources are in coincidence. That is, a continuous phase frequency-shift is assumed. Figure 3.4 depicts the situation described here. The reference signal, representing a positive frequency step, is given as

$$v_i(t) = - V_i \sin \left[\omega_c t + \phi_i(t)\right] , \qquad (3.12)$$

where

$$\phi_i(t) = \begin{cases} - \Delta\omega t \text{ for } t < 0 \ , \\ + \Delta\omega t \text{ for } t > 0 \ , \end{cases}$$

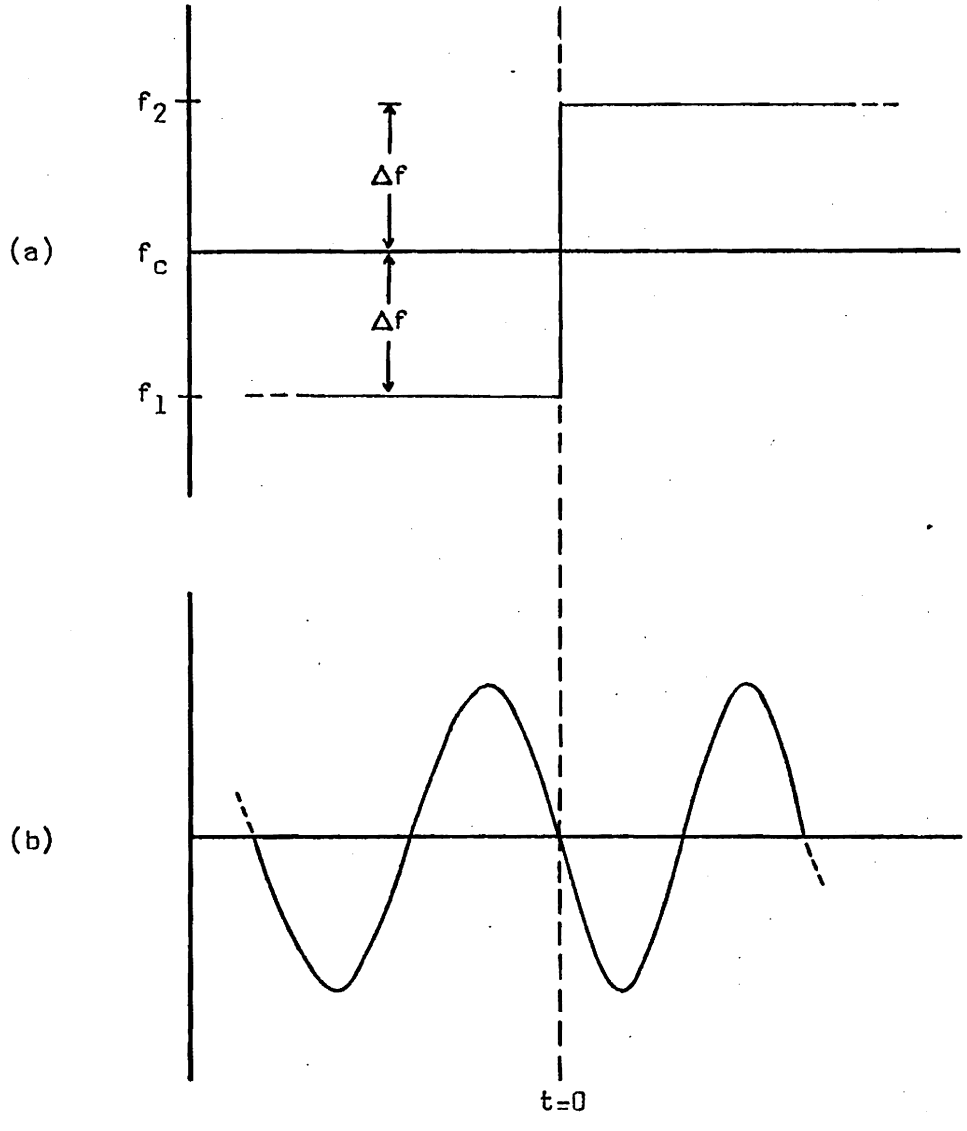

Figure 3.4. Continuous phase frequency shift, (a) modulating waveform and (b) modulated signal.

and ω_c is equal to the natural frequency of the VCO.

Utilizing Equations (3.10) and (3.11), the PLL's integro-differential equation can be written as*

$$\ddot{\phi}(t) = k_o \int_0^t h(x)\, \dot{v}_e(t - x)dx \tag{3.13}$$

and from (3.7)

$$\dot{v}_e(t) = k_c \left[\dot{\phi}_i(t) - \dot{\phi}(t)\right] .$$

Solution of (3.13) is obtained by Laplace transform techniques, and the PLL output phase-time function becomes

$$\phi(t) = \omega t - \frac{\Delta\omega}{K} + \frac{2\Delta\omega}{\omega_n}\sqrt{\frac{1 - 2\delta\omega_n/K + \omega_n^2/K^2}{1 - \delta^2}}\, e^{-\delta\omega_n t} \sin\left[\omega_n\sqrt{1 - \delta^2}\, t + \theta\right] \tag{3.14}$$

where

$$\theta = \arctan\left[\frac{\omega_n\sqrt{1 - \delta^2}/K}{\delta\omega_n/K - 1}\right],$$

$$K = k_o k_c , \tag{3.15}$$

$$\omega_n = \sqrt{K/t_a} , \tag{3.16}$$

---

*A detailed analysis of the PLL is presented in Appendix A. Dots placed above variables indicate time derivatives.

and

$$\delta = \frac{Kt_b + 1}{2t_a\omega_n} \cdot \tag{3.17}$$

The initial conditions imposed upon the solution above are

$$\phi_i(0) = 0 ,$$

$$\dot{\phi}(0) = \Delta\omega/K$$

and

$$\dot{\phi}(0) = -\Delta\omega \cdot$$

The frequency-time function, representing the instantaneous frequency of the PLL output, is obtained by taking the time derivative of (3.14) as

$$\omega(t) = \dot{\phi}(t) = \Delta\omega + 2\Delta\omega \sqrt{\frac{1 - 2\delta\omega_n/K + \omega_n^2/K^2}{1 - \delta^2}}\, e^{-\delta\omega_n t} \sin\left[\omega_n\sqrt{1 - \delta^2}\, t + \gamma\right] , \tag{3.18}$$

where

$$\gamma = \arctan\left[\frac{-\sqrt{1 - \delta^2}}{\delta - \omega_n/K}\right] \cdot$$

The solutions (3.14) and (3.18) are applicable for positive and negative frequency steps by supplying the appropriate sign with $\Delta\omega$. Families of normalized phase-error and frequency curves are shown in Figures 3.5, 3.6 and 3.7 for constant values of δ and ω_n/K. From (3.17),

$$t_b = \frac{2\delta}{\omega_n} - \frac{1}{K}, \tag{3.19}$$

where the up-break frequency, ω_b, of the phase lag filter is equal to $1/t_b$. When $t_b = 0$,

$$2\delta = \frac{\omega_n}{K}, \tag{3.20}$$

and each family of curves degenerates to a single curve, and the filter is reduced to the simple RC circuit. Thus, the effect of the up-break frequency on the phase error and frequency is observed.

3.3 Physical Realizability

Certain restrictions on the values of PLL parameters must be observed in order to effect a physically realizable design. In terms of the loop parameters defined by (3.16) and (3.17), an inequality exists which places bounds on the values of these parameters.

The restrictions placed on the break frequencies of the phase lag filter are

$$\omega_a < \omega_b \leq \infty . \tag{3.21}$$

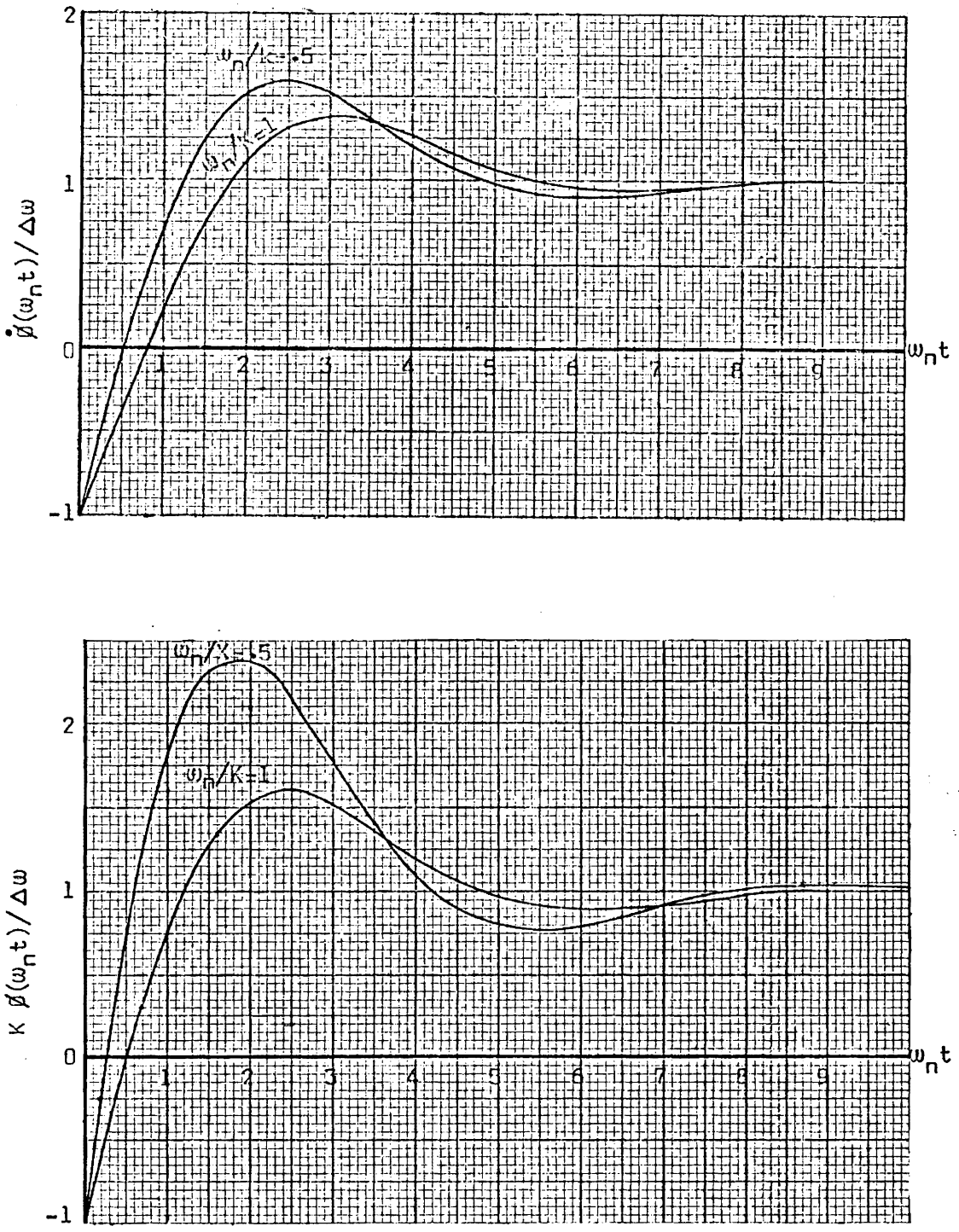

Figure 3.5. Phase-locked-loop response corresponding to $\delta = 0.5$, (a) frequency and (b) phase.

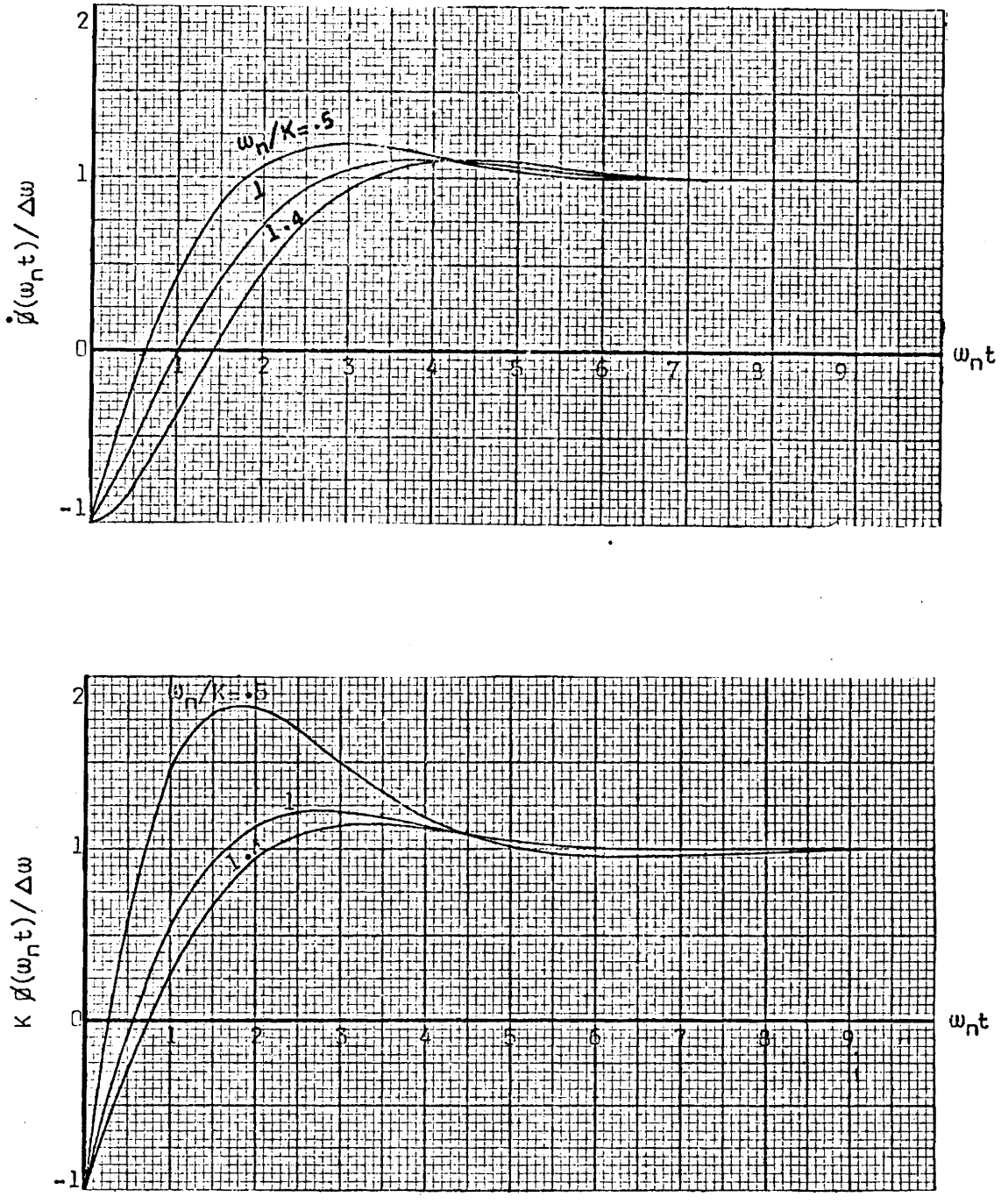

Figure 3.6. Phase-locked-loop response corresponding to $\delta=0.7$, (a) frequency and (b) phase.

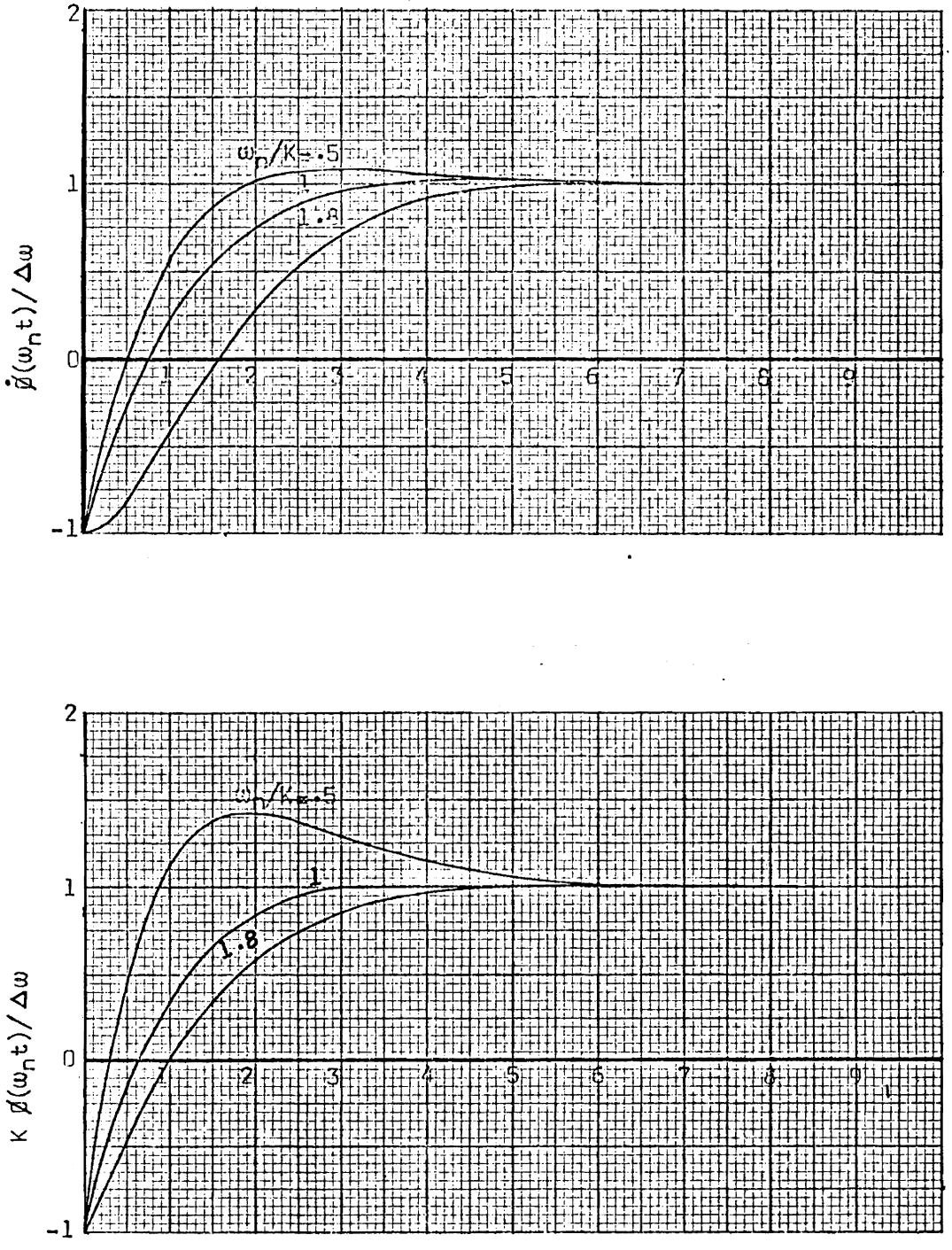

Figure 3.7. Phase-locked-loop response corresponding to $\delta=0.9$, (a) frequency and (b) phase.

Solving (3.17) for t_b and substituting into (3.21) gives

$$\frac{\omega_n}{K} \leq 2\delta < \frac{\omega_n}{K} + \frac{K}{\omega_n} \tag{3.22}$$

The literature [32] normally considers the case where K is large and therefore ω_n/K is negligible. Under such conditions, (3.22) is always satisfied. In cases where the loop gain is not sufficiently high to allow this approximation, bounds on δ and ω_n/K must be determined. The location of the up-break frequency relative to the down-break frequency is given by $N = \omega_b/\omega_a$, and from (3.17)

$$2\delta = \frac{\omega_n}{K} + \frac{1}{N}\frac{K}{\omega_n} .$$

Utilizing the inequality of (3.22) and the above equation, the relationship between N and ω_n/K is shown in Figure 3.8 for several values of δ. Large values of N give good high frequency attenuation in the low pass filter, providing a more nearly ideal control voltage. However, the upper-break frequency affects the loop's pull-in range, and this effect must be considered in some applications. For loop operation near critical damping ($\delta \simeq 1$), ω_n/K is restricted to values less than two (see Equation 3.22). The effects of small values of ω_n/K on phase and frequency is seen in Figures 3.5, 3.6 and 3.7. These graphs allow the designer to select the shape of frequency transition desired, while satisfying (3.22).

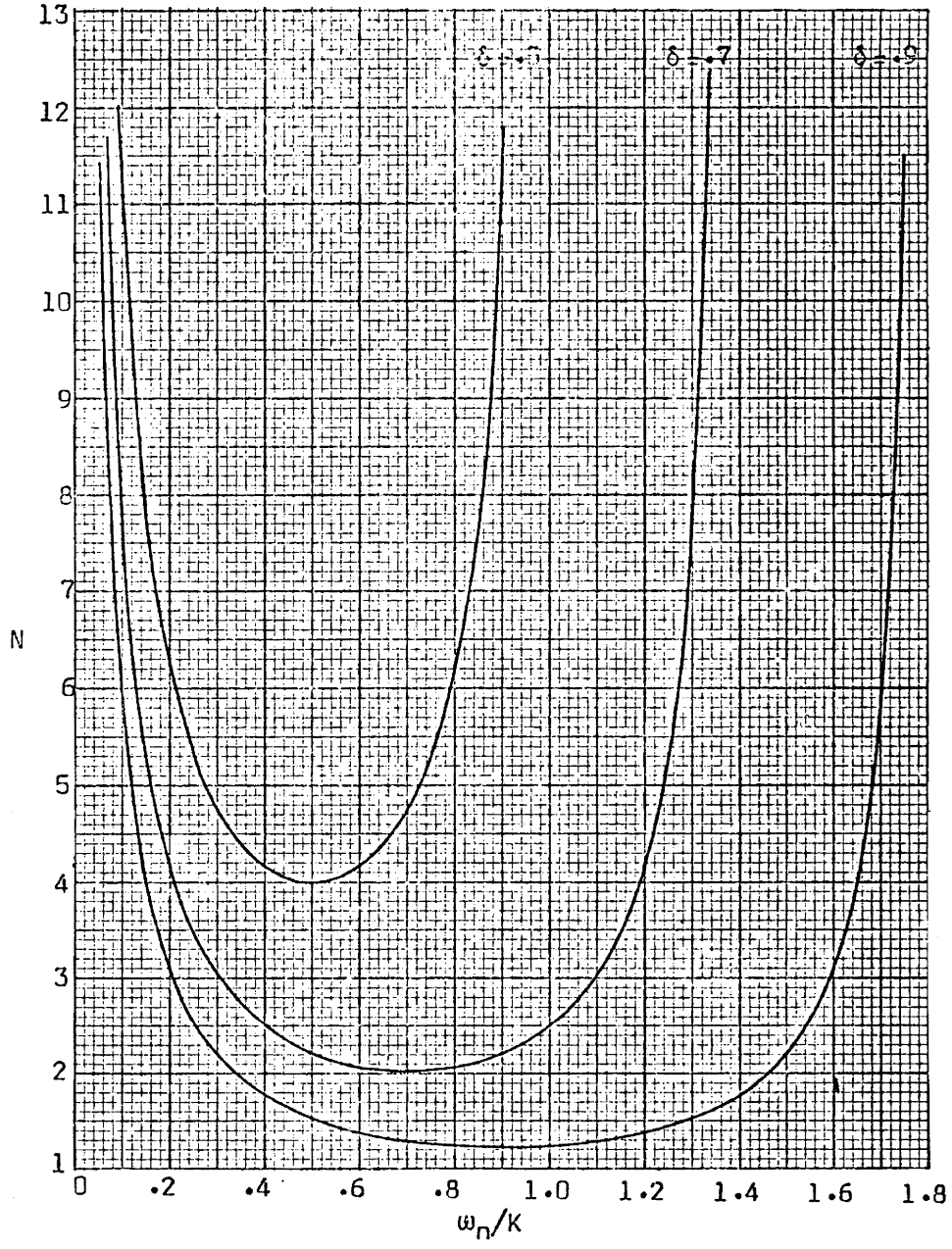

Figure 3.8. Break frequency ratio, $N \equiv \omega_b/\omega_a$, versus ω_n/K for constant values of δ.

The effects of the frequency transition on the PLL output signal bandwidth, and the response of systems excited by such, are determined by the magnitude of the frequency shift and the derivatives of frequency (or simply the shape of the frequency transition). Since a wide range of frequency transition shapes can be obtained for values of δ less than unity, as seen in the normalized frequency graphs, the remainder of this investigation is concerned with such a range of δ values.

3.4 Series Representation of the Phase-locked-loop Output Signal

The response of networks to arbitrary frequency-modulated carriers cannot be expressed in closed form. In general, the network response involves evaluation of at least one integral whose integrand is quite complex. Thus, some type of series representation is normally utilized, even where approximate solutions are acceptable. In order to utilize the PLL as a frequency-shifted carrier source for linear networks, the signal is expressed as an infinite series. Then, for any linear network, the response may be determined by superimposing the responses of the network to each individual term in the series. The series developed here involves the phase time function in the form of (3.14).

In an effort to simplify the mathematical expressions, equation (3.14) is rewritten as

$$\phi(t) = \Delta\omega t + Me^{-\alpha t} \sin(\beta t + \theta) - \phi_s \; ; \qquad (3.23)$$

where

$$M = \frac{2\omega}{\omega_n}\sqrt{\frac{1 - 2\delta\omega_n/K + \omega_n^2/K^2}{1 - \delta^2}}\ , \tag{3.24}$$

$$\alpha = \delta\omega_n\ , \text{ the damping factor}\ , \tag{3.25}$$

$$\beta = \omega_n\sqrt{1 - \delta^2}\ , \text{ the damped natural frequency}\ , \tag{3.26}$$

and

$$\phi_s = \Delta\omega/K\ , \text{ the steady-state phase error}\ . \tag{3.27}$$

Utilizing equation (3.3), the PLL output signal can be expressed as

$$v(t) = V \sin\left[\omega_2 t + Me^{-\alpha t}\sin(\beta t + \theta) - \phi_s\right]\ , \tag{3.28}$$

where

$$\omega_2 = \omega_c + \Delta\omega\ .$$

A Maclaurin expansion [38] is utilized to develop a series consisting of a steady-state term plus damped sinusoidal terms. The development of this series is presented in Appendix B, and from (B.8) several terms of the series are written as follows

$$v_o(t) = G_o \sin(\omega_2 t) - \phi_s)$$

$$+ G_1 \left(\sin\left[(\omega_2 + \beta)t - \phi_s + \theta\right] - \sin\left[(\omega_2 - \beta)t - \phi_s - \theta\right]\right)$$

$$+ G_2 \left(\sin\left[(\omega_2 + 2\beta)t - \phi_s + 2\theta\right] + \sin\left[(\omega_2 - 2\beta)t - \phi_s - 2\theta\right]\right)$$

$$+ G_3 \left(\sin\left[(\omega_2 + 3\beta)t - \phi_s + 3\theta\right] - \sin\left[(\omega_2 - 3\beta)t - \phi_s - 3\theta\right]\right)$$

$$+ \ldots .$$

$$+ G_p \left(\sin\left[(\omega_2 + p\beta)t - \phi_2 + p\theta\right]\right.$$

$$\left. + (-1)^p \sin\left[(\omega_2 - p\beta)t - \phi_s - p\theta\right]\right), \qquad (3.29)$$

where

$$G_p = G_p(M,\alpha t) =$$

$$= V \sum_{k=0}^{\infty} \frac{(-1)^k M^{2k+p} e^{-(2k+p)\alpha t}}{2^p 4^k k!\,(k+p)!} \qquad (3.30)$$

and

$$p = 0,1,2, \ldots .$$

With the exception of the first term in $G_p(M,\alpha t)$, which represents the steady state component, all terms decay with time. The contribution of $G_p(M,\alpha t)$ to the composite signal, $v(t)$, is indicated in Figures 3.9, 3.10 and 3.11, where the range of M values is representative of those values encountered in this investigation.

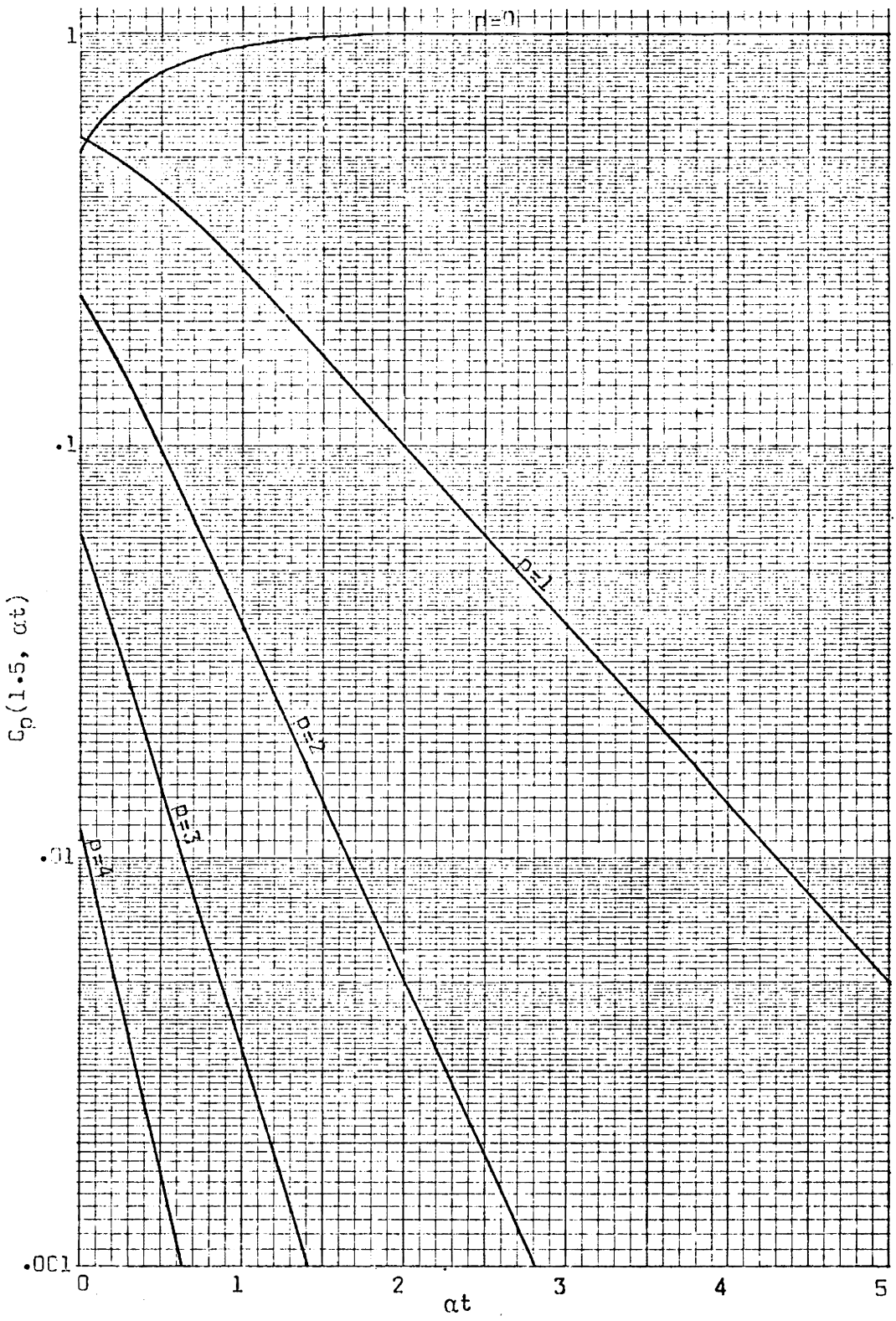

Figure 3.9. Graph of $G_p(M,\alpha t)$.

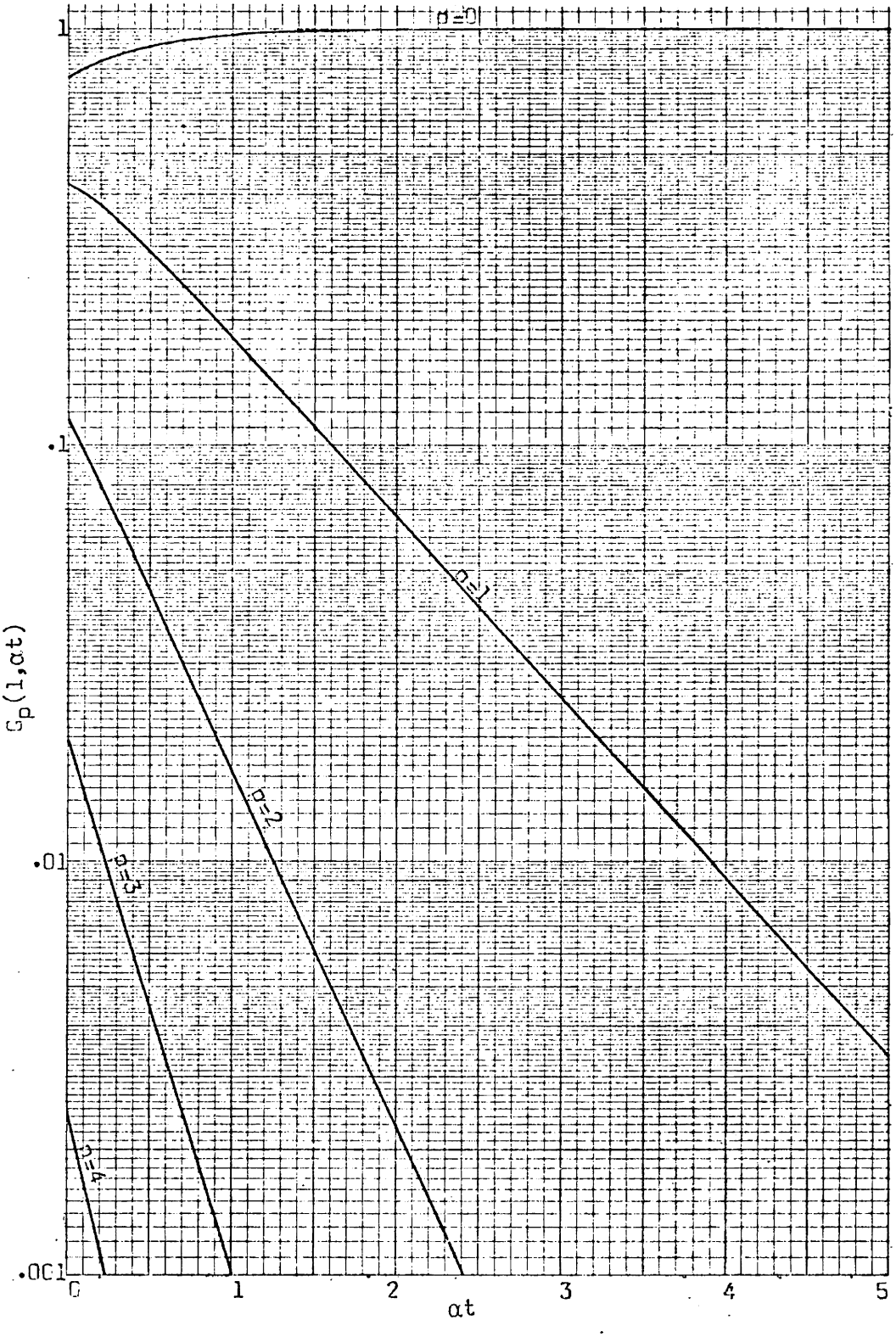

Figure 3.10. Graph of $G_p(M,\alpha t)$.

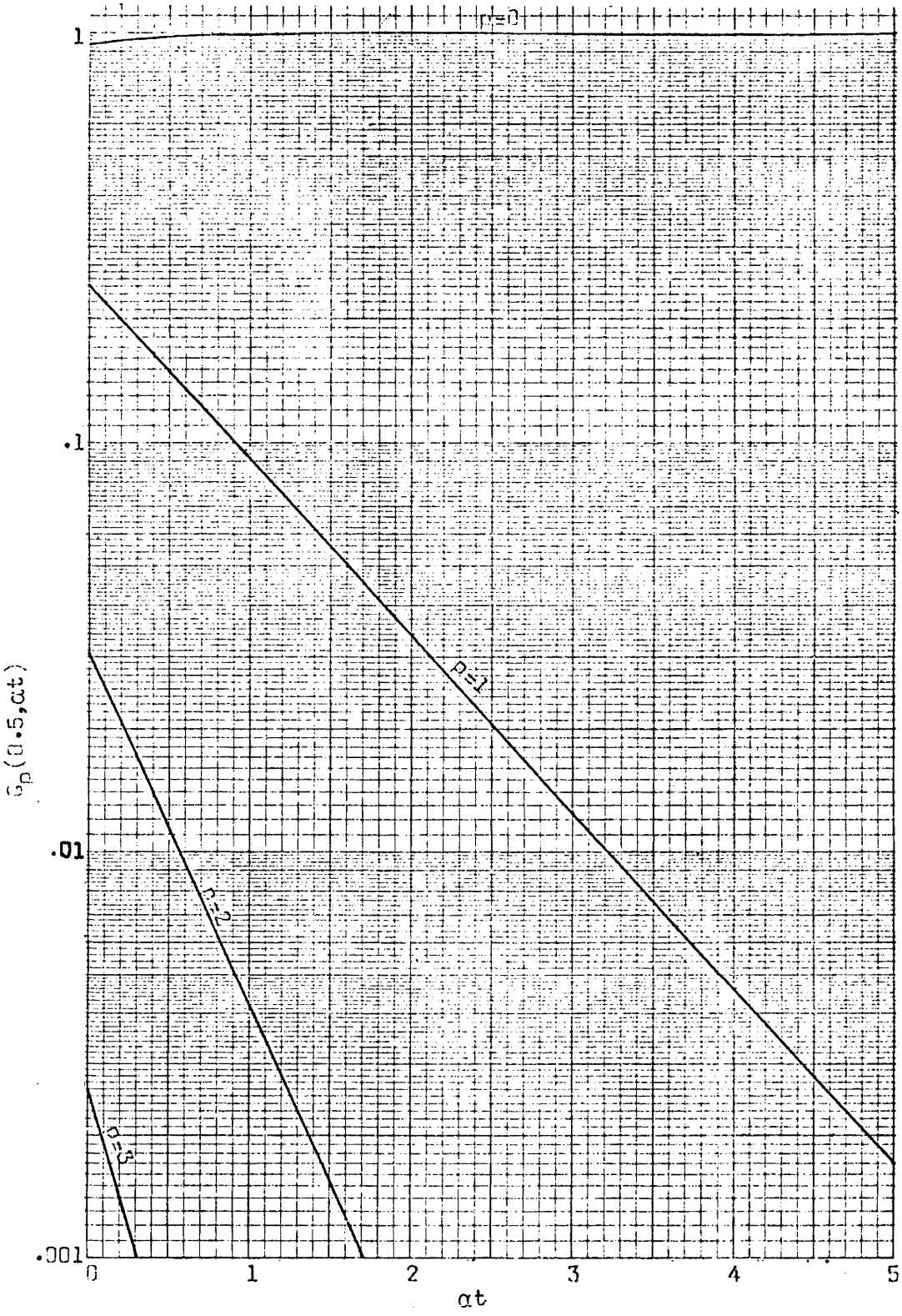

Figure 3.11. Graph of $G_p(M,\alpha t)$.

It is interesting to note that in the limit, when $\alpha \rightarrow 0$, Equations (3.29) and (3.30) can be identified with the Bessel-Fourier series encountered in sinusoidal frequency modulated carriers [39]. From a physical point of view, this is to be expected. In this case the PLL is excited by the frequency step and the VCO continues to be sinusoidally frequency modulated, by the undamped transient, at the natural frequency of the loop.

IV. SPECTRAL ANALYSIS OF PHASE-LOCKED-LOOP OUTPUT

The PLL output signal can be expressed in terms of its frequency spectrum. This assumes that the PLL reference signal takes the form of a square wave frequency modulated carrier, resulting in a periodically keyed PLL. The significant frequency components which constitute the signal and determine its bandwidth are functions of the rate of change of freqneucy during any frequency transition. Figure 4.1 depicts a typical frequency transition, and a transition time interval, t_s, is defined. The transition interval is selected as the time required for 90% of the total change in frequency, where t_s is measured from time $t = 0$. The effect of t_s on signal bandwidth will be determined for the case of a frequency-shifted phase-locked-loop (FS-PLL), periodically switched at a frequency, f hertz.

4.1 Keying Conditions

Consider the FS-PLL reference signal to be frequency-modulated by means of a square wave, as shown in Figure 4.2. The frequency transition is instantaneous ($t_s = 0$), and the phase is assumed to be continuous. It is further assumed that the phase has a zero value, referenced to a sine wave, at the switching instant.

The conditions necessary to provide the assumed keying conditions are determined as follows. An integral number of cycles must occupy any single bit time-interval; and in the first half keying cycle

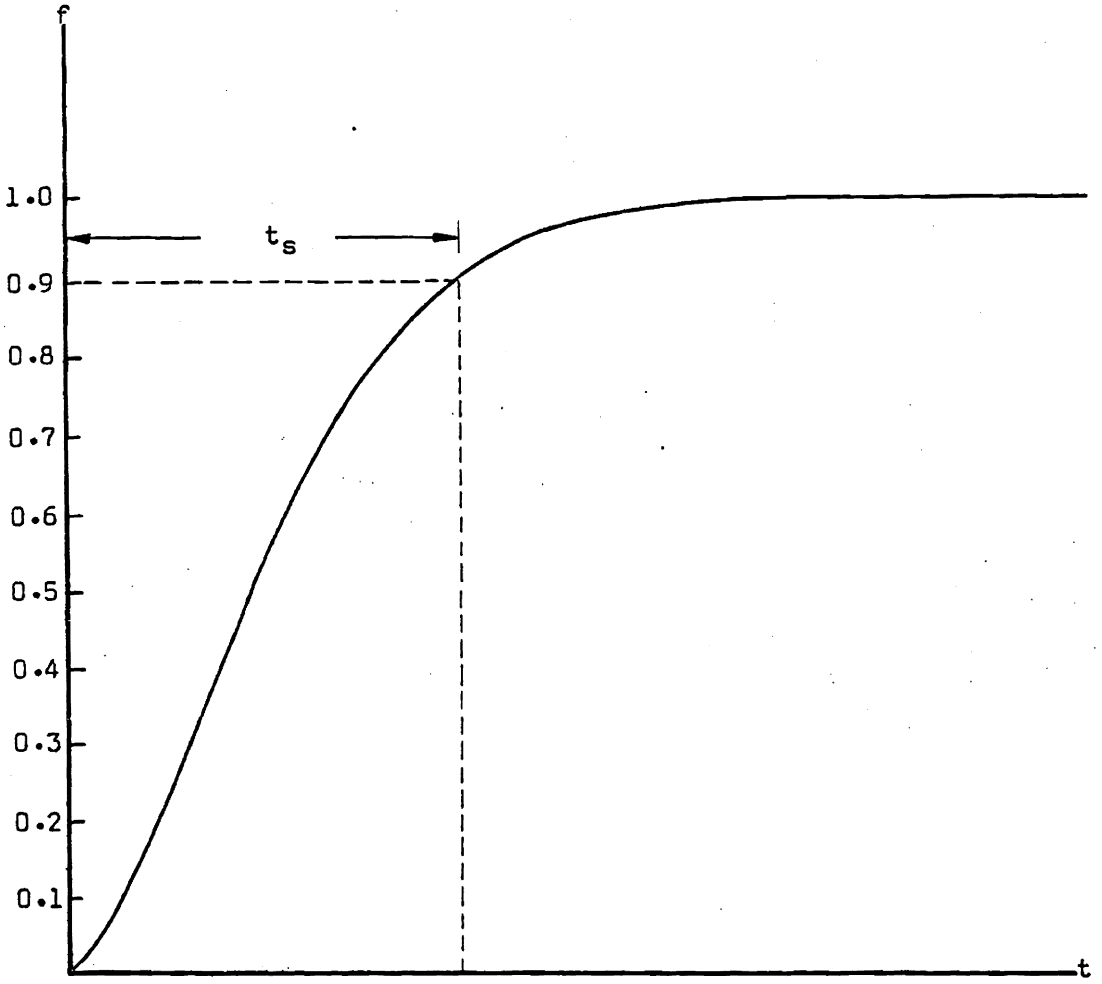

Figure 4.1. Representative frequency transition, where the change in frequency is given relative to the total frequency shift.

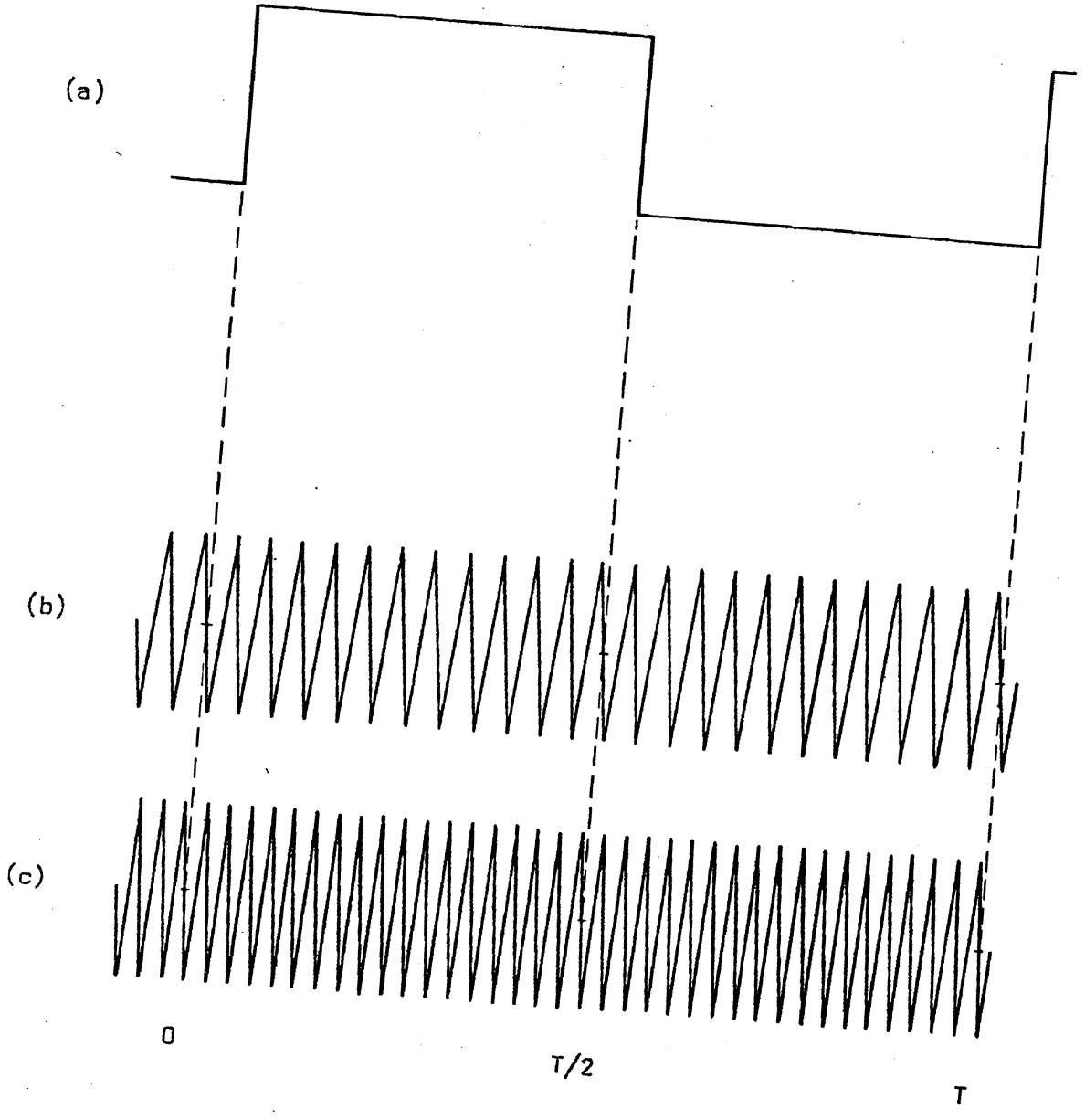

Figure 4.2. Illustration of keying conditions, (a) keying (modulation) signal, (b) frequency f_1 and (c) frequency f_2.

$$\omega_1 T/2 = 2\pi q_1 \quad , \quad q_1 = 1,2,3, \cdots \; ; \tag{4.1}$$

where T is the period of the keying, or modulating frequency. Thus

$$q_1 = f_1/2f \; . \tag{4.2}$$

Likewise, for the second half keying cycle,

$$q_2 = f_2/2f \tag{4.3}$$

where

$$q_2 = 1,2,3, \cdots \; .$$

Letting f_2 be greater than f_1, solving (4.2) and (4.3) for the two frequencies involved and subtracting provides a relation between the modulating frequency and the total carrier shift,

$$f_2 - f_1 = 2(q_2 - q_1)f = 2mf \; . \tag{4.4}$$

Since q_1 and q_2 are integers, the value of m must also be an integer. Noting that the difference frequency on the left of (4.4) is the total frequency shift, this equation can be rewritten as

$$m = \frac{f_2 - f_1}{2f} = \frac{\Delta f}{f} \; , \tag{4.5}$$

which is the expression for modulation index. The amount of frequency deviation from the center, or carrier, frequency is given by Δf.

In the analysis which follows, the restrictions of equations (4.2), (4.3) and (4.5) are observed, and a modulation index of m=1 is used (narrowband bindary FSK operation).

A periodically frequency-shift-keyed carrier can be expressed in terms of a Fourier series by means of[40].

$$v(t) = \frac{a_0}{2} + \sum_{n=1}^{\infty} |C_n| \cos (n\omega t + \theta_n) , \tag{4.6}$$

where

$$C_n = \frac{2}{T} \int_0^T v(t) e^{-jn\omega t} \, dt .$$

The Fourier coefficients, $|C_n|$, are of primary interest in determining signal bandwidth, where $|C_n|$ is the magnitude of the nth discrete harmonic present in the frequency spectrum. In general, the modulated carrier is given as

$$v(t) = V \sin [\omega_c t + \phi(t)] , \tag{4.7}$$

where $\phi(t)$ describes the modulation about the carrier frequency ω_c.

Square Wave Frequency Modulated Carrier Spectrum. The frequency spectrum for square wave frequency modulation is presented here for periodic frequency shifts between the two frequencies f_1 and f_2. The binary modulation function is

$$\phi(t) = \begin{cases} (\omega_2-\omega_c)t = \Delta\omega t & , \quad 0 < t < T/2 \\ (\omega_1-\omega_c)t = -\Delta\omega t & , \quad T/2 < t < T \end{cases} . \tag{4.8}$$

Employing these expressions for the modulated carrier along with (4.6), the Fourier coefficients can be obtained by straightforward methods as

$$C_n = \frac{1}{2}\left(\left[\frac{\sin(2q_2-n)\pi/2}{(2q_2-n)\pi/2} - \frac{\sin(2q_2+n)\pi/2}{(2q_2+n)\pi/2}\right]\right.$$

$$\left. - (-1)^n \left[\frac{\sin(2q_1-n)\pi/2}{(2q_1-n)\pi/2} - \frac{\sin(2q_1+n)\pi/2}{(2q_1+n(\pi/2}\right]\right) e^{j(2q_1-n+1)\pi/2} , \tag{4.9}$$

for q_1 and q_2 as defined in (4.2) and (4.3) and a modulation index, m=1. This result appears in the literature [15-16] .

Determination of signal bandwidth can be facilitated by utilizing a discrete spectral component envelope. Such an envelope is obtained by drawing a smooth curve through the points which represent the maximum values of the spectral magnitudes $|C_n|$. Equation (4.9) can be modified to provide an expression for the spectral magnitudes which are applicable throughout the range of significant frequency components. Using (4.9) and letting r designate the order of the spectral component relative to the carrier frequency, the discrete spectral component envelope is given approximately by

$$|\hat{C}_r| = \frac{2}{(r^2-1)\pi} , \quad r = 0, \pm 2, \pm 3 , \ \ldots\ ; \tag{4.10}$$

and for $r = \pm 1$,

$$|C_{\pm 1}| = \frac{1}{2} \cdot$$

The following substitutions have been made in deriving (4.10):

$$r-1 = 2q_2-n \quad ,$$

and

$$r+1 = 2q_1-n \quad .$$

Equation (4.10) is valid when $|r| \ll 2n$, which includes the range of significant frequency components about the carrier frequency.

Frequency-shifted Phase-locked-loop Output Spectrum. The Fourier series is defined by (4.6). For non-elementary time functions v(t), conventional mathematics are not expected to yield the frequency spectrum C_n. Computerized numerical integration methods can be utilized for the purpose of evaluating C_n in cases where v(t) is quite complex. Equation (3.29), which is readily handled by the digital computer, is available in this investigation. In many practical cases only a few terms of (3.29) are needed to accurately represent the frequency transition, and the Fourier series coefficients may be found with a minimum of computer time as contrasted to the computer time required to find the coefficients by numerical integration. The advantage in using (3.29) is greatest for small values of t_s.

The FS-PLL output is given by

$$v(t) = \begin{cases} V \sin\left[\omega_c t + \phi(t)\right] , & 0 < t < T/2 \\ V \sin\left[\omega_c t - \phi(t)\right] , & T/2 < t < T \end{cases} \tag{4.11}$$

where $\phi(t)$ is given by (3.14). Equation (4.11) represents frequency shifts from f_1 to f_2 and f_2 to f_1, respectively. Substituting the series from (3.29) for v(t) in the expression for C_n of (4.6) provides the frequency spectrum by evaluation of the integrals term by term. The spectrum found is

$$C_n = \sum_{P=0}^{\infty} \sum_{k=0}^{\infty} c_{n,p,k} \tag{4.12}$$

where $c_{n,p,k}$ represents the contribution to the spectrum of each term in the series of (3.29). Expressions for $c_{n,p,k}$ are developed in Appendix C as (C.4) and (C.5).

The square wave frequency modulated carrier spectrum of (4.9) is shown in Figure 4.3(a) for the purpose of comparison with FS-PLL specta. Equation (4.12) is used to calculate the FS-PLL signal's midband frequency components, for several values of t_s, corresponding to the smooth transition of Figure 4.1. These spectra appear as Figures 4.3(b) and (c). It is seen from this figure that an increase in the value of t_s tends to concentrate the signal energy in the neighborhood of the signal's midband frequency.

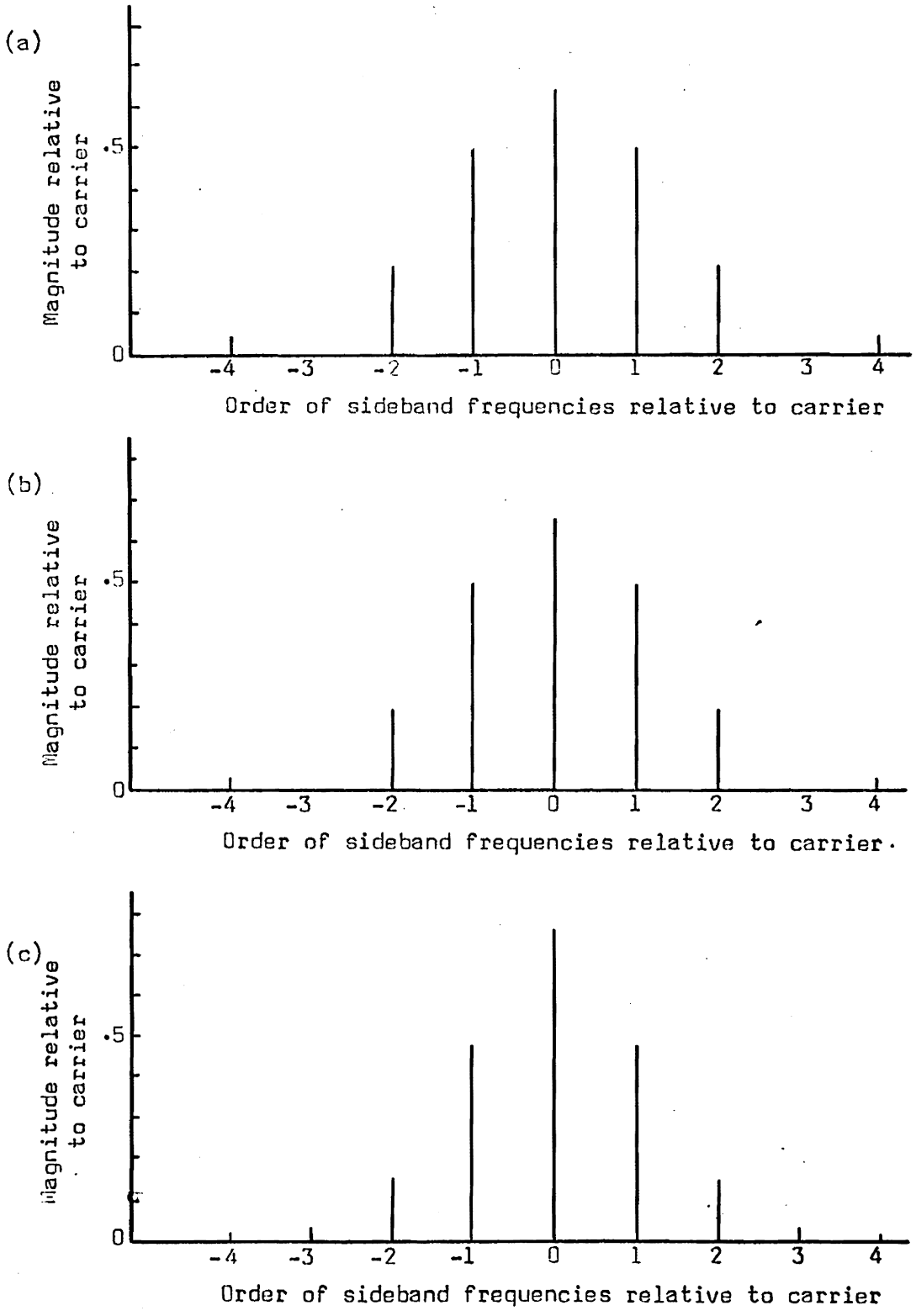

Figure 4.3. Comparison of frequency spectra for (a) square wave keying, t_s=0, (b) t_s=5ms and (c) t_s=10ms.

In order to facilitate the presentation of various spectra, a spectral component envelope is employed. Furthermore, only the upper half of each spectrum is shown, since the spectral magnitudes are symmetrical about the carrier frequency. The most noticeable effect of t_s on the spectral composition, or bandwidth of a signal is found at frequencies removed from midband, as shown by Figure 4.4. In this figure the spectral envelopes are compared with that of the square wave frequency modulated carrier given by (4.10).

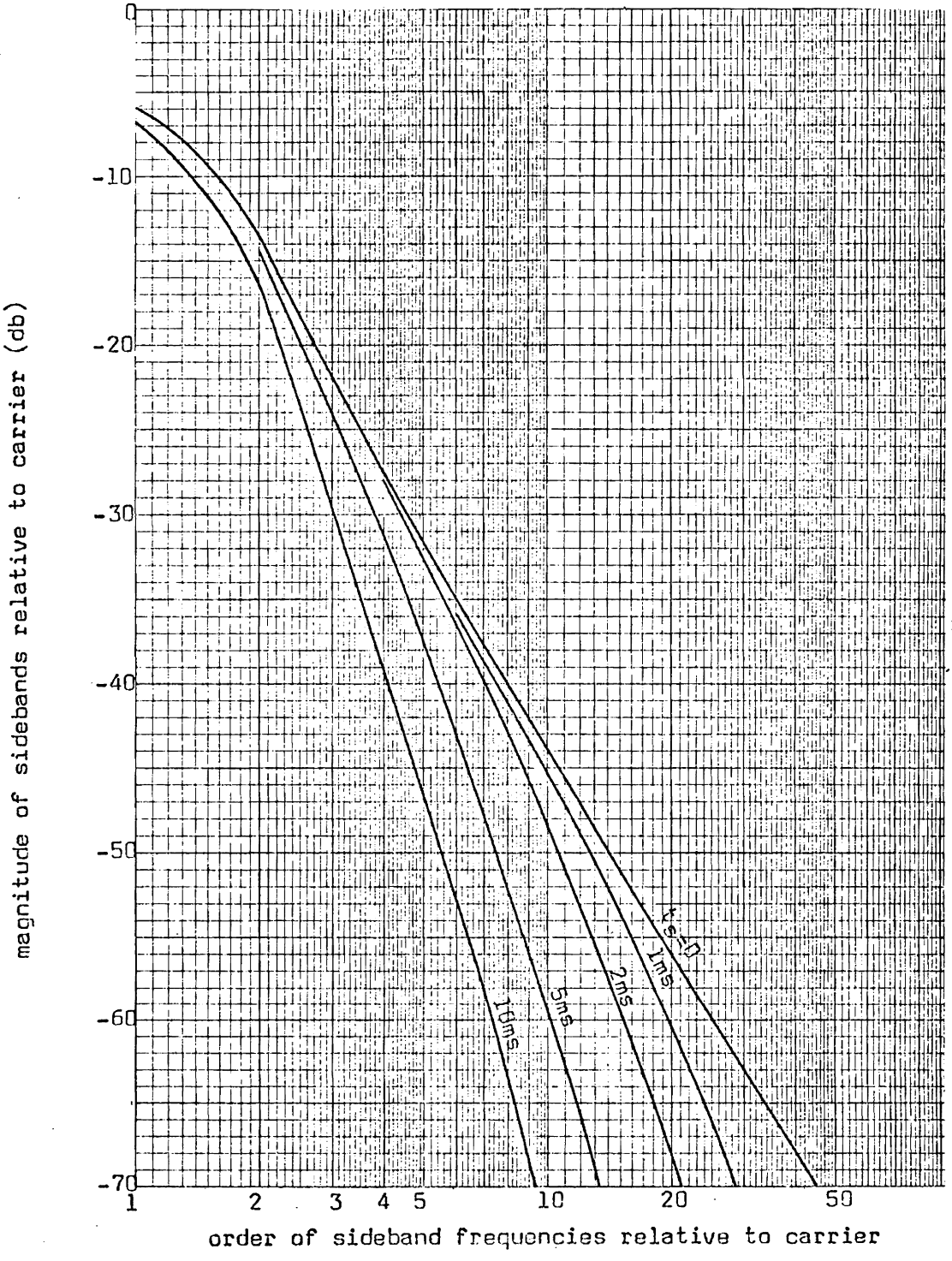

Figure 4.4. Spectral envelopes for representative values of t_s.

V. RESPONSE OF A SERIES TUNED CIRCUIT EXCITED BY A FREQUENCY-SHIFTED PHASE-LOCKED-LOOP

The FS-PLL output signal has been characterized in the time and frequency domains. This section of this paper considers the response of a simple network driven by the FS-PLL. The particular network considered here is a narrowband series tuned circuit. The primary reason for selecting the series tuned circuit in this investigation is because it is used as an equivalent circuit of the VLF transmitting antenna [41]. Analyses and conclusions provided here can be applied equally well to the parallel tuned circuit by employing the duality principle.

5.1 System Description and Initial Conditions

The narrowband series tuned circuit excited by means of a constant amplitude frequency stepped carrier has received considerable attention in the literature [10,12,13]. In contrast to the instantaneous transition of the frequency step, the effect on circuit response of a finite frequency transition interval is of primary interest here. The circuit employed for analysis is presented in Figure 5.1, along with its steady-state frequency response characteristics. The voltage source of the tuned circuit is the FS-PLL.

Consider that the PLL's reference frequency is subjected to a step, from f_1 to f_2. The PLL does not respond instantaneously, thus

its output frequency shifts from f_1 to f_2 over some finite time interval, as determined by the loop gain and bandwidth. A representative frequency transition appears in Figure 4.1, where a transition time interval, t_s, is defined. The frequency shift is symmetrical with respect to the circuit's resonant frequency. That is, f_1 and f_2 are equal power frequencies, on their respective sides of resonance. The two equal power frequencies are related to the resonant frequency, f_r, of the tuned circuit by

$$f_r = \sqrt{f_1 f_2} \quad , \tag{5.1}$$

where the resonant frequency is that frequency which makes the input impedance of the series tuned circuit purely resistive. For narrowband signals,

$$|f_1 - f_2| \ll f_r \quad ,$$

and (5.1) can be approximated by

$$f_r - f_1 \cong f_2 - f_r \cong \Delta f \tag{5.2}$$

It is assumed that the RLC series tuned circuit is in the steady state at time zero, being driven at a frequency f_1. The initial current in the inductor, I_o, and voltage across the capacitor, V_o, is obtained from the steady state response of the circuit. The steady state excitation is given by

$$v(t) = V \sin(\omega_1 t + \phi_s) \quad , \quad \text{for } t < 0 \quad . \tag{5.3}$$

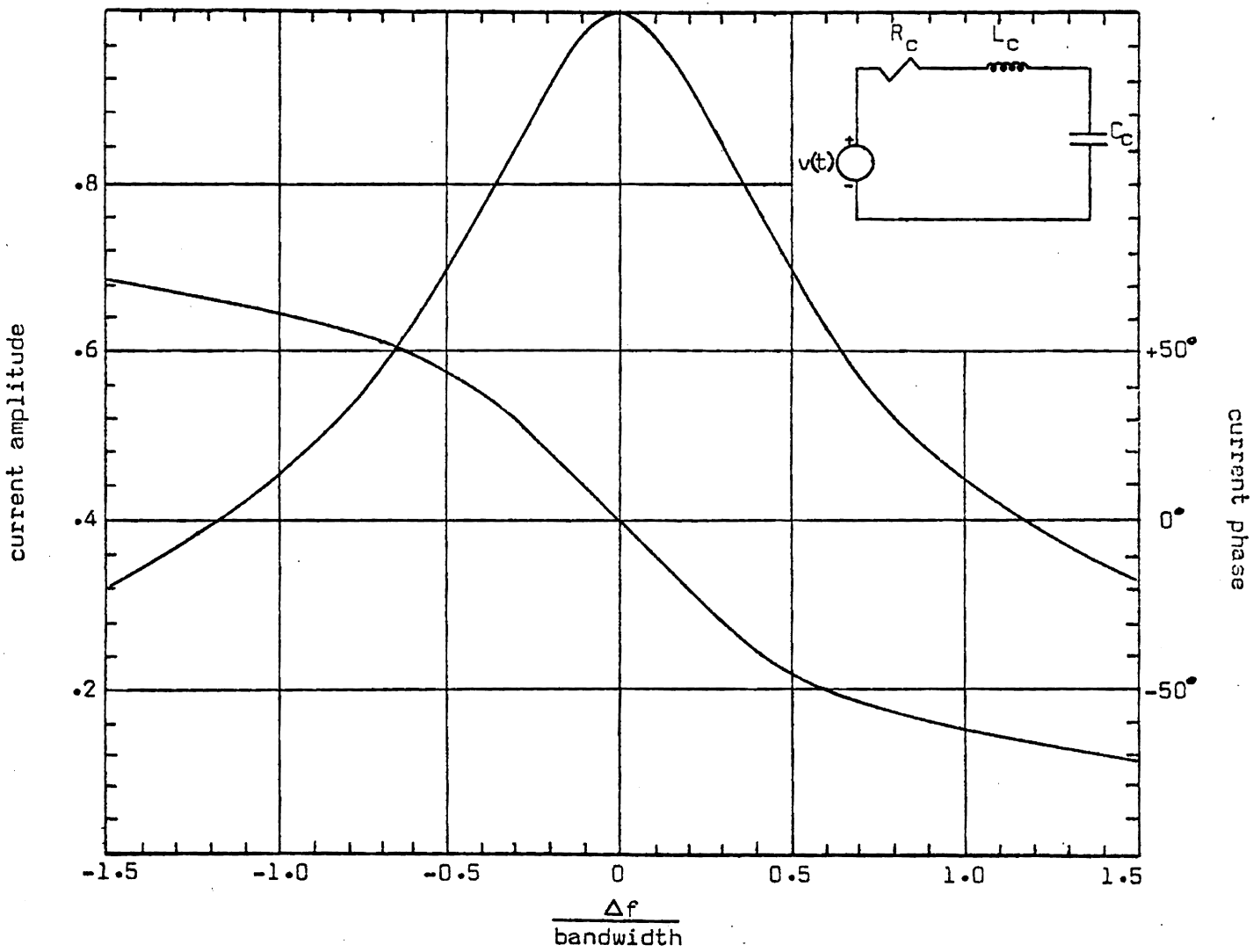

Figure 5.1. RLC series tuned circuit response, relative to source voltage.

Equation (5.3) is obtained from (3.29) by using

$$f_1 = f_c - \Delta f \quad ,$$

and the assumption that all time-decaying terms have been reduced to zero. The steady state response and initial conditions are presented in Appendix D.

5.2 Response Analysis

As discussed in Section 3.4, the response of networks to frequency modulation other than square wave frequency modulation cannot be obtained by straightforward network analysis. For this reason, a series of elementary terms has been developed which can be used for term-by-term excitation of any linear network. The total response is then obtained by superposition. Response of the RLC series tuned circuit can now be found by utilizing familiar Laplace transform techniques.

Upon transforming the RLC circuit, and representing the initial inductor current and capacitor voltage as voltage generators, the circuit of Figure 5.2 results. From this figure, the circuit current is given by

$$I = \frac{V}{Z} + \frac{SLI_o - V_o}{SZ} \quad , \qquad (5.4)$$

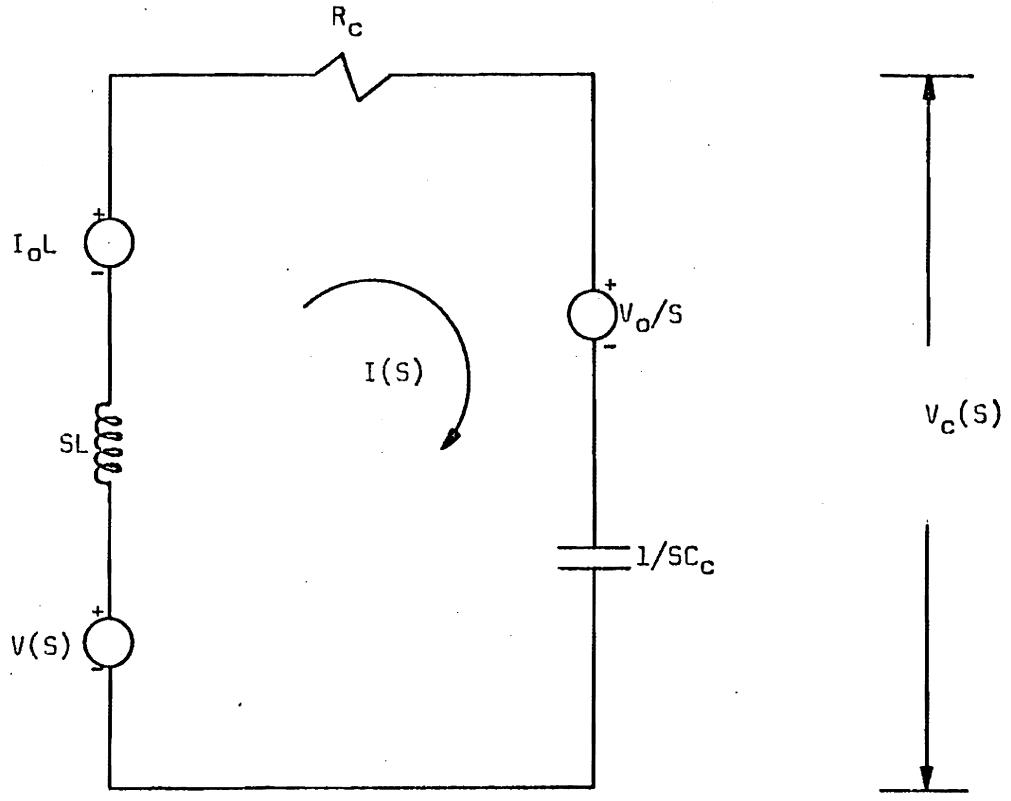

Figure 5.2. Laplace transformed RLC series tuned circuit, including initial conditions.

where I, V and Z are functions of the Laplace transform variable, S. The transformed impedance is

$$Z = \frac{L}{S}(S^2 + SR/L + 1/LC) \quad , \tag{5.5}$$

and the resonant frequency is defined as

$$\omega_r = \sqrt{1/LC} \quad .$$

At time zero, the reference frequency of the PLL is stepped by $2\Delta f$*, from f_1 to f_2. The ensuing FS-PLL output signal (circuit's input) is expressed by (3.28) or the series of (3.29). Considering that the circuit is excited separately by each term in the series (3.29), the current given by (5.4) can be rewritten as

$$I = \frac{\sum\sum F_{p,k}}{Z} + \frac{SLI_o - V_o}{SZ} \quad . \tag{5.6}$$

The quantity $F_{p,k}$ represents the Laplace transform of the general term in (3.29) and the summation on $F_{p,k}$ represents the sum of all such terms. Details concerning the inverse transformation of (5.6) are presented as Appendices D and E.

---

*A PLL reference frequency step of $2\Delta\omega$ is equivalent to step modulating the carrier by an amount $\Delta\omega$, which results in a total frequency change of $2\Delta\omega$ of the PLL output signal.

From (D.6) and (E.19), the current response time function can be expressed symbolically as

$$i(t) = i_{ic}(t) + \sum_{p=o}^{\infty} \sum_{k=o}^{\infty} r_{p,k}(t) \cdot \qquad (5.7)$$

The first term on the right is the current resulting from initial conditions, and the double summation represents the current due to the source. The quantity $r_{p,k}(t)$ represents the response to each term of the series.

5.3 Representative Response Calculations

Calculation of representative series tuned circuit responses to FS-PLL excitation can be effected by programming (5.7) on the digital computer. Such a program is employed here and the resulting data are presented in the form of families of curves. These curves represent the envelope of the positive peaks of the rf carrier. The amplitudes plotted are relative to the steady state current values.

Corresponding to the frequency transition for $2\delta = \omega_n/K = 1.8$ of Figure 3.7, examples of the response for various values of t_s, Δf and circuit bandwidth are shown in Figures 5.3 through 5.5. The current phase presented is relative to the phase of the source voltage. For comparison, the frequency step circuit amplitude response and the

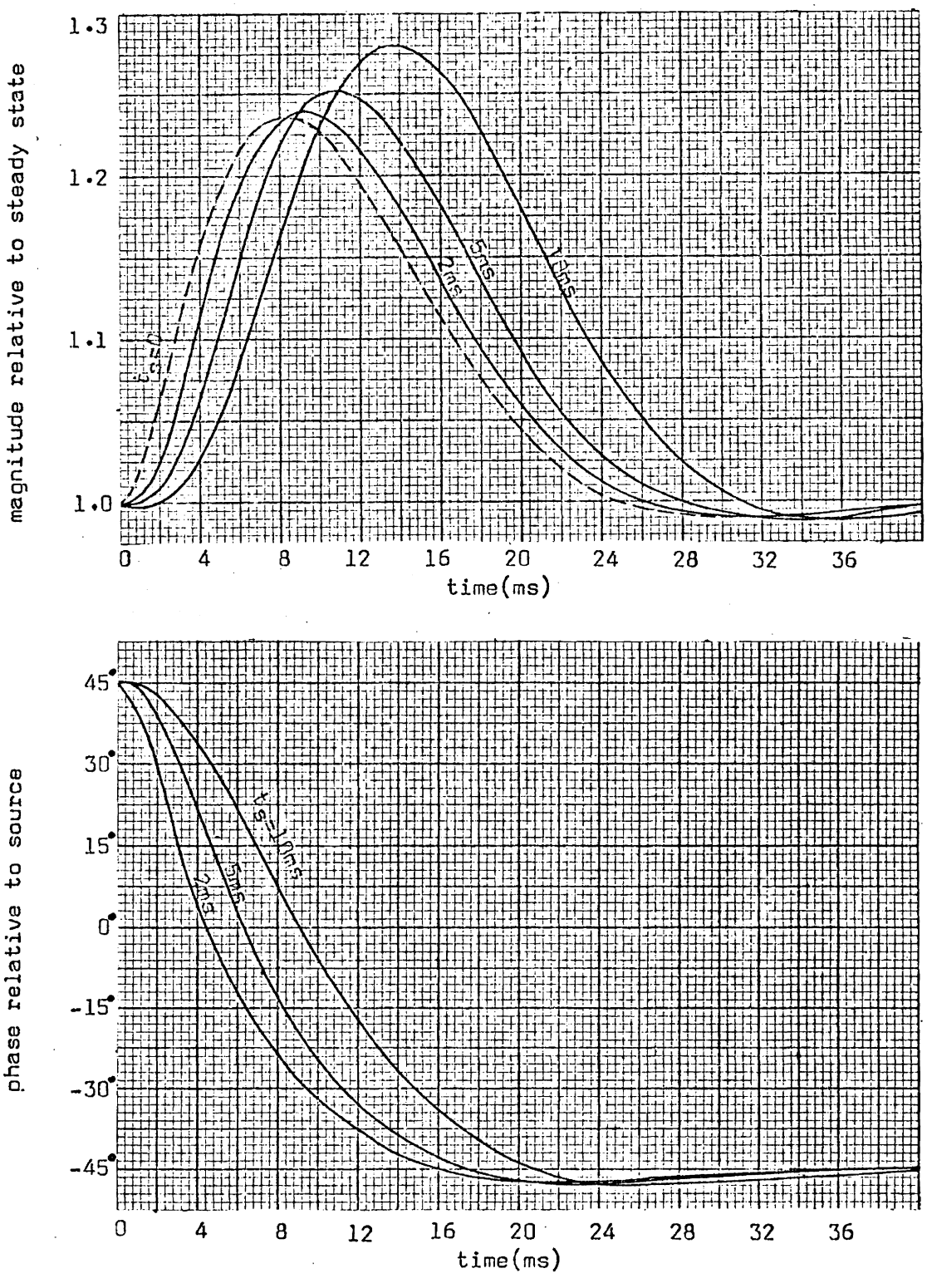

Figure 5.3. Response of series tuned circuit for Δf=25 hertz and circuit bandwidth of 50 hertz.

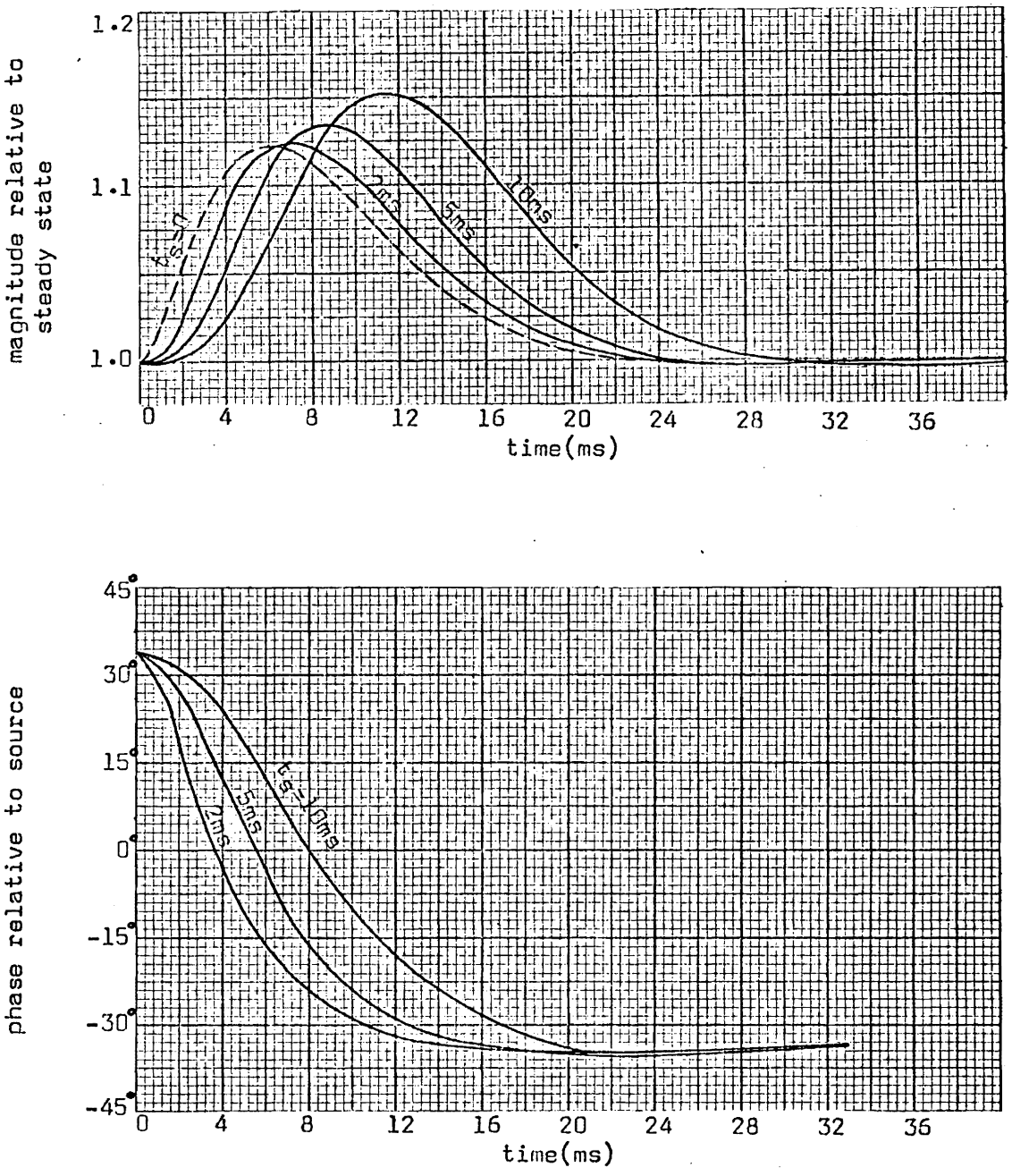

Figure 5.4. Response of series tuned circuit for Δf=25 hertz and circuit bandwidth of 75 hertz.

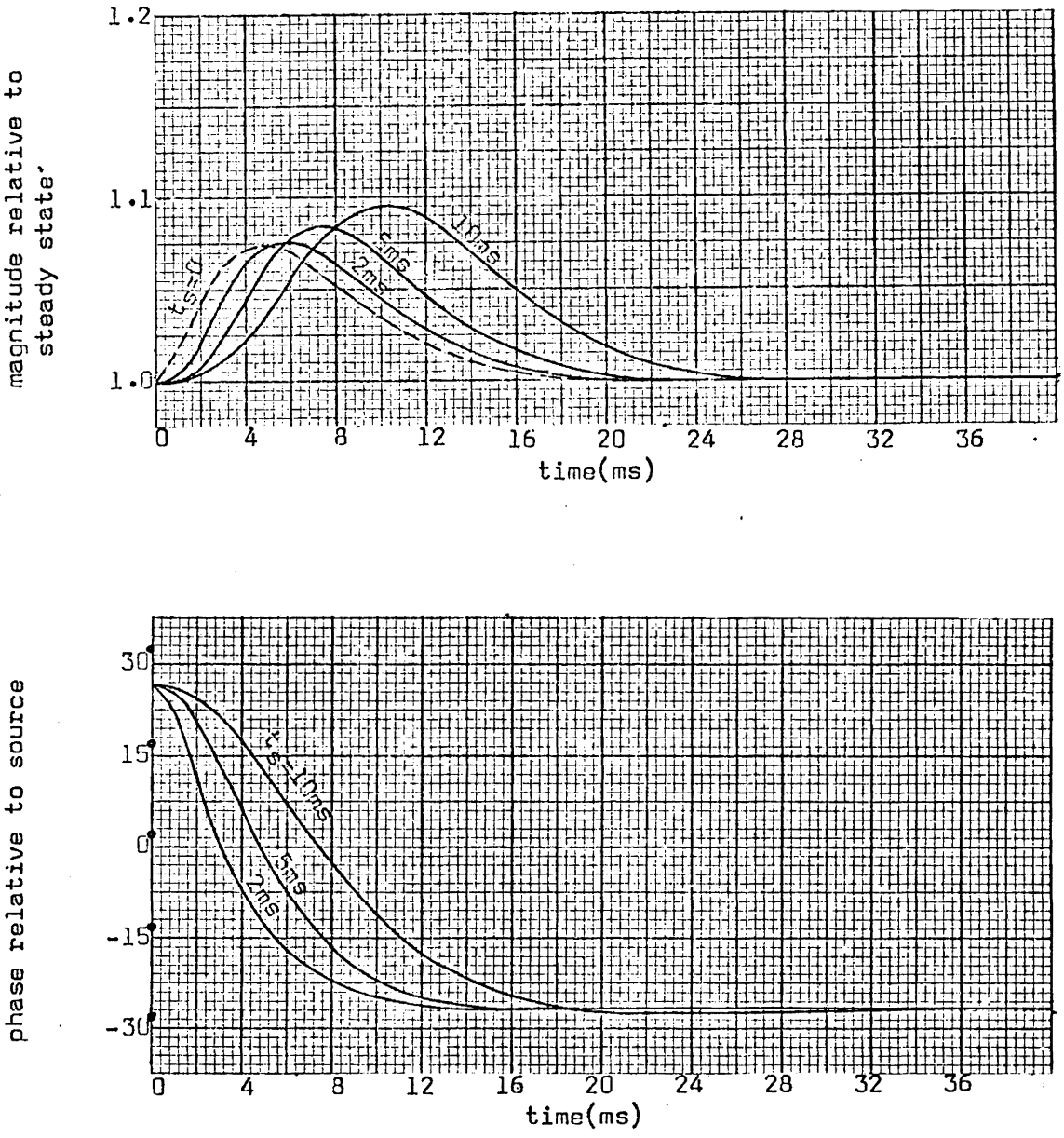

Figure 5.5. Response of series tuned circuit for Δf=25 hertz and circuit bandwidth of 100 hertz.

quasi-stationary peak response level are also included with each figure. These figures show that the peak response varies directly as t_s and inversely as circuit bandwidth. The relationship between the response of a high Q circuit excited by the FS-PLL (t_s = 5 ms) and the quasi-stationary response is illustrated by the curves of Figure 5.6, where the frequency transition corresponds to δ = 0.9 of Figure 3.7. Time varying values for the quasi-stationary response envelope are obtained by substituting values of time varying frequency in place of the constant frequency appearing in the steady state response given by (D.2). This example is a case where considerable error would result if the response were assumed to be either quasi-stationary or that of a circuit excited by an instantaneous frequency shift (frequency step).

The transient response which is a direct consequence of a frequency shift is indicative of the inability of a circuit to adjust to the phase variations of its source. Conversely, if a circuit acquires its steady state phase immediately after the frequency shift, then there is no transient response. Figure 5.7 depicts the actual phase of the current relative to the quasi-stationary phase for several values of t_s. This figure illustrates the circuit's inability to follow the phase variations of its source, and it is apparent that the circuit is able to follow the slower frequency shifts, t_s large, much better than it can fast variations. Since the peak response

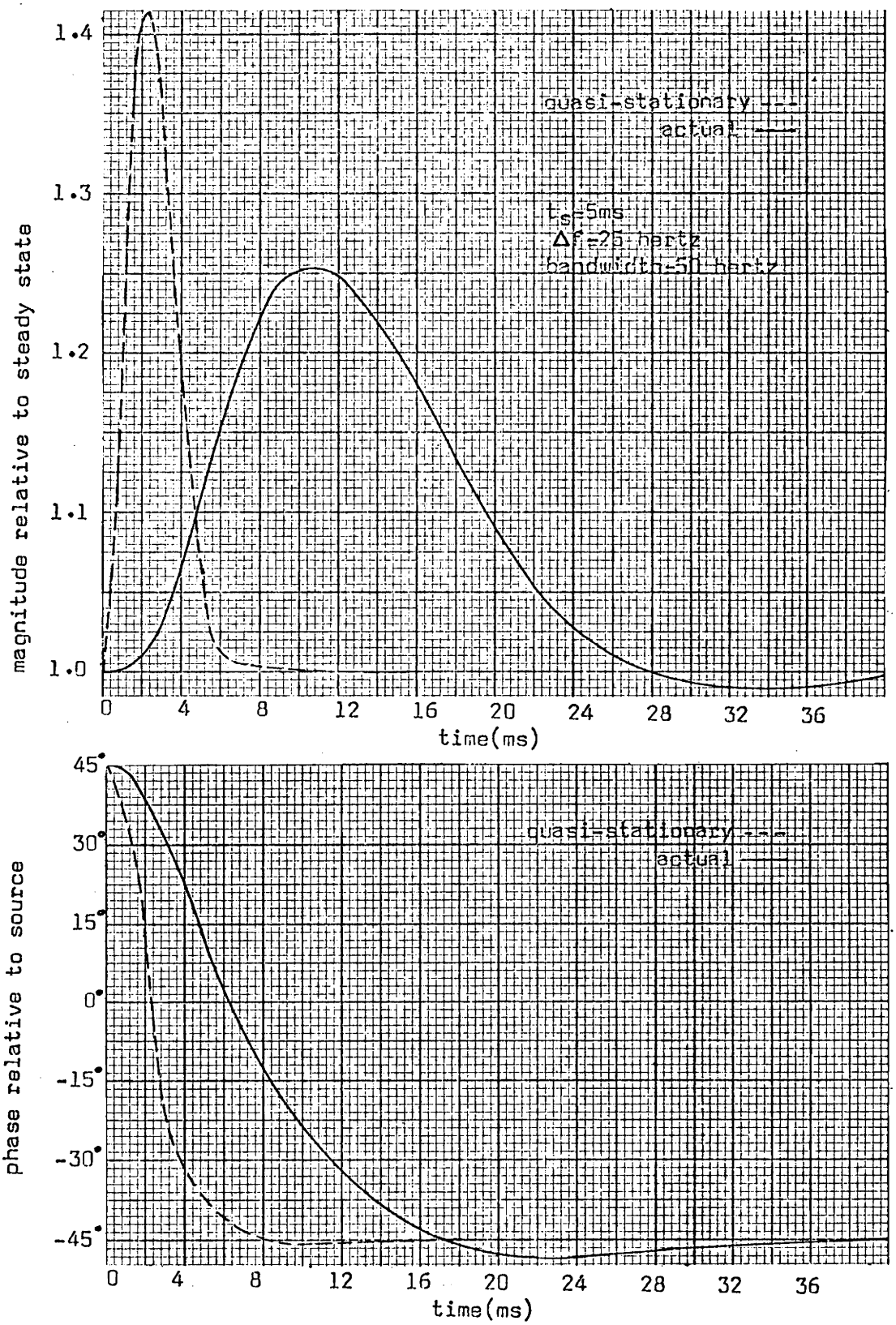

Figure 5.6. Comparison of quasi-stationary and actual response.

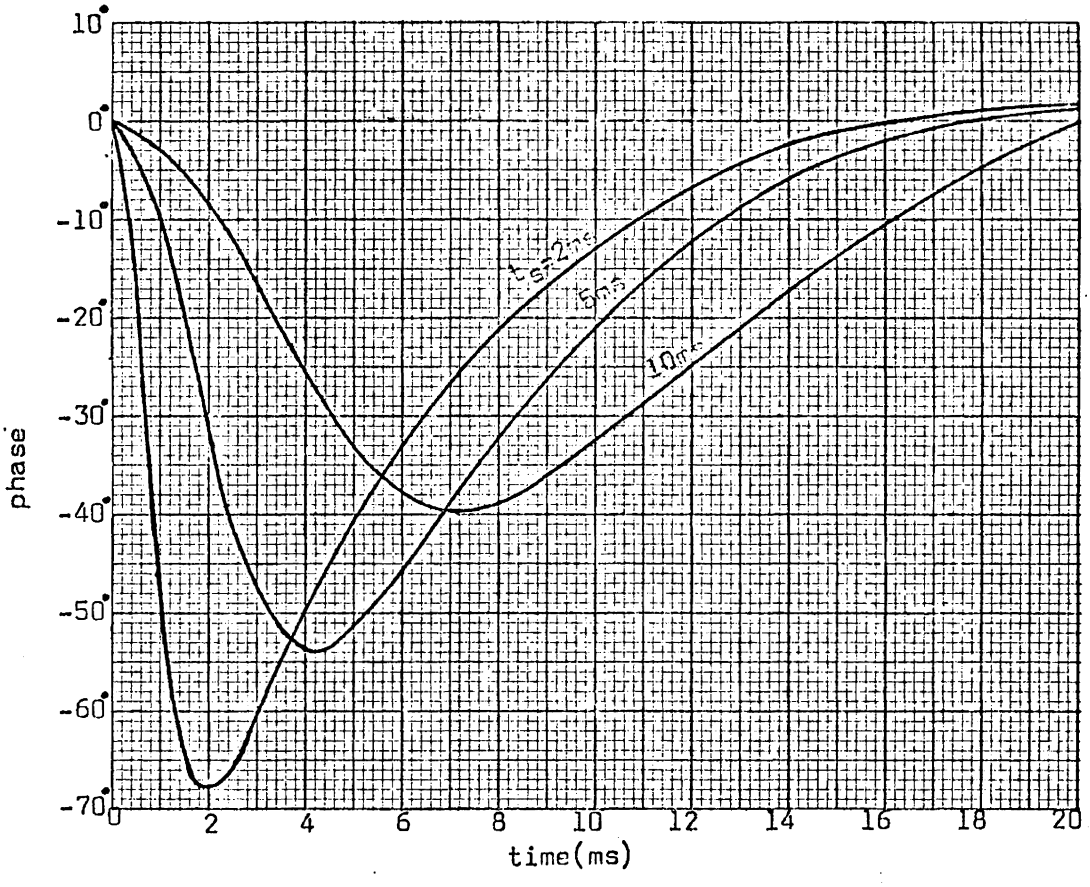

Figure 5.7 Series tuned circuit phase response relative to quasi-stationary phase for δ=0.9, ω_n/K=1.8, circuit bandwidth equal 50 hertz and Δf=25 hertz.

varies directly as t_s, the increase in the peak value over that of a frequency step must be due to a quasi-stationary effect rather than being a direct result of the frequency shift. That is, the circuit responds to the instantaneous frequency as the time varying frequency passes through the circuit's midband. This situation is quite pronounced in cases where the value of t_s is approximately equal to, or greater than, the circuit's time constant.

VI. EXPERIMENTAL INVESTIGATION

The experimental investigation is designed to verify the theory presented and to substantiate the analytical methods employed throughout the foregoing analyses. More specifically, this experiment is devised to provide experimental data on the phase and frequency variations of the FS-PLL, its frequency spectra and the tuned circuit response to the FS-PLL output. The experimental apparatus is described and the resulting data are compared with the analysis.

6.1 Description of the Experimental Apparatus

Operation of the experimental system is designed to simulate VLF-FSK communications conditions, where the FS-PLL is utilized as the frequency-shifted carrier source. The network load on the FS-PLL is the circuit equivalent of the VLF transmitting antenna. Figure 6.1 is a block diagram representation of the system.

Frequency Synthesizer. In order to conduct the experimental investigation under the initial conditions and keying conditions prescribed in Sections 3.2 and 4.1, respectively, it is necessary that the frequencies f_1, f_2 and f maintain an exact relation to each other. This condition can be satisfied by synthesizing each frequency from a single stable source or reference, such as a crystal controlled oscillator.

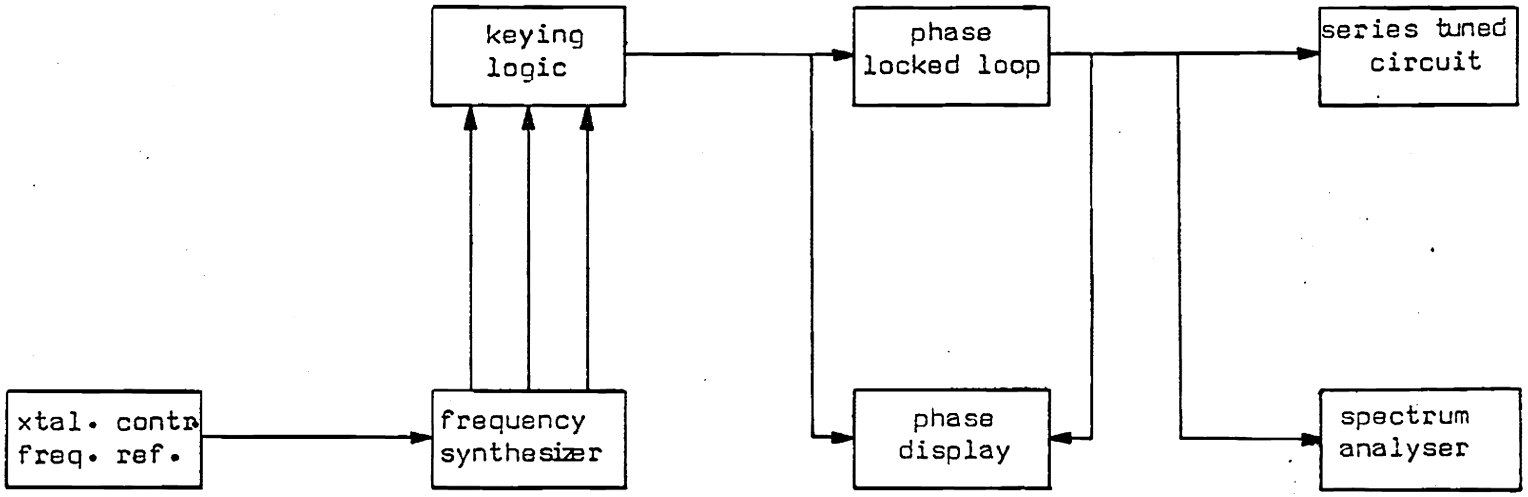

Figure 6.1. Block diagram of experimental system.

Techniques employed to generate the frequencies of interest are illustrated in Figure 6.2. The output of the VCO is mixed with the reference, producing a difference frequency, $5(f_2-f_1)$, which is compared in phase with an identical frequency that is obtained by reference frequency division. The output of the phase comparator is used to control the VCO. Hence, if the mixer output differs from $5(f_2-f_1)$, the phase comparator provides a signal to correct the VCO. Finally, the VCO output is divided to provide f_2. Frequency f_1 is obtained by direct division of the reference frequency. A square-wave keying signal of frequency f is available by division of the reference, or of the mixer output. It is interesting to note that the latter source of f always satisfies the keying condition which requires f to be a sub-multiple of (f_2-f_1), regardless of variations in the reference frequency.

Keying Logic. The output signals from the synthesizer, with frequencies f_1 and f_2, are in the form of rectangular waves. It is necessary to determine the instant in time when these two signals are phase coincident. Differentiation of each rectangular wave produces one very narrow positive pulse per cycle. The pulses associated with each signal are chosen as the zero phase references. When a pulse from each signal arrives at the coincidence detector simultaneously, a coincidence output pulse is produced by the detector. Operation of the keying logic and the corresponding waveforms are depicted in Figures 6.3 and 6.4, respectively.

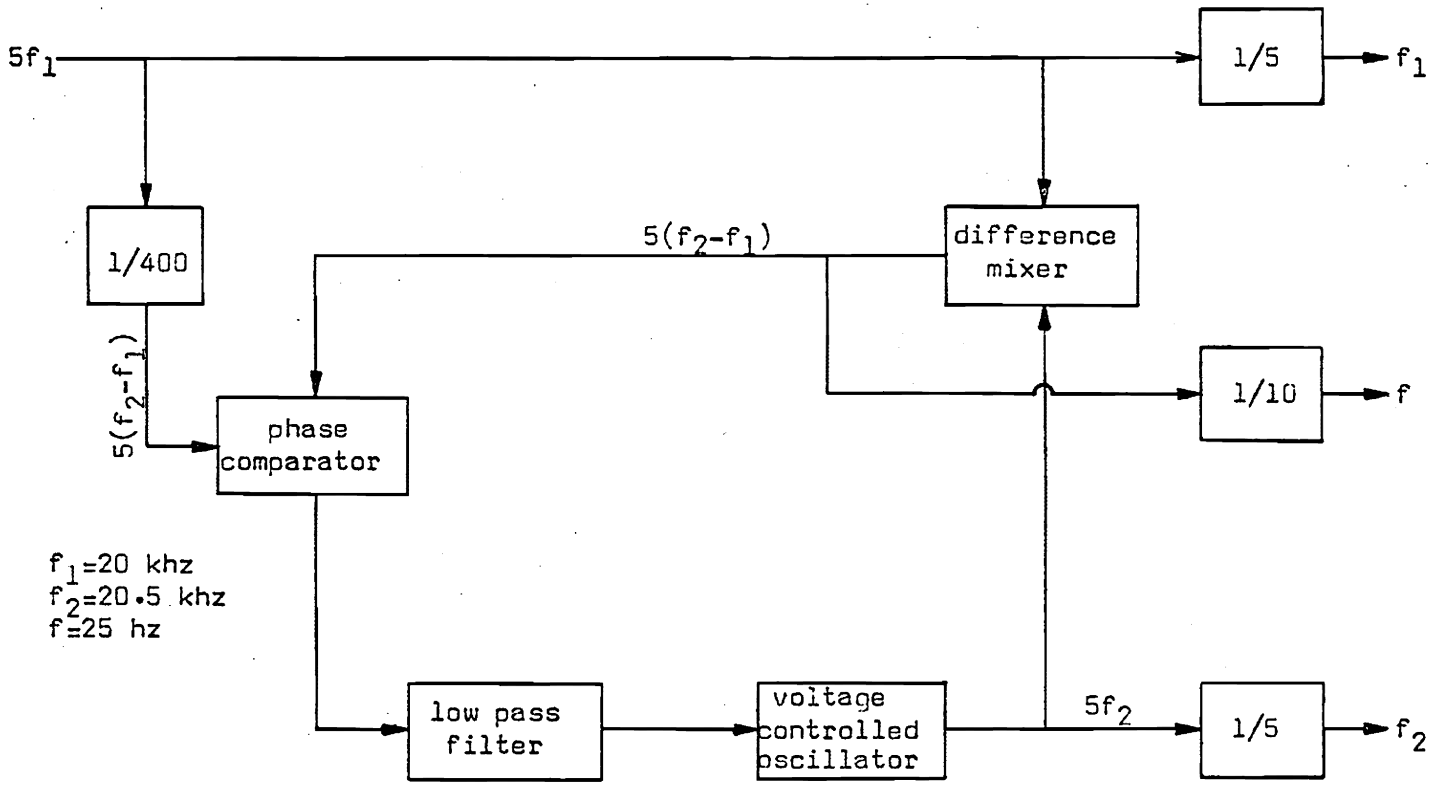

Figure 6.2. Frequency synthesizer

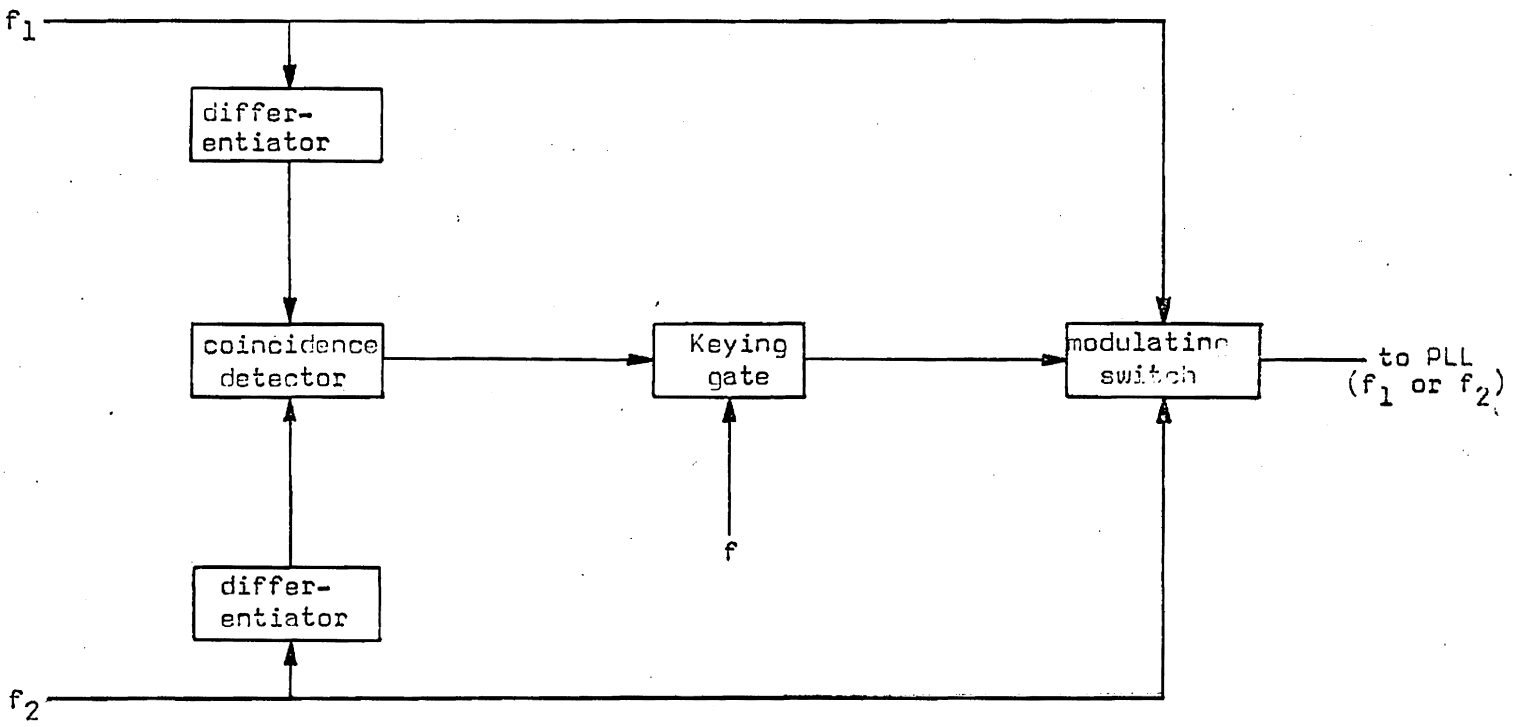

Figure 6.3. Keying logic.

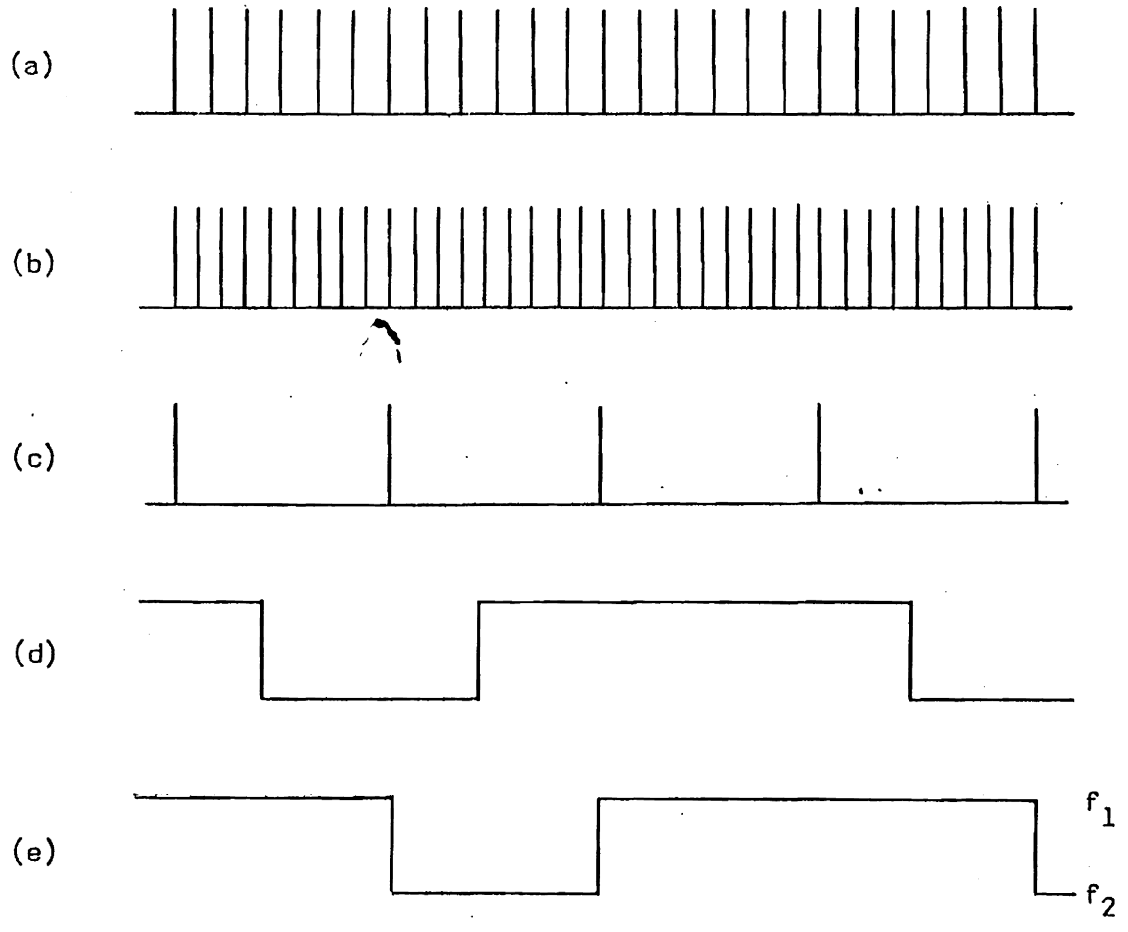

Figure 6.4. Keying logic waveforms, (a) frequency f_1, (b) frequency f_2, (c) coincidence detector output, (d) keying waveform and (e) frequency out of modulating switch.

The presence of a coincidence pulse indicates that the necessary phase conditions exist for a frequency shift to take place. Whether a shift occurs or not depends on the keying signal. The keying gate is operated by the keying signal (such as a teletype code signal), and the gate passes a coincidence pulse each time a frequency shift is called for by the keying code. Passage of a coincidence pulse by the keying gate actuates the modulation switch. The switch selects f_1 or f_2, and for all practical purposes it operates instantaneously.

Phase-locked-loop. A functional description of the PLL is given in Section 3.1. Figure 6.5 gives a block diagram representation of the particular PLL employed in this experiment. The PLL reference signal is obtained from the output of the modulation switch. A broadband dc amplifier is included in the loop to provide additional loop gain, and also a means of varying the gain. Further control over the loop's operation is made available through the down-break frequency, ω_a, of the loop filter. The up-break frequency, ω_b, is placed at infinity ($R_2 = 0$ in Figure 3.3).

Voltage control of the PLL's oscillator is made possible by utilizing voltage-variable capacitors in parallel with the oscillator tank circuit [42]. The VCO transfer characteristics are shown in Figure 6.6.

Narrowband Series Tuned Circuit. In order to simulate a VLF transmitting antenna, it is necessary to construct a RLC series circuit having a very high Q inductor (antenna Q's range from 200 to 400

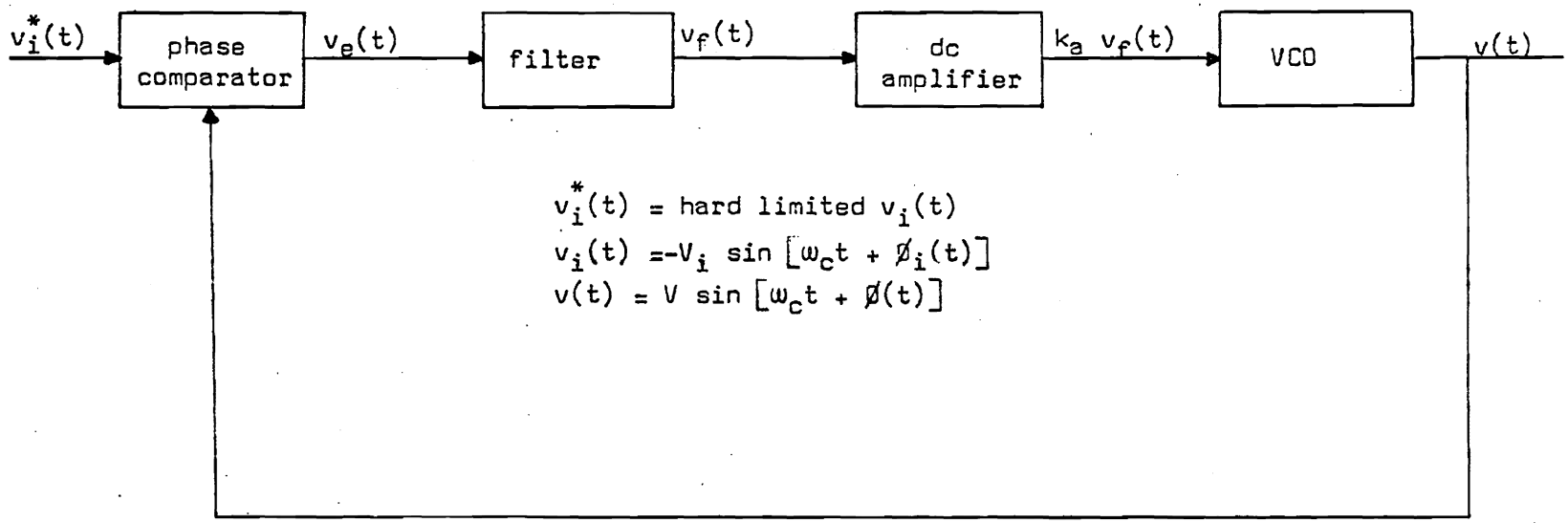

Figure 6.5. Experimental phase-locked-loop.

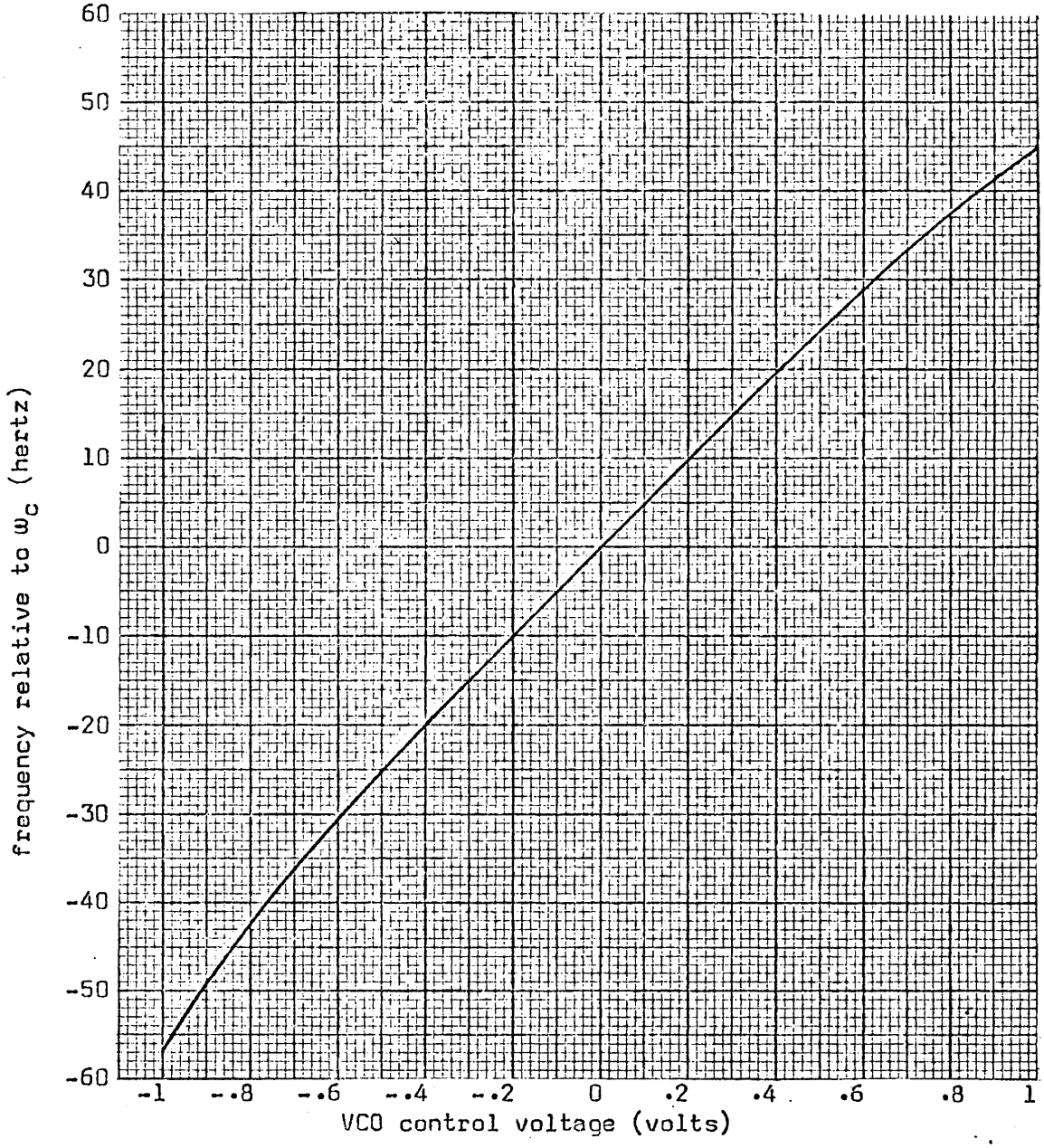

Figure 6.6. Experimentally determined VCO transfer characteristics.

at 20khz). The necessary inductor Q is obtained by winding 172 turns of litz wire (125 strands of no. 30 copper wire) on an air core form measuring 30 inches in height by 20 inches in diameter. This coil configuration provides an inductance of 7.9 milli-henrys with a maximum Q of 445 at 20khz. The schematic of the equivalent antenna and the frequency response of the circuit are shown in Figure 6.7. Adjustment of the circuit Q is accomplished by changing the value of the series resistor, R_c.

The output of the modulation switch acts as the PLL reference signal and in turn the PLL provides a frequency shifted source for the tuned circuit. The tuned circuit analysis assumed an ideal voltage source which was approximated with the aid of a low output impedance amplifier. It was experimentally verified that the amplifier frequency response was flat over the signal bandwidth, and that the amplifier output resistance was approximately 0.1 ohm.

6.2 Measurement of Time Varying Phase and Frequency

Throughout this investigation, the time varying frequency of the PLL output has been of primary concern. Experimentally, it was necessary to obtain accurate data on the frequency transition, to substantiate the theoretical predictions. Normal discriminator techniques used in frequency demodulation are limited in their ability to detect narrowband frequency variations at very low frequencies. The problem is that of the inherent low frequency response of a

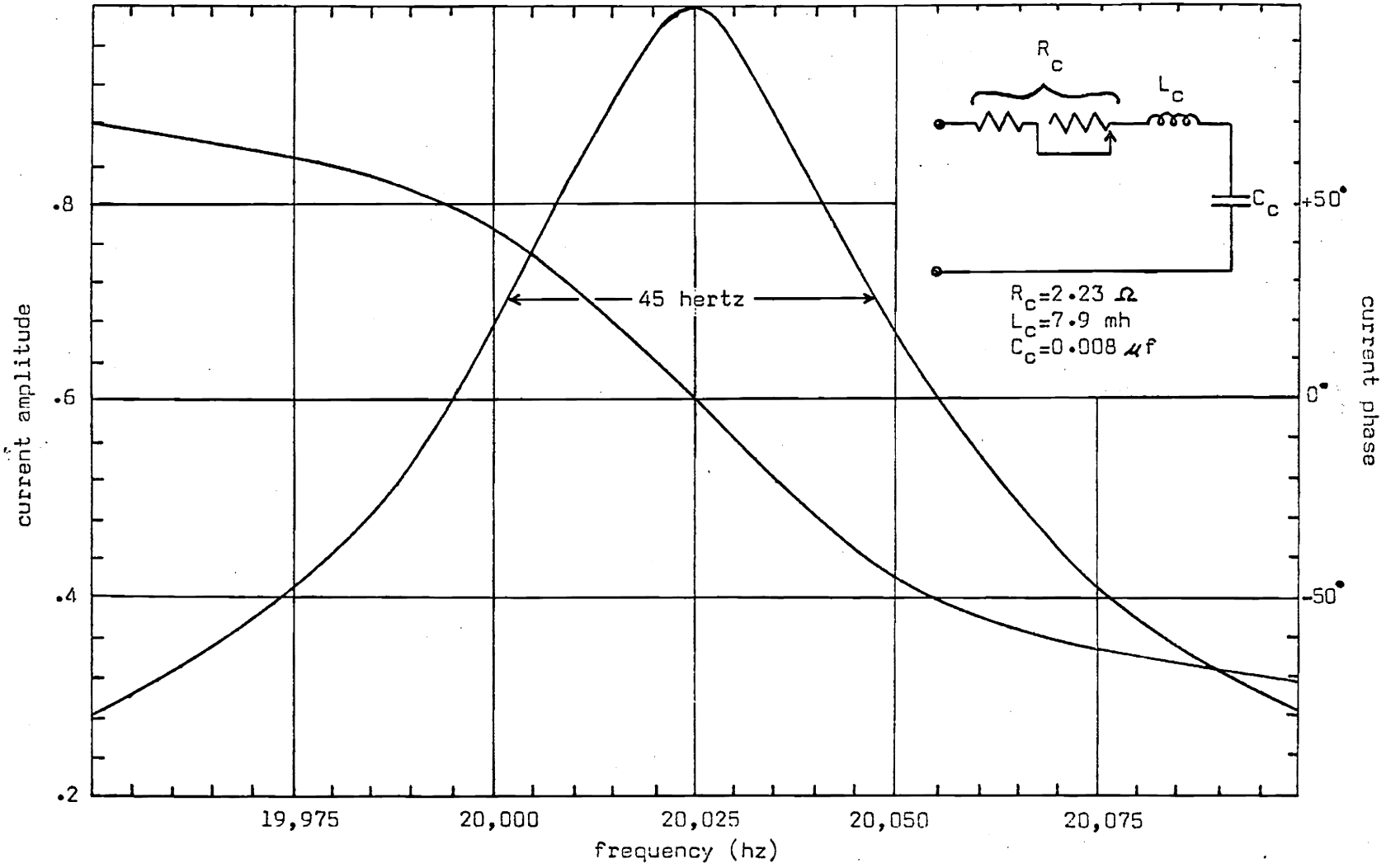

Figure 6.7. Response of experimental RLC series tuned circuit corresponding to minimum circuit bandwidth, where the response data is plotted relative to the source voltage.

narrowband discriminator. The response problem can be solved, somewhat indirectly, by means of an intensity modulated oscilloscope technique. This technique detects the change in phase of one signal relative to a second. But frequency is the time rate of change of phase; hence, frequency information is indirectly available by taking a time derivative. The disadvantage here lies in the fact that the phase changes might be too small to yield accurate measurement, while the rate of change of phase might be quite large.

The intensity modulated oscilloscope phase discriminator operation is illustrated pictorially by Figure 6.8. With application to measurement of the PLL's output time varying phase, operation is described as follows. The PLL reference signal, which is in the form of a rectangular wave, is differentiated and the resulting negative (or positive, depending on the oscilloscope) pulses are amplified and applied to the oscilloscope's Z axis. From Equation (3.3), the PLL's reference signal is given by

$$v_i(t) = - V_i \sin (\omega_2 t)$$

where $\omega_2 = \omega_c + \Delta\omega$ for a positive frequency step. Letting the pulses occur once each cycle at

$$\omega_2 t = 0, 2\pi, 4\pi, \quad \cdots \quad \ell(2\pi) , \tag{6.1}$$

the reference becomes

$$v_i(\ell T_2) = - V_i \sin (\ell 2\pi) , \tag{6.2}$$

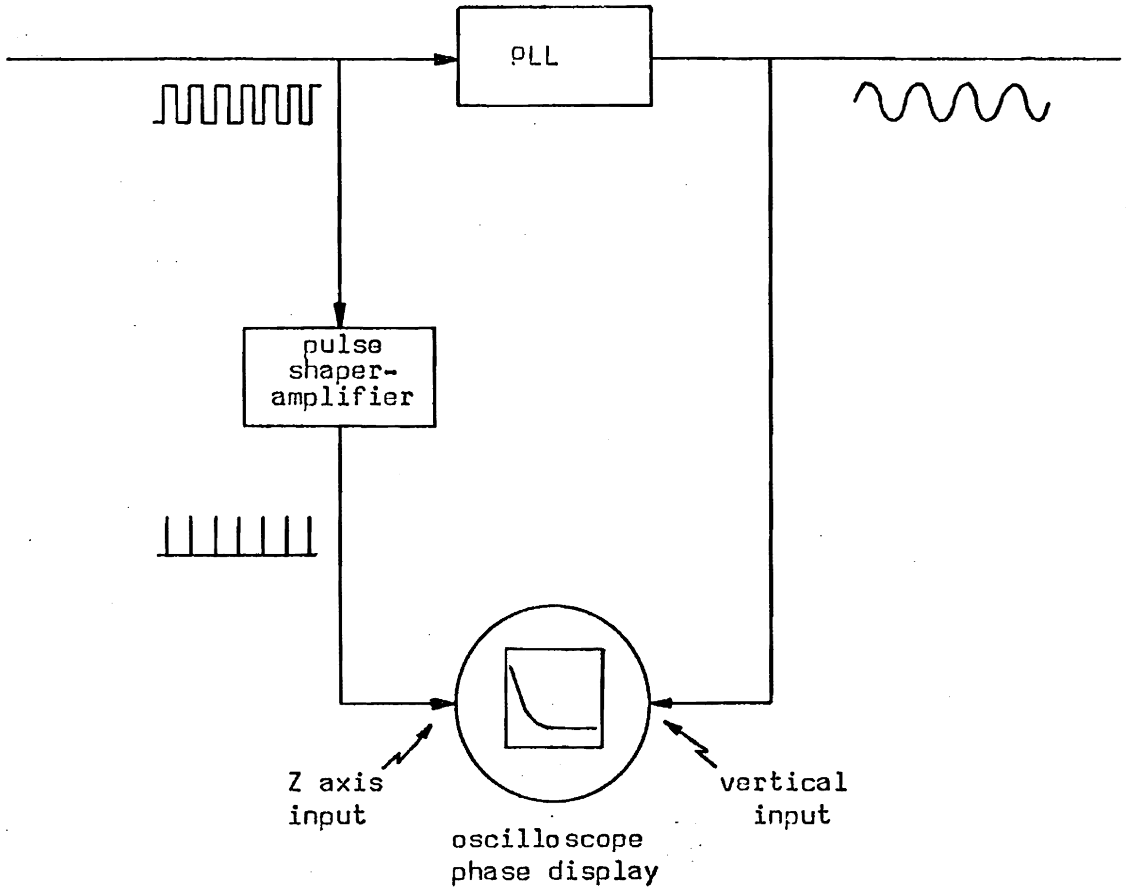

Figure 6.8. Block Diagram of phase discriminator.

where $T_2 = 1/f_2$. Observing the intensity modulated PLL output on the oscilloscope screen, an intensity dot profile is seen. From (3.4), (3.5) and (6.1), the dots occur at

$$v(\ell T_2) = V \sin \left[(\ell 2\pi) - \phi_e(\ell T_2) \right] . \tag{6.3}$$

Comparison of the arguments of (6.2) and (6.3) shows that the dot profile differs from the signal's $\ell(2\pi)$ phase position by the negative of the phase error, $\phi_e(t)$. A typical dot profile representing a PLL frequency shift is shown in Figure 6.9, as it would appear superimposed on the envelope of a sinusoidal output signal.

Assuming that the signal observed on the oscilloscope screen is near sinusoidal over that portion of the cycle which involves phase measurement, the phase error can be evaluated by

$$- \phi_e(\ell T_2) = \arcsin \left[v(\ell T_2)/V \right] . \tag{6.4}$$

Since data resulting from (6.4) provide the phase error, the time derivative yields the instantaneous frequency error. Taking the derivative of (3.5) the variation of frequency about the carrier (the modulation) is

$$\begin{aligned} \dot{\phi}(t) &= \dot{\phi}_i(t) - \dot{\phi}_e(t) \\ &= \frac{d}{dt} (\phi_i - \phi_e) . \end{aligned} \tag{6.5}$$

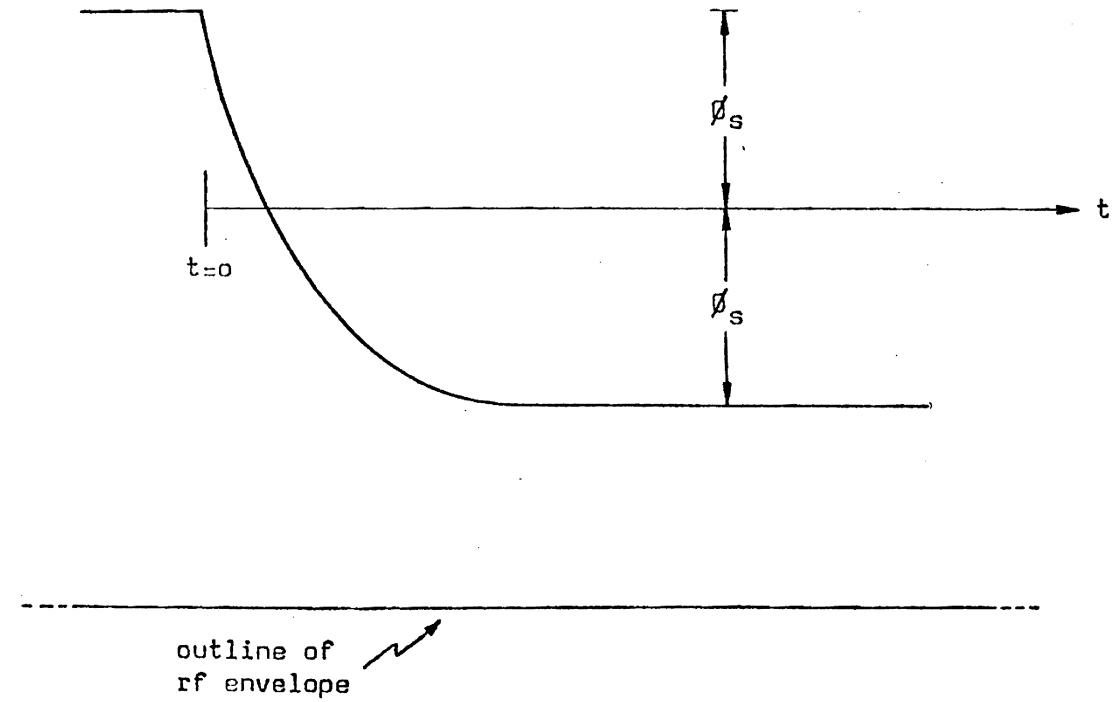

Figure 6.9. Phase-locked-loop output phase profile.

It is obvious that the measurement technique described above can also be employed to determine the phase characteristics of networks.

6.3 Experimental Data

Experimental apparatus and procedures have been discussed. Design of the PLL can be effected using the data in Figures 3.5 through 3.7 and relationships appearing in Section 3.2. Selecting a suitable frequency transition and value of t_s, the corresponding values of ω_n, δ and ω_n/K can be obtained from the figures. Equation (3.16) and Equation (3.19) give the filter break-frequencies. The loop employed in this experiment corresponds to $2\delta = \omega_n/K = 1.8$. Design calculations for three values of t_s appear in Table 6.1. The designs presented here are meant to aid in substantiating the theory, and are not intended as an attempt to optimize the FS-PLL.

Utilizing the design outlined above, data were taken to establish the validity of the analytical models and methods employed throughout the investigation. Photographs of representative dot profiles of the phase error, as given by (6.4), are presented in Figures 6.10, 6.11 and 6.12 for frequency transitions which are practically useful. The sinusoidal rf envelope of the FS-PLL output appears as the background, where the more intense curve is the dot profile of the phase error. Figures 6.13 through 6.21 include photographs of tuned circuit responses corresponding to the frequency transitions of the three preceding figures. The dot profile, as

	Case I	Case II	Case III
t_s(ms)	2	5	10
δ(1/rad)	0.9	0.9	0.9
ω_n(rad/sec)	1700	680	340
K(1/sec)	944	378	189
ω_n/K(rad)	1.8	1.8	1.8
ω_a(rad/sec)	3060	1222	611
ω_b(rad/sec)	∞	∞	∞
R_1(ohms)	32.7K	81.7K	163.4K
R_2(ohms)	0	0	0
C(farads)	10^{-8}	10^{-8}	10^{-8}

Table 6.1. Phase-locked-loop design calculations.

appearing in each of these photographs, is used to determine the zero time reference which is indicated by the sudden change of the dot profile slope. Finally, Figure 6.22 provides experimental data for the FS-PLL output spectra. This data was obtained by means of a spectrum analyzer, as indicated in Figure 6.1; and it corresponds to the frequency transitions displayed in Figures 6.10 through 6.12.

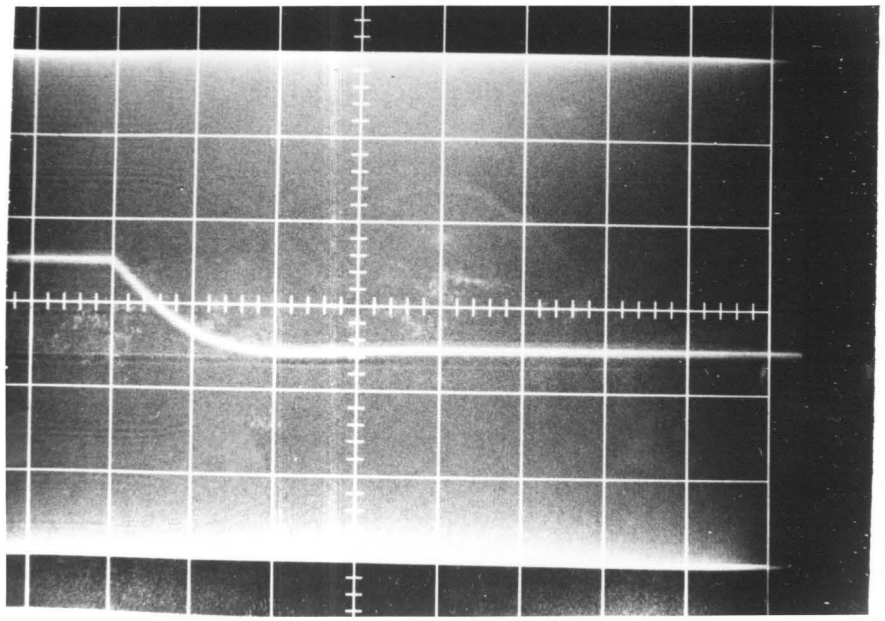

sweep ± 1ms/div

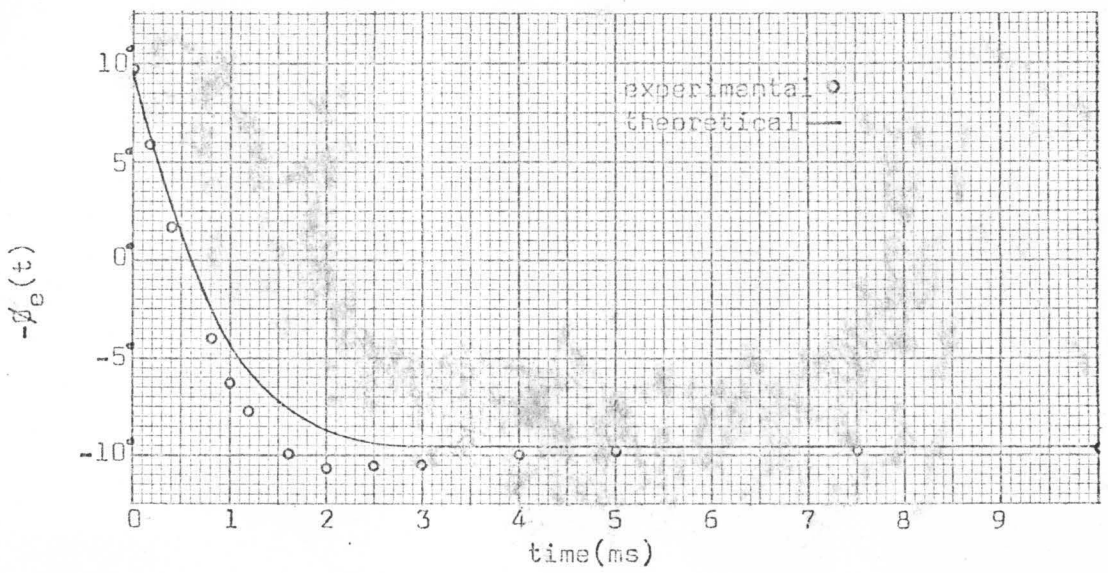

Figure 6.10. Dot profile corresponding to t_s=2ms and ω_n/K=1.8.

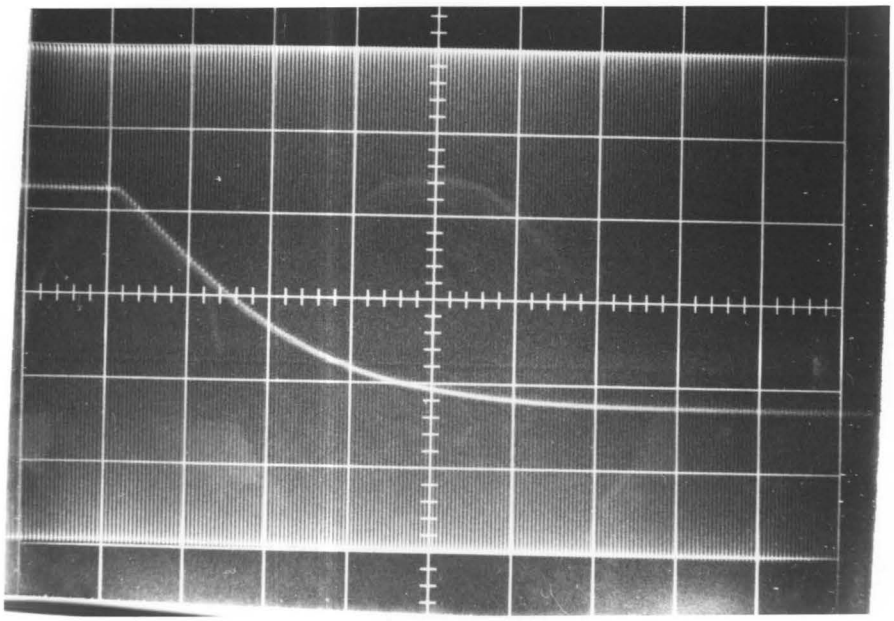

sweep = 1ms/div

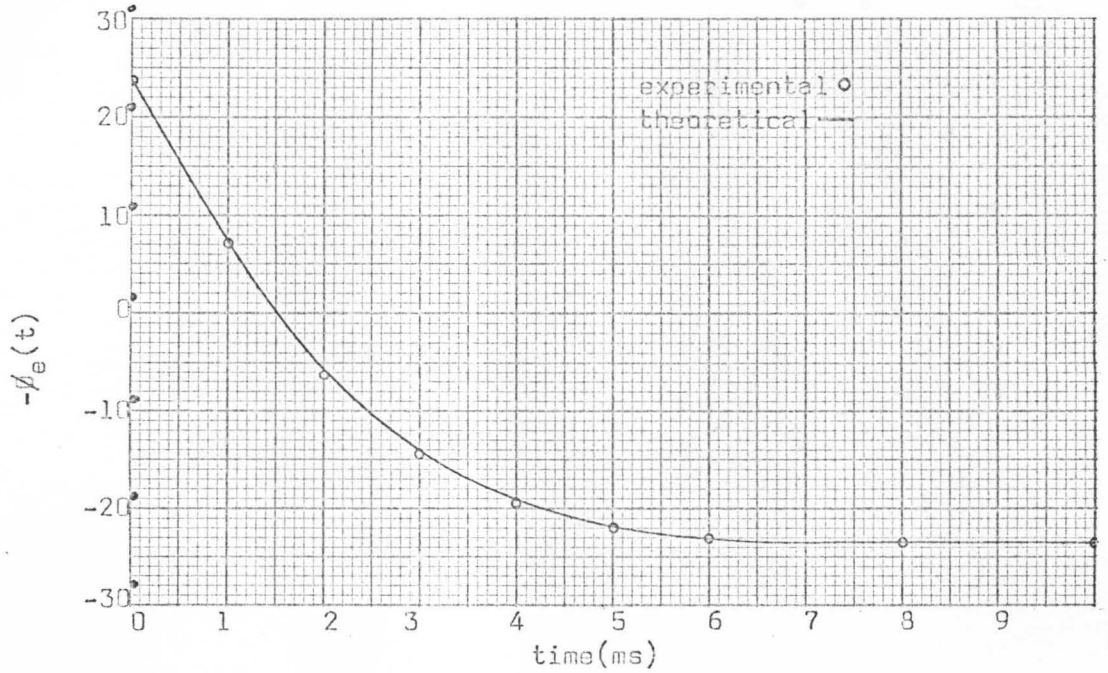

Figure 6.11. Dot profile corresponding to t_s=5ms and ω_n/K=1.8.

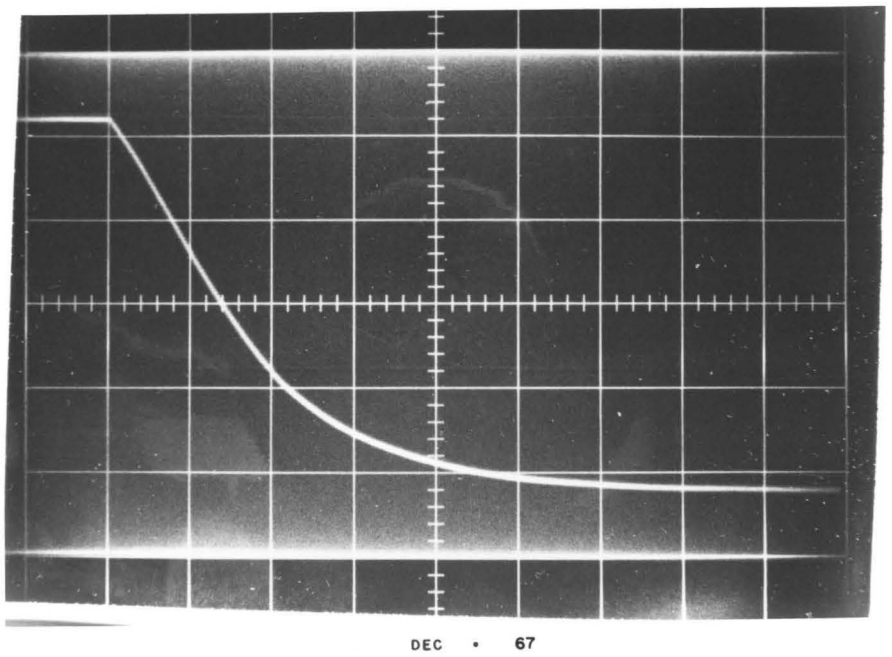

sweep = 2ms/div

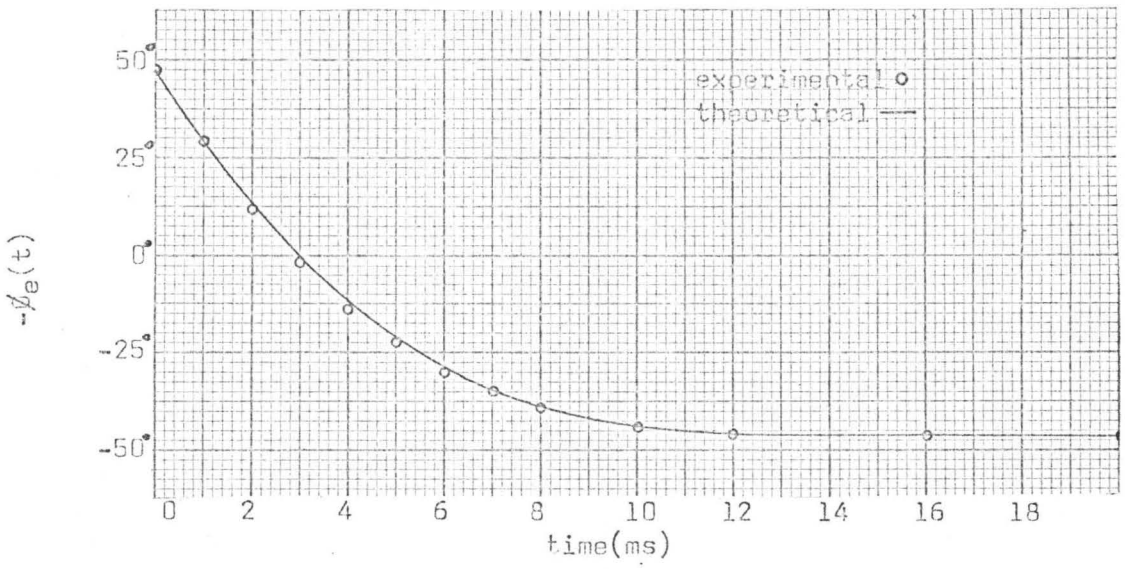

Figure 6.12. Dot profile corresponding to t_s=10ms and ω_n/K=1.8.

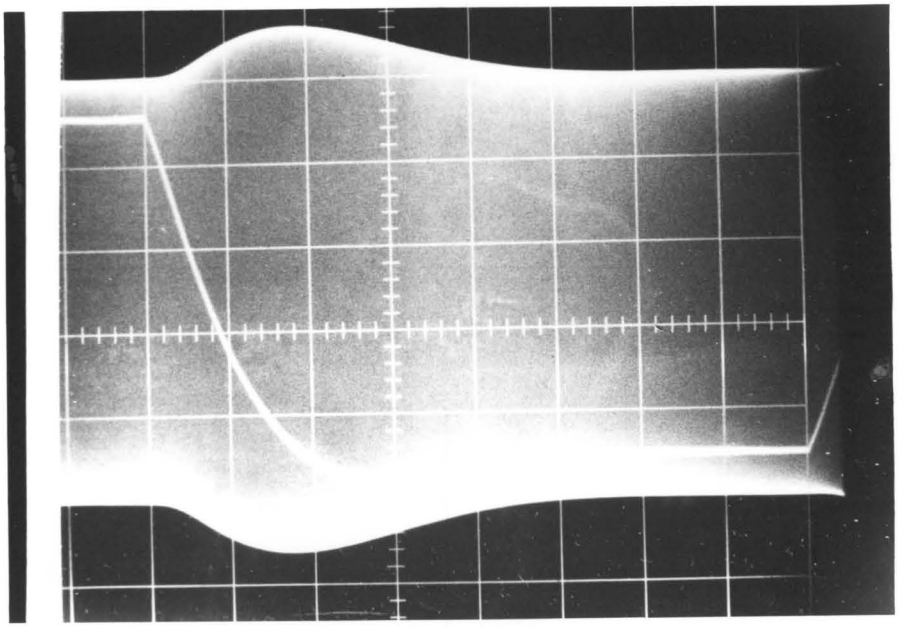

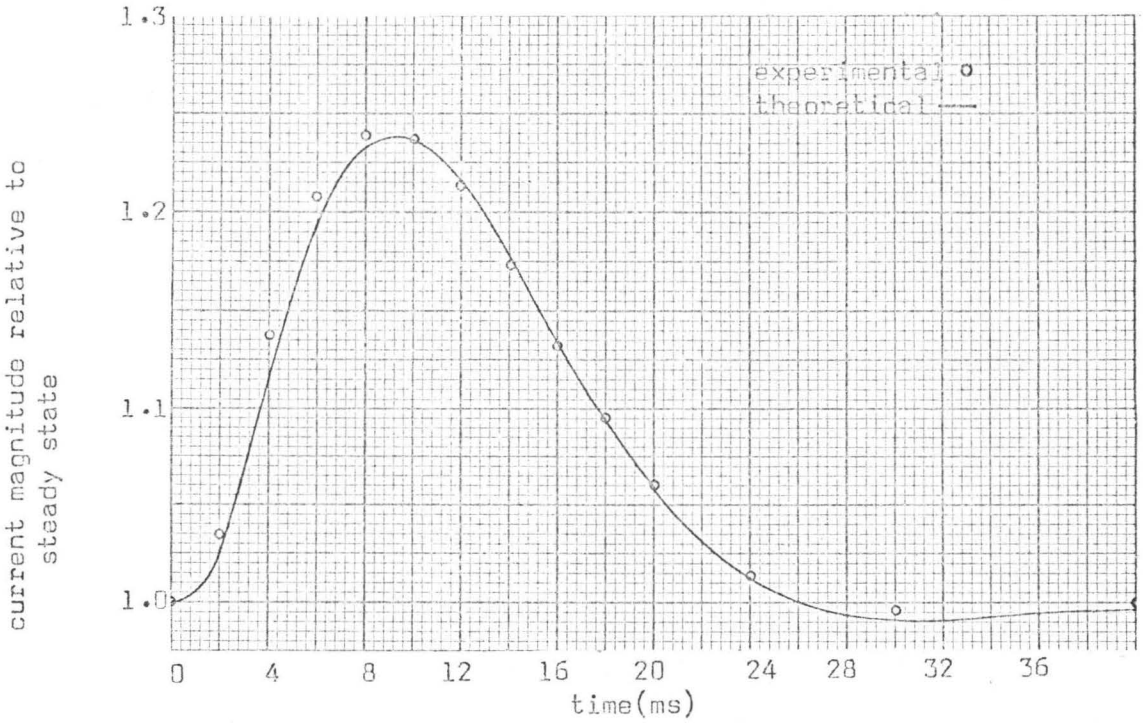

Figure 6.13. Magnitude response of series tuned circuit for Δf=25 hertz, t_s=2ms and circuit bandwidth of 50 hertz.

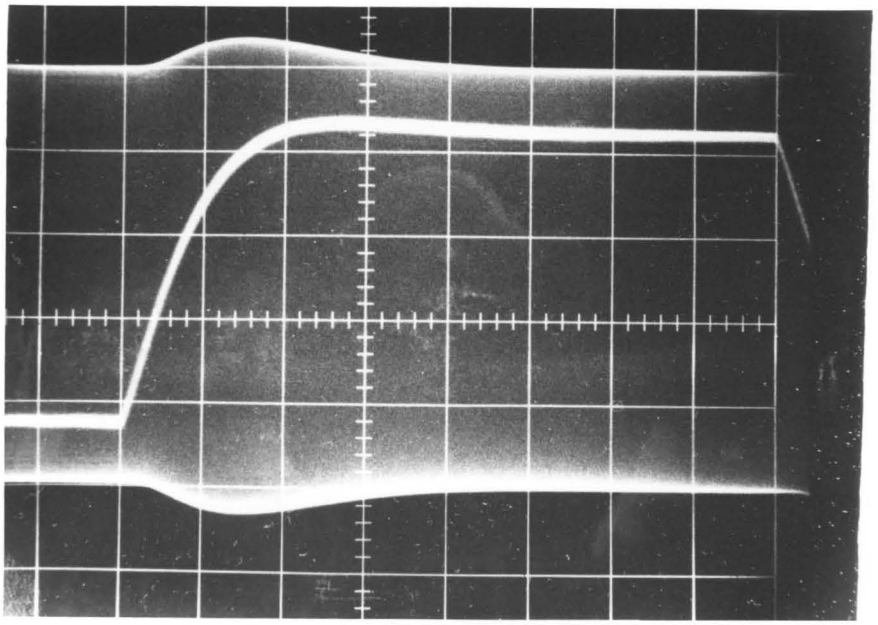

sweep = 5ms/div

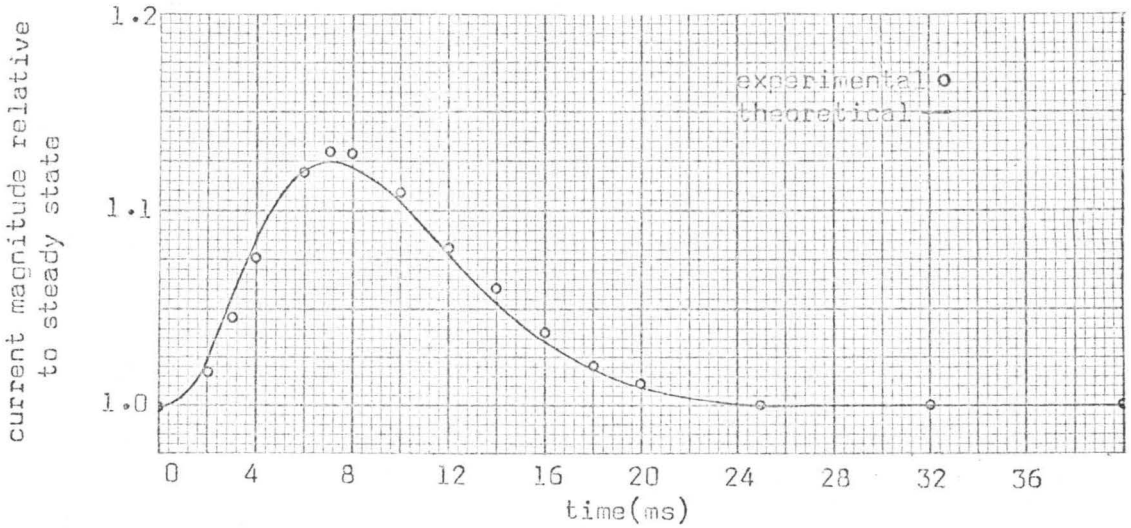

Figure 6.14. Magnitude response of series tuned circuit for Δf=25 hertz, t_s=2ms and circuit bandwidth of 75 hertz.

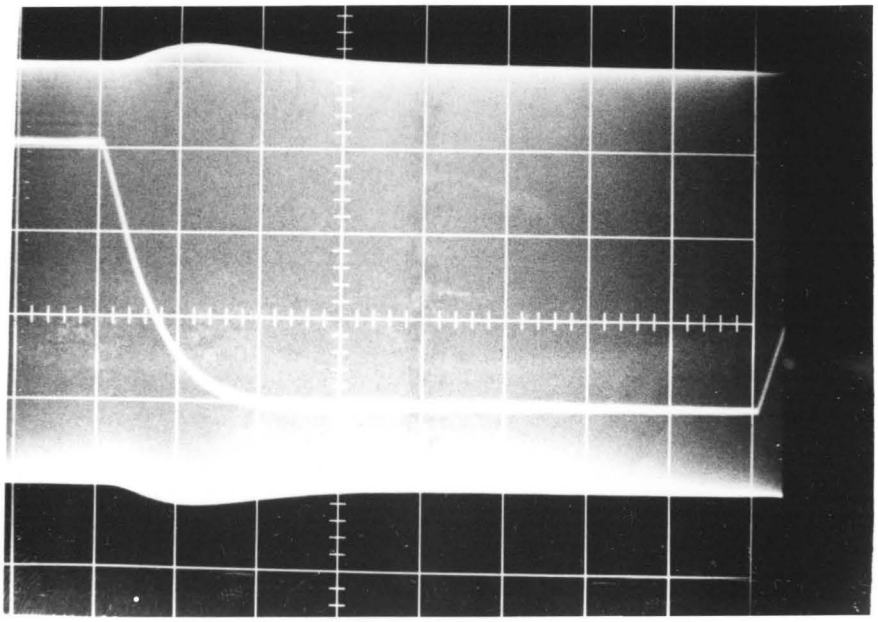

sweep = 5ms/div

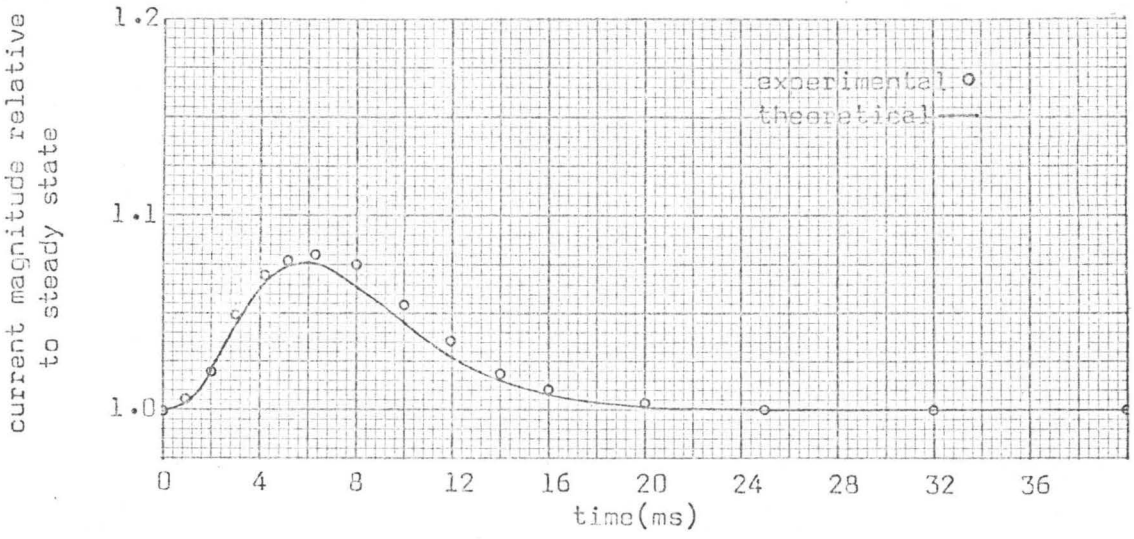

Figure 6.15. Magnitude response of series tuned circuit for Δf=25 hertz, t_s=2ms and circuit bandwidth of 100 hertz.

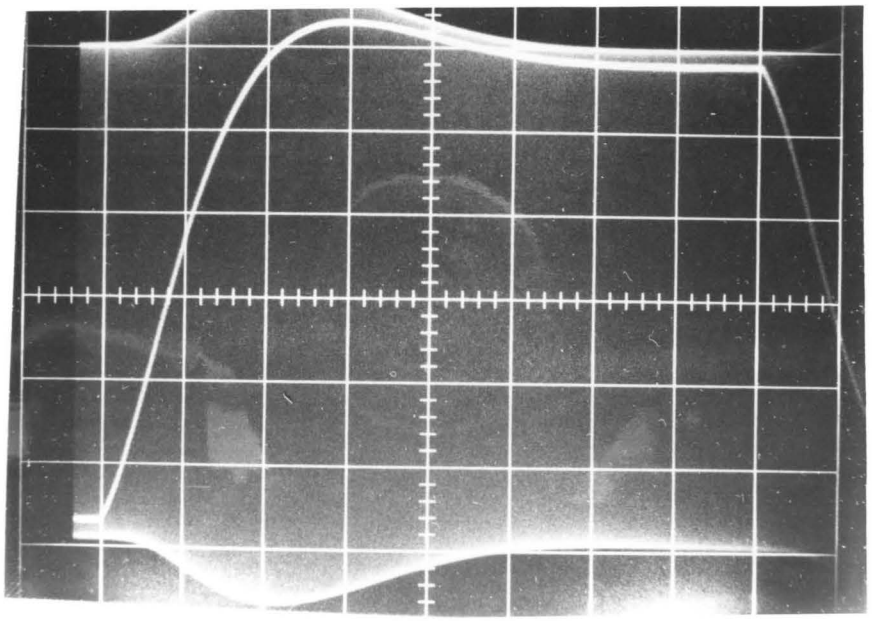

sweep = 5ms/div

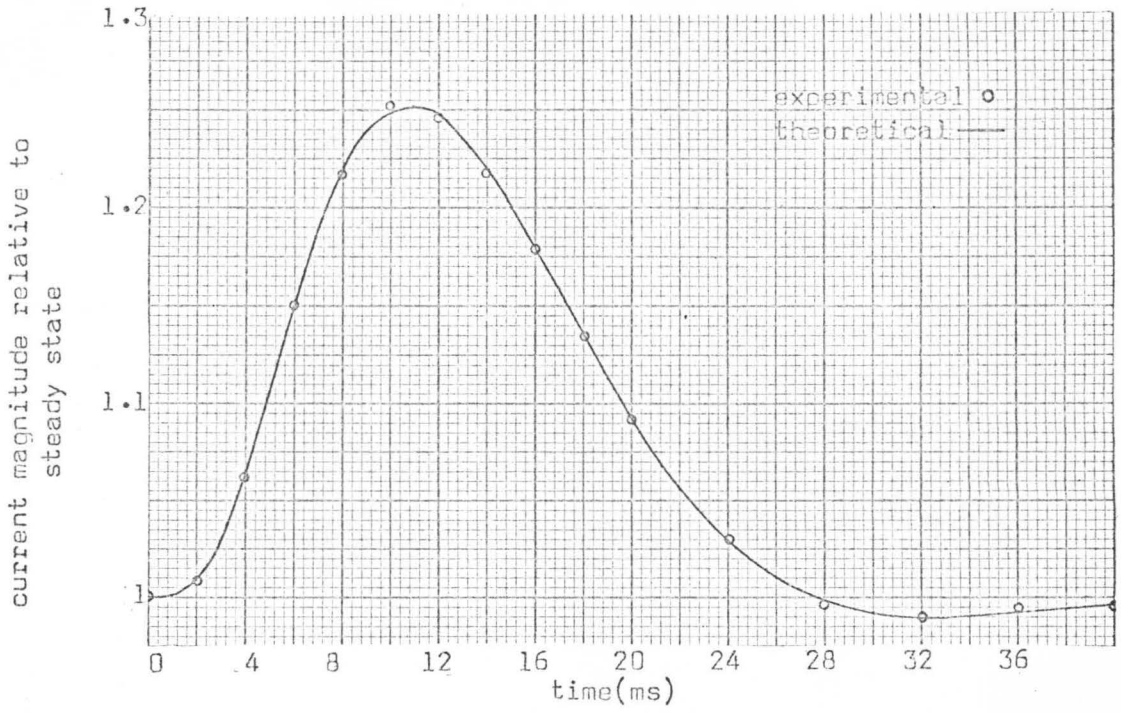

Figure 6.16. Magnitude response of series tuned circuit for Δf=25 hertz, t_s=5ms and circuit bandwidth of 50 hertz.

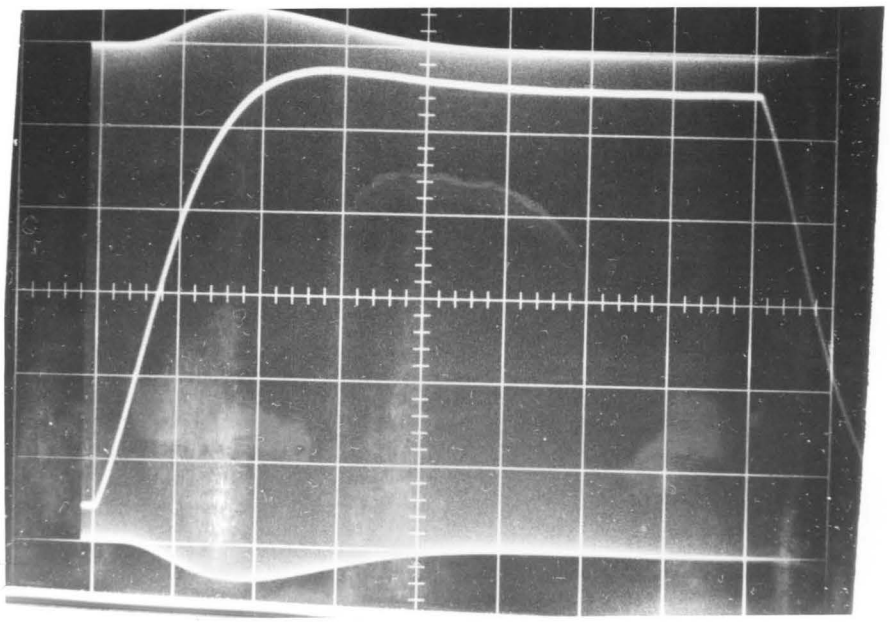

sweep = 5ms/div

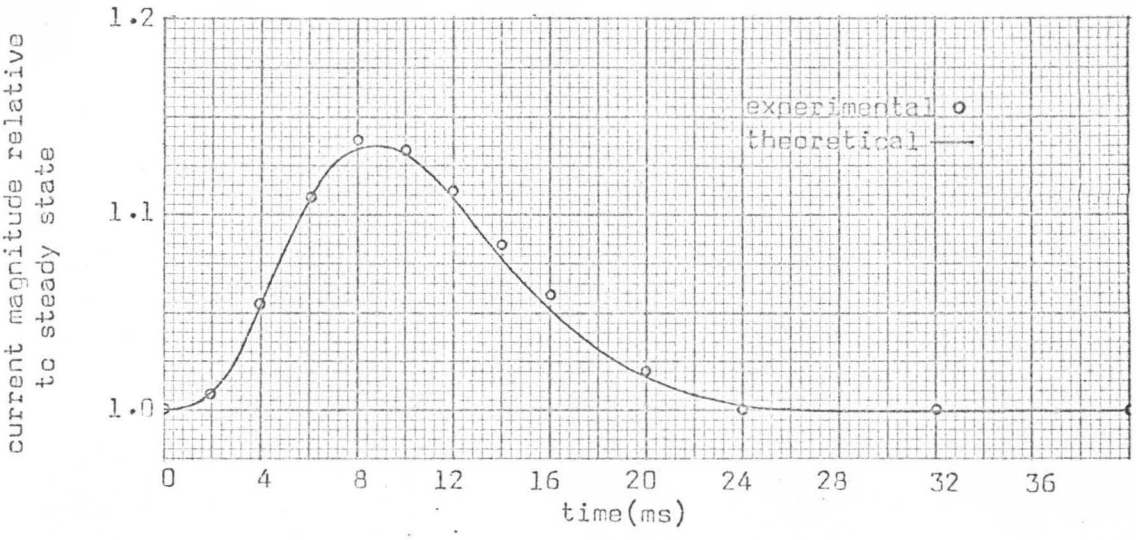

Figure 6.17. Magnitude response of series tuned circuit for Δf=25 hertz, t_s=5ms and circuit bandwidth of 75 hertz.

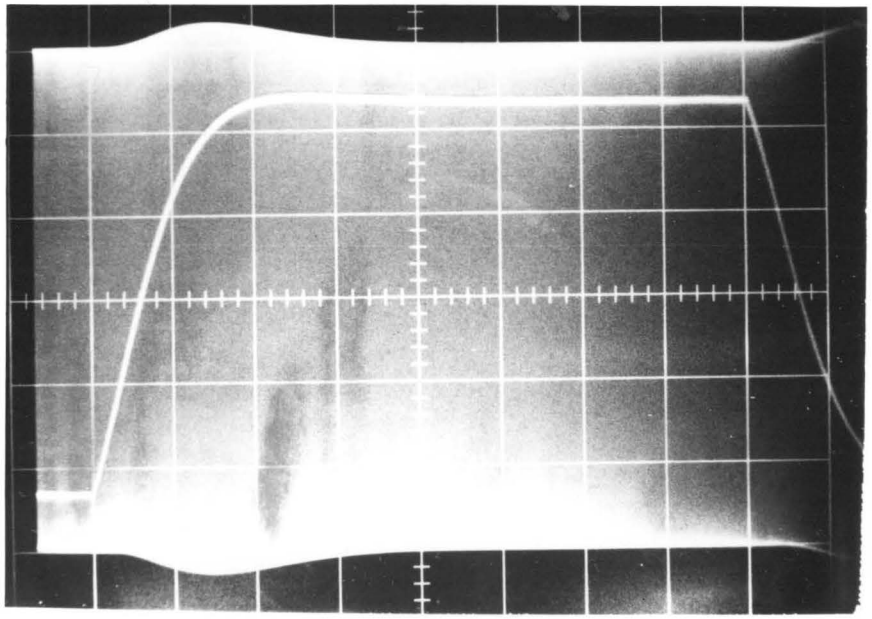

sweep = 5ms/div

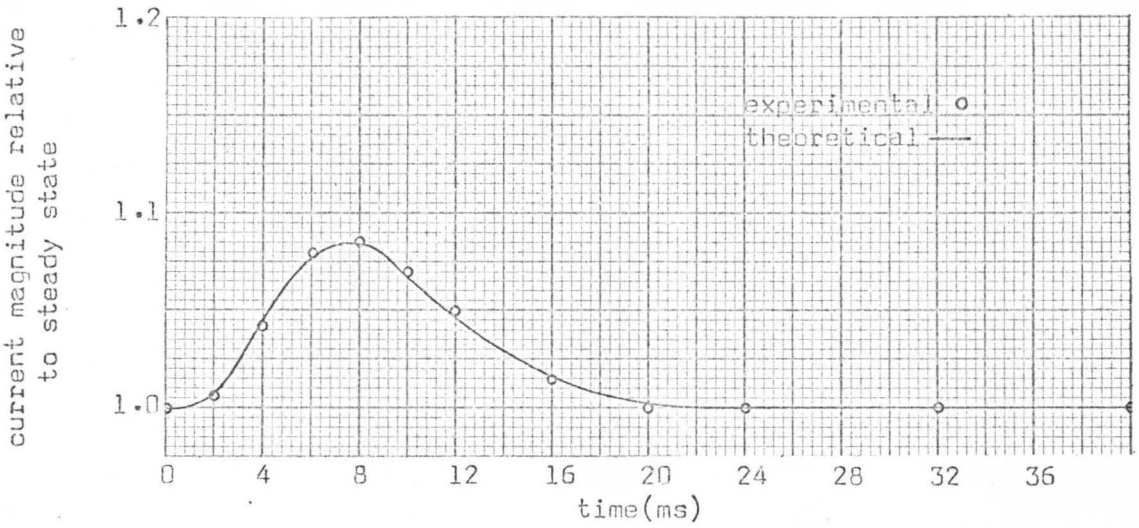

Figure 6.18. Magnitude response of series tuned circuit for Δf=25 hertz, t_s=5ms and circuit bandwidth of 100 hertz.

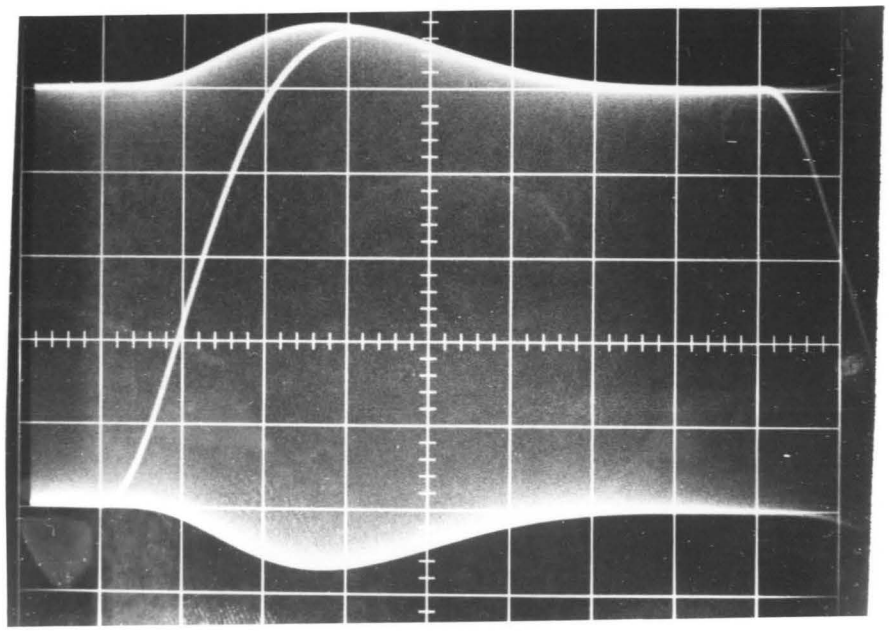

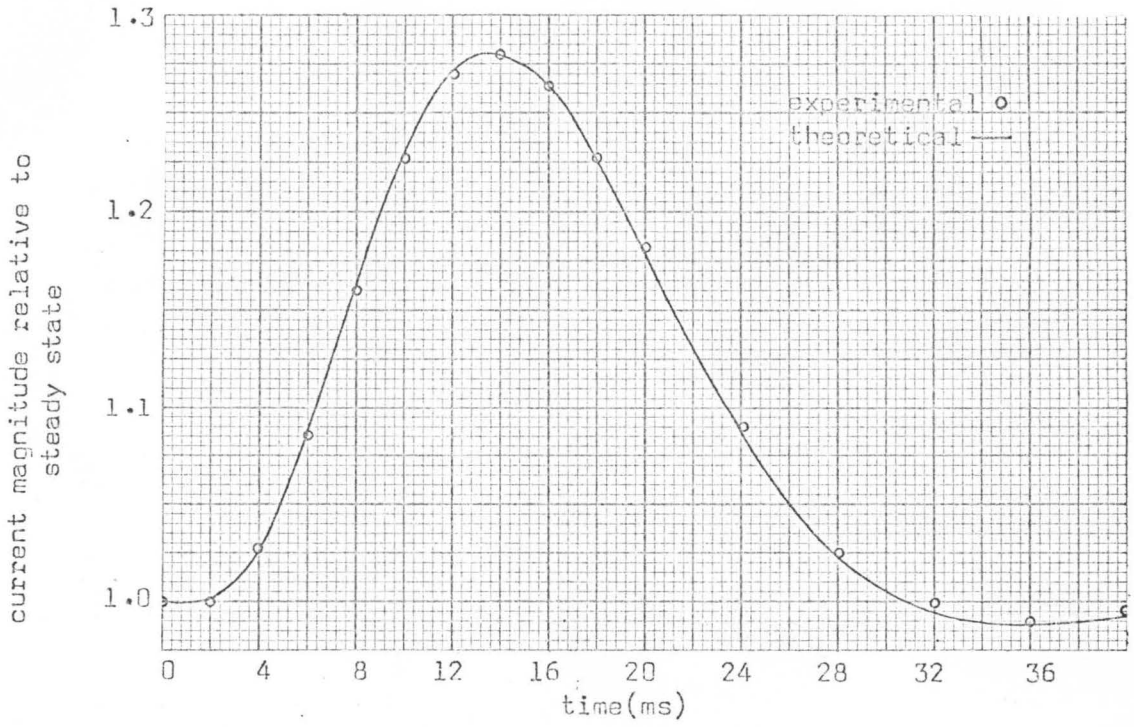

Figure 6.19. Magnitude response of series tuned circuit for Δf=25 hertz, t_s=10ms and circuit bandwidth of 50 hertz.

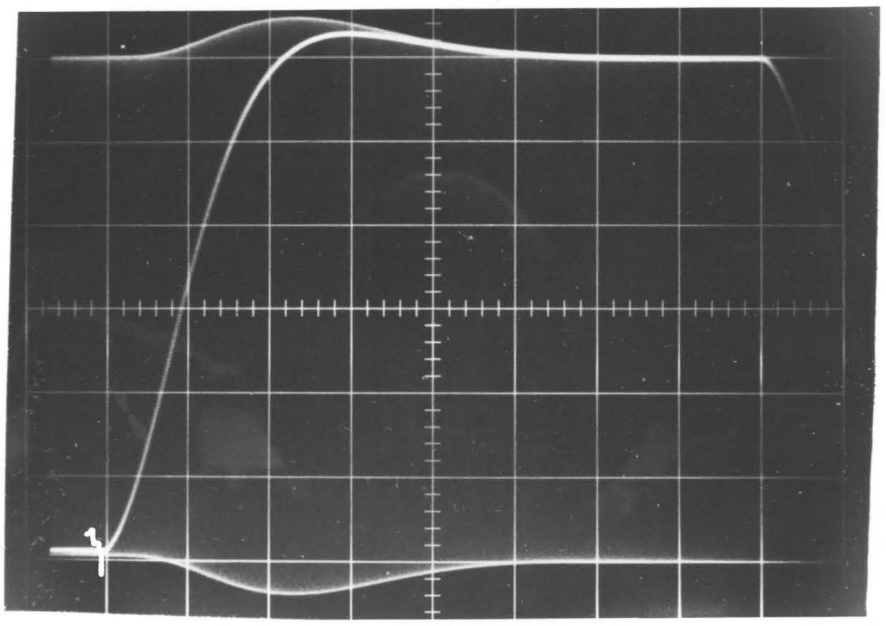

sweep = 5ms/div

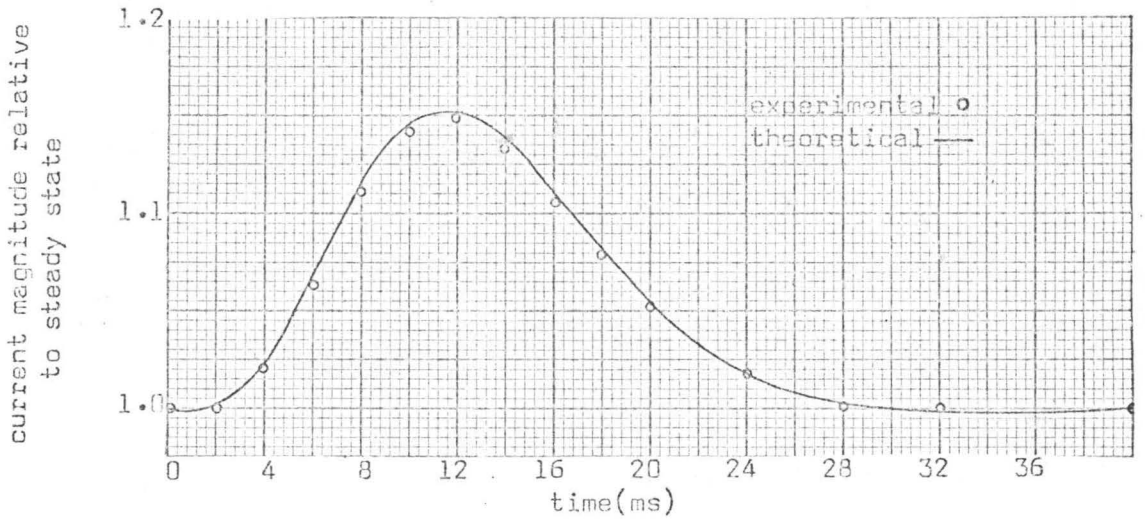

Figure 6.20. Magnitude response of series tuned circuit for Δf=25 hertz, t_s=10ms and circuit bandwidth of 75 hertz.

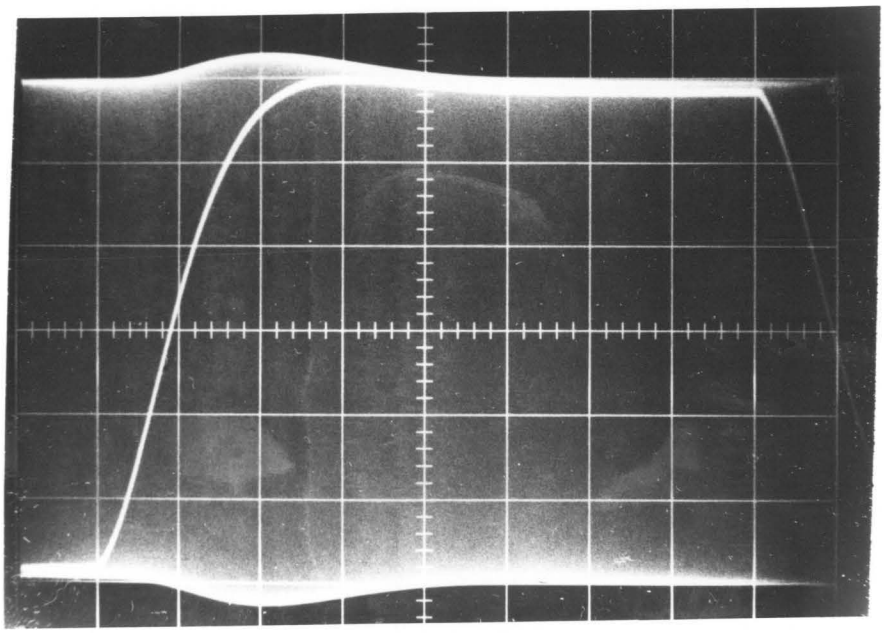

sweep = 5ms/div

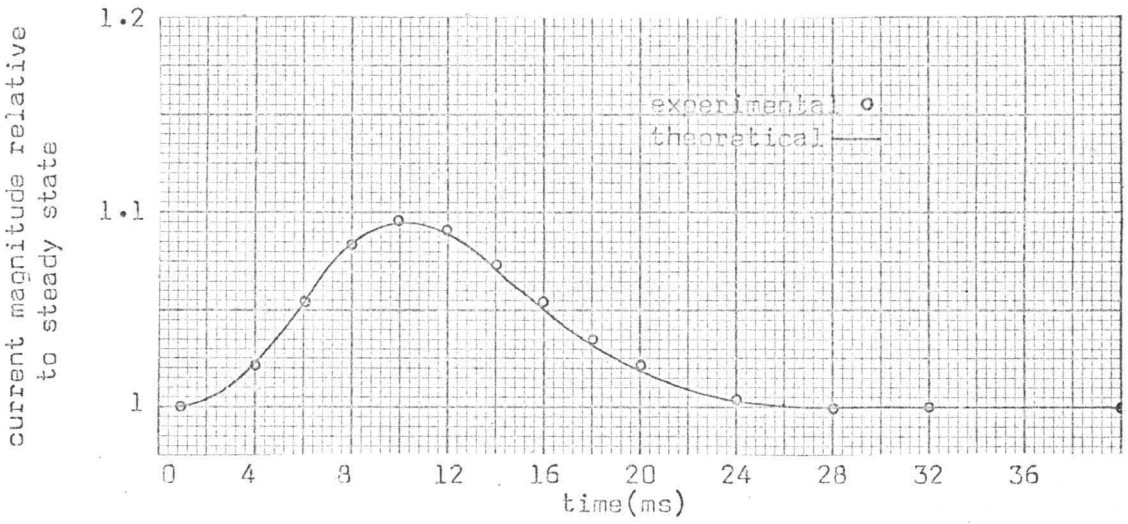

Figure 6.21. Magnitude response of series tuned circuit for Δf=25 hertz, t_s=10ms and circuit bandwidth of 100 hertz.

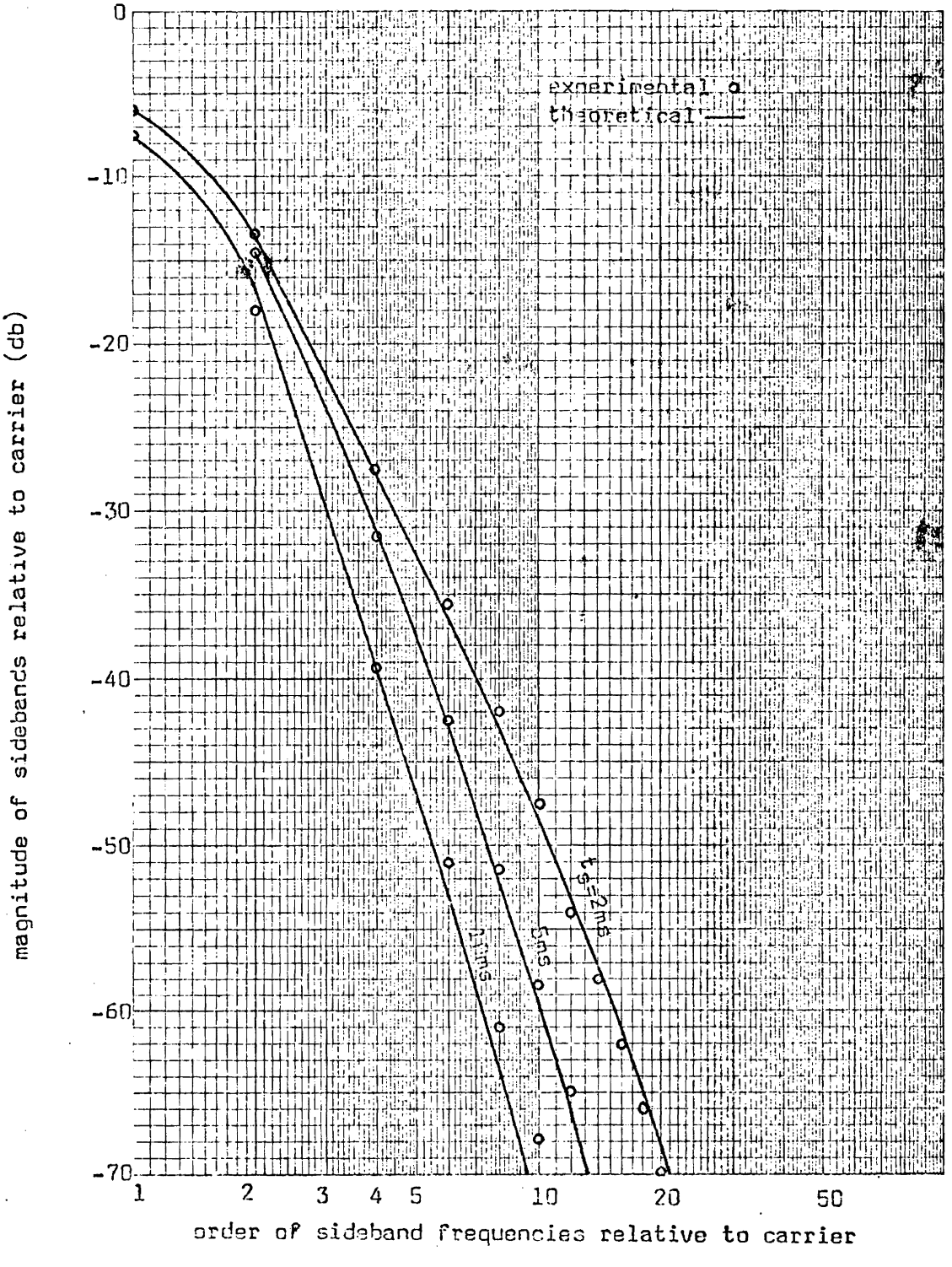

Figure 6.22. Spectral envelopes for representative values of t_s.

VII. RESULTS AND CONCLUSIONS

The investigation undertaken here is primarily concerned with characterization of the output signal of a frequency-shifted phase-locked-loop. Expressions are presented for the output signal and the modulation waveform resulting from a step change in the frequency of the PLL reference signal. Graphical evidence of the dependence of the modulation waveform on the loop parameters, gain and bandwidth, is presented. In order to facilitate the analysis of linear networks excited by the FS-PLL, an infinite series of damped sinusoidal terms representing the PLL output signal is developed. This series is also used to determine the coefficients of the Fourier series representation of a periodically keyed PLL. Using this result, the signal bandwidth was shown to vary directly as the loop response. Application of the FS-PLL as a voltage source was made for the purpose of studying the response of the equivalent circuit (a high Q series tuned circuit) of a VLF transmitting antenna. Representative curves are provided which show that the circuit transient response is in general the superposition of a transient component resulting from a change in frequency and a quasi-stationary component. The nature of the response discussed above is peculiar to the series tuned circuit only. A network characterized by flat response between f_1 and f_2 would not be expected to exhibit the quasi-stationary response component. In such cases, the transient amplitude response of the network would vary inversely as t_s.

Theory and experiment are compared in Figures 6.10 through 6.22 for the three design cases included in Table 6.1. Analytical and experimental considerations have covered a broad range of parameter values; thus, the accuracy, and certain limitations, of the techniques employed here are observed in the many curves presented in Section 6.3. These Figures generally show good agreement between the analytical and experimental data.

7.1. Observations and Limitations

During the experimental portion of this investigation, some error was observed in the dot profiles for frequency transition intervals smaller than approximately 3ms. For such values of t_s, the transition tended to be faster than predicted, and more overshoot was observed than was anticipated. An example of this is found in Figure 6.10, where t_s=2ms. A possible explanation of this performance lies in an initial assumption concerning the phase comparator. It was assumed that the sawtooth comparator operates as a continuous time device when the comparator input frequency is large compared to the natural frequency of the PLL [36]. The question here concerns the definition of "large". Experiment indicates that a factor between 50 and 100 is necessary to satisfy this assumption.

Final consideration concerning the analytical methods employed here primarily involves the two infinite series which have been utilized. It must be recalled that truncation of the series developed for a single frequency transition, Equation (3.29), is proportional to

the frequency transition interval, t_s. That is, small values of t_s require fewer terms of this series to accurately represent the FS-PLL output. Concerning the Fourier series developed for the periodically keyed PLL, it is necessary to remember that this development assumes that a half-period of the keying waveform is greater than approximately 2.2 times t_s (this figure is based on the presupposition that a simple damped exponential has a negligible value after five time constants). Some deviation from the theoretical spectral curves, for t_s=10ms, is observed in Figure 6.22. This value of t_s, considering that the keying wave half-period is 20ms, approaches the limit set forth for accurate representation of the periodically keyed PLL output by means of the Fourier series of Equation (4.12). The assumption connected with (4.12) involves the keying conditions set on the PLL, as well as, direct involvement of the mathematical assumptions.

7.2 Suggestions for Further Study

Application of the analytical methods employed in this investigation can be extended to include response analysis of a broad class of networks excited by the FS-PLL. Besides time-invariant networks, certain time-variant networks are also of interest. Again with application to very low frequency narrowband FSK, the response characteristics of a series tuned circuit, whose resonant frequency is time variant, is of considerable importance. This investigator has shown that the transient response of such a circuit, whose resonant frequency is made to vary synchronously with the FS-PLL frequency

transition, approaches a zero value under certain conditions. For the most part, this result is based on the assumptions that the network Q is constant over the signal bandwidth, and that the rate of change of frequency is small when compared with the carrier frequency. These assumed conditions are not restrictive in practice, but the necessary synchronism is difficult to achieve. Hence, further investigation could yield useful information concerning the effect on network response of the network's inability to ideally track the FS-PLL.

VIII BIBLIOGRAPHY

Literature Cited

1. Davey, J. R. and Matte, A. L., "Frequency-Shift Telegraphy-Radio and Wire Applications", Transactions A.I.E.E., Vol. 66, pp. 479-493, 1947.

2. Walter, John C., "Very Low Frequency Antennas are Going Back to Work", Electronics, Vol. 38, No. 1, January 11, 1965, pp. 80-86.

3. Stone, R. R. and Gee, T. H., "Incorporating FSK into VLF Transmissions", Frequency, Vol. 2, No. 4, July-August 1964, pp. 20-23.

4. Hupert, J. J., "Transient Response of Narrow-Band Networks to Angle-Modulated Signals", Proceedings of the National Electronics Conference, Vol. 18, October 1962, pp. 458-468.

5. Carson, J. R. and Fry, T. C., "Variable-Frequency Electric Circuit Theory", Bell Systems Technical Journal, Vol. 16, October 1937, pp. 513-540.

6. Van der Pol, B., "The Fundamental Principles of Frequency Modulation," Journal I.E.E. (London), pt. 3, Vol. 93, May 1946, pp. 153-158.

7. Stumpers, F. L. H. M., "Distortion of Frequency Modulated Signals in Electrical Networks", Communication News, Vol. 9, April 1948, pp. 82-92.

8. Baghdady, E. J., Lectures on Communications Theory , New York, McGraw Hill, 1961, pp. 460-466.

9. Rowe, H. E., "Distortion of Angle-Modulated Waves by Linear Networks" I.R.E. Transactions on Circuit Theory, Vol. CT-9, September 1962, pp. 286-290.

10. Weiner, D. D. and Leon, B. J., "The Quasi-Stationary Response of Linear Systems to Modulated Waveforms", Proceedings I.E.E.E., Vol. 53, No. 6, June 1965, pp. 564-575.

11. Johnson, P. B., "Band Limited FM Spectrum Analysis", Ph.D. Dissertation, Virginia Polytechnic Institute, Blacksburg, Virginia, 1966.

12. Hartley, H. F., "Transient Response of Narrow-Band Networks to Narrow-Band Signals With Application to Frequency Shift Keying", I.E.E.E. Transactions on Communications Technology, Vol. COM-14, No. 4, August 1966, pp. 470-477.

13. Gee, T. H., "An Analysis of Keying Conditions for Mimimum Transient in a High Q Resonant Circuit Excited by FSK", Master's Thesis, Virginia Polytechnic Institute, Blacksburg, Virginia, June 1965.

14. DeRusso, P. M., Roy, R. J. and Close, C. M., State Variables for Engineers, John Wiley and Sons Inc., New York, 1965.

15. Van der Pol, B., "Frequency Modulation", Proceedings I.R.E., Vol. 18, pp. 1194-1205, July 1930.

16. Corrington, M. S., "Variation of Bandwidth with Modulation Index in Frequency Modulation", Proceedings I.R.E., Vol. 35, No. 10, pp. 1013-1020, August 1947.

17. Cawthra, W. A. and Thomson, W. E., "Bandwidth of a Sinusoidal Carrier Wave, Frequency Modulated by a Rectangular Wave with Half-Sine-Wave Build-Up", Proceedings I.E.E. (London), Pt. 3, Vol. 98, pp. 69-74, 1951.

18. Allnott, J. N. and Jones, E. D. J., "An Investigation of the Spectra of Binary Frequency-Modulated Signals with Various Build-up Waveforms", Proceedings I.E.E., Vol. 104, Pt. B, No. 14, pp. 111-116, March 1957.

19. Watt, A. D., Zurich, V. J. and Coon, R. M., "Reduction of Adjacent-Channel Interference from Frequency-Shift-Keyed Carriers", National Bureau of Standards Report 5096, June 25, 1957

20. Bennett, W. R. and Rice, S. O., "Spectral Density and Auto Correlation Functions Associated with Binary Frequency-Shift-Keying", The Bell System Technical Journal, Vol. 42, No. 5, pp. 2355-2385, September 1963.

21. Chaffe, J. G., "The Application of Negative Feedback to Frequency Modulation Systems", Proceedings I.R.E., pp. 317-331, May 1939.

22. Gruen, W.J., "Theory of AFC Synchronization", Proceedings I.R.E., Vol. 41, pp. 1043-1048, August 1953.

23. Richman, D., "Color Carrier Reference Phase Synchronization Accuracy in NTSC Color TV", Proceedings I.R.E., Vol. 42, pp. 106-153, January 1954.

24. Ulicki, E. M., "Cubic Inch Frequency Synthesizers", Proceedings' 19th Annual Symposium on Frequency Control, April 1965.

25. Filipowsky and Muehldorf, Space Communications Systems, Prentice Hall, Englewood, N.J., 1965, pp. 264.

26. Panter, P. F., Modulation, Noise, and Spectral Analysis, McGraw Hill, New York, 1965, pp. 495.

27. Viterbi, A. J., "Phase-lock-loop Systems", Space Communications, McGraw Hill, 1963, pp. 123-142.

28. Benes, V. E., "Ultimately Periodic Solutions to a Non-Linear Integrodifferential Equation", Bell Systems Technical Journal, Vol. 41, January 1962, pp. 257.

29. Richman, D., "The DC Quadricorrelator: A Two-Mode Synchronization System", Proceedings I.R.E., Vol. 42, 1954, pp. 288.

30. Barnard, R. D., "Variational Techniques Applied to Capture in Phase-Controlled Oscillators", Bell Systems Technical Journal, Vol. 41, January 1962, pp. 227.

31. Jaffe, R. and Rechtin, E., "Design and Performance of Phase-lock Circuits Capable of Near-Optimum Performance Over a Wide Range of Input Signal and Noise Levels", I.R.E. Trans. on Information Theory, Vol. IT-1, March 1955, pp. 66-72.

32. Gardner, F. M., Phaselock Techniques, John Wiley and Sons, New York, 1966.

33. Robinson, L. M., "Tanlock: A Phase-lock loop of extended tracking capability", Proceedings National Winter Conference on Military Electronics, 1962.

34. Rideout, V. C., Active Networks, Prentice-Hall Inc., New York, 1954, pp. 368.

35. Goldstein, A. J., "Analysis of the Phase-Controlled Loop with a Sawtooth Comparator", Bell Systems Technical Journal, Vol. 41, March 1962, pp. 603.

36. Byrne, C. J., "Properties and Design of the Phase Controlled Oscillator with a Sawtooth Comparator", Bell Systems Technical Journal, Vol. 41, March 1962, pp. 559.

37. Splitt, F. G., "Design and Analysis of a Linear Phase-Locked Loop of Wide Dynamic Range", I.E.E.E. Transactions on Communication Technology, Vol. COM-14, No. 4, August 1966, pp. 432.

38. Granville, W. A., Smith, P. F. and Longley, W. R., Elements of Calculus, Ginn and Company, New York, 1946, pp. 352-353.

39. Terman, F. E., Electronic and Radio Engineering, McGraw Hill Book Company, New York, 1955, pp. 588-589.

40. Schwartz, M., Information Transmission, Modulation and Noise, McGraw Hill, New York, 1959, pp. 24.

41. Laport, Edmund A., Radio Antenna Engineering, McGraw Hill Book Company, Inc., New York, 1952, pp. 21-22.

42. Boyle, P. J., "A Design Approach to Transistorized Voltage-Controlled Crystal Oscillators", Electronic Design, March 2, 1964, pp. 22-26.

43. Scott, R. E., Linear Circuits, Pt. 1, pp. 441, 1960, Addison-Wesley Publishing Company, Inc., Reading, Mass.

44. Gardner, M. F. and Barnes, J. L., Transients in Linear Systems, John Wiley and Sons, Inc., New York, 1963, pp. 334-354.

45. Abrahamowitz, M. and Stegun, I. (Editors), Handbook of Mathematical Functions, National Bureau of Standards, U. S. Government Printing Office, Washington, D. C.

APPENDIX A

Phase-locked-loop Analysis

The integro-differential equation which describes the linear in-lock operation of the PLL can be obtained by means of Figure 3.1 and the discussion of Section 3.1. Various forms of this equation appear in the literature [35,37], but it will be developed here for continuity.

Utilizing the convolution integral, the output of the loop filter can be written as

$$v(t) = \int_{-\infty}^{t} h(x)v_e(t-x)dx = v(0) + \int_{0}^{t} h(x)v_e(t-x)dx \quad ,$$

where $h(t)$ is the impulse response of the filter and $v_e(t)$ is the filter input. Taking the time derivative [43] of the above expression gives

$$\dot{v}(t) = \int_{0}^{t} h(x)\dot{v}_e(t-x)dx \quad . \tag{A.1}$$

The VCO frequency is given by

$$\omega_c + \dot{\phi}(t) = \omega_c + k_o v_f(t) \quad ,$$

or

$$\ddot{\phi}(t) = k_o \dot{v}_f(t) \quad . \tag{A.2}$$

It should be noted here that the equations above are independent of the VCO's natural frequency, ω_c. The oscillator gain constant, k_o, has units of radians per second per volt. Combining (A.1) and (A.2)

$$\dot{\phi}(t) = k_o \int_o^t h(x)\dot{v}_e(t-x)dx \quad , \tag{A.3}$$

where the error voltage $v_e(t)$ is

$$v_e(t) = k_c[\phi_i(t) - \phi(t)] \quad ,$$

and the phase difference is restricted to the region of linear operation of the phase comparator. The time derivative of the error voltage can be written as

$$\dot{v}_e(t) = k_c[\dot{\phi}_i(t) - \dot{\phi}(t)] \quad , \tag{A.4}$$

and k_c is the comparator gain constant with units of volts per radian. Equations (A.3) and (A.4) describe the in-lock operation of a PLL employing a linear phase comparator.

In order to obtain the solution for the output phase, $\phi(t)$, Laplace transform methods will be used. Using appropriate Laplace transformations,* [39], equations (A.3) and (A.4) transform into

---

*The quantities V_e, H, ϕ_i and ϕ are Laplace transformed quantities and functions of the Laplace transform variable, S.

$$S^2\phi - S\phi(0) - \dot{\phi}(0) = Sk_oHV_e \qquad (A.5)$$

and

$$SV_e = K_c\left[S\phi_i - \phi_i(0) - S\phi + \phi(0)\right] \quad . \qquad (A.6)$$

Substituting (A.6) into (A.5) and solving for ϕ gives

$$\phi = \frac{KH\phi_i}{S + KH} + \frac{\phi(0)}{S} + \frac{\dot{\phi}(0)}{S[S + KH]} - \frac{KH\phi_i(0)}{S[S + KH]} \quad . \qquad (A.7)$$

In the above expression, $K = k_ok_c$. Additional loop gain, k_a, may be introduced into the loop in the form of an amplifier, and then $K = k_ak_ok_c$. The initial conditions $\phi(0)$, $\dot{\phi}(0)$ and $\phi_i(0)$ are evaluated at time equal zero minus ($t = 0^-$). For $t < 0$, the PLL is operating at the steady state input (reference) frequency,

$$\omega_c + \dot{\phi}_i(t) = \omega_c - \Delta\omega \quad , \quad \text{for} \quad t < 0 \quad ; \qquad (A.8)$$

and

$$\dot{\phi}(0) = \dot{\phi}_i(0) = -\Delta\omega \quad . \qquad (A.9)$$

A frequency step is applied at $t = 0$ and the input reference frequency becomes

$$\omega_c + \dot{\phi}_i(t) = \omega_c + \Delta\omega \quad , \quad \text{for} \quad t > 0 \quad ,$$

where ω_c is the VCO's natural frequency. Integration of the frequency gives the excitation in terms of phase,

$$\phi_i(t) = \Delta\omega t \quad , \quad \text{for} \quad t > 0 \quad . \tag{A.10}$$

It is further assumed that the time origin, $t = 0$, is selected such that

$$\phi_i(0) = 0 \quad . \tag{A.11}$$

The remaining initial condition is

$$\phi(0) = \phi_i(0) - \phi_e(0) \quad , \tag{A.12}$$

and $\phi_e(0)$ is the steady state phase error as seen by the phase comparator. If the VCO is locked to a reference signal whose frequency is not equal to the VCO's natural frequency, there must be a steady state phase error. The comparator converts this phase error into the voltage required to tune the VCO to the reference frequency. The gain, K, is the conversion gain from phase error to frequency. It is the change in the VCO frequency that results from a one radian change in phase error. The mistuning of the oscillator $-\Delta\omega$ is therefore produced by a steady state phase error given by

$$\phi_e = -\Delta\omega/K \quad . \tag{A.13}$$

Finally, by means of (A.8), (A.11), (A.12) and (A.13), the initial value of output phase becomes

$$\phi(0) = \Delta\omega/K \tag{A.14}$$

The transfer function for the PLL filter, as given in Section 3.1, is

$$H = \frac{t_b S + 1}{t_a S + 1} \quad . \tag{A.15}$$

Introducing the Laplace transform of (A.10), the initial conditions from (A.9), (A.11) and (A.14) along with the filter transfer function into (A.7) gives

$$\phi = \frac{\Delta\omega}{S^2} \frac{S(2\delta\omega_n - \omega_n^2/K) + \omega_n^2}{S^2 + 2\delta\omega_n S + \omega_n^2} + \frac{\Delta\omega}{K} \frac{(S + 2\delta\omega_n)}{(S^2 + 2\delta\omega_n S + \omega_n^2)}$$

$$- \frac{\Delta\omega}{S^2 + 2\delta\omega_n S + \omega_n^2} ,$$

where the loop parameters have been expressed in terms of

$$\omega_n = \sqrt{K/t_a} \tag{A.16}$$

and

$$\delta = \frac{Kt_b + 1}{2t_a\omega_n} \quad . \tag{A.17}$$

The inverse Laplace transformation can be obtained from tables such as those provided by Gardner and Barnes [44]. After considerable algebraic manipulations, the phase time function can be shown to be

$$\phi(t) = \Delta\omega t - \frac{\Delta\omega}{K}$$

$$+ \frac{2\,\Delta\omega}{\omega_n} \sqrt{\frac{1 - 2\delta\omega_n + \omega_n^2/K}{1 - \delta^2}} \; e^{-\delta\omega_n t} \sin(\omega_n \sqrt{1-\delta^2}\, t + \theta), \tag{A.18}$$

where

$$\theta = \arctan\left[\frac{\omega_n\sqrt{1-\delta^2}/K}{\delta\omega_n/K - 1}\right], \quad \delta < 1 \quad .$$

The instantaneous frequency of the VCO, upon taking the time derivative of (A.18), becomes

$$\dot{\phi}(t) = \Delta\omega + 2\Delta\omega\sqrt{\frac{1 - 2\delta\omega_n + \omega_n^2/K}{1-\delta^2}}\, e^{-\delta\omega_n t}\sin(\omega_n\sqrt{1-\delta^2}\, t + \gamma), \quad (A.19)$$

and

$$\gamma = \arctan\left[\frac{-\sqrt{1-\delta^2}}{\delta - \omega_n/K}\right], \quad \delta < 1 \quad .$$

Equations (A.18) and (A.19) are in their most elementary form for the underdamped case, $\delta < 1$. For the overdamped case, $\delta > 1$, these equations can be written in terms of hyperbolic functions as

$$\phi(t) = \Delta\omega t + \frac{2\Delta\omega}{\omega_n\sqrt{\delta^2-1}} e^{-\delta\omega_n t}\left[(\delta\omega_n/K - 1)\sinh(\omega_n\sqrt{\delta^2-1}\, t)\right.$$

$$\left. + (\omega_n\sqrt{\delta^2-1}/K)\cosh(\omega_n\sqrt{\delta^2-1}\, t)\right] - \frac{\omega}{K}, \quad \delta > 1 \; ; \qquad (A.20)$$

and

$$\dot{\phi}(t) = \Delta\omega + \frac{2\,\Delta\omega}{\sqrt{\delta^2-1}}\, e^{-\delta\omega_n t}\left[(\delta - \omega_n/K)\sinh\left(\omega_n\sqrt{\delta^2-1}\;t\right)\right.$$

$$\left. -\sqrt{\delta^2-1}\cosh\left(\omega_n\sqrt{\delta^2-1}\;t\right)\right] \quad , \quad \delta > 1 \quad . \qquad (A.21)$$

When the loop is critically damped, $\delta = 1$, (A.18) and (A.19) are not applicable in their present form. By taking the limit as $\delta \to 1$, the phase and frequency time functions become

$$\phi(t) = \Delta\omega t - \Delta\omega/K + 2\,\Delta\omega\left[(\omega_n/K - 1)\,t + 1/K\right]e^{-\omega_n t}, \quad \delta = 1 \; ; \qquad (A.22)$$

and

$$\dot{\phi}(t) = \Delta\omega + 2\,\Delta\omega\left[\omega_n(1 - \omega_n/K)t - 1\right]e^{-\omega_n t}, \quad \delta = 1 \quad . \qquad (A.23)$$

APPENDIX B

Derivation of the Series Expression for the FS-PLL Output

The output signal of a PLL that is subjected to a frequency step at time zero is given by

$$v(t) = V \sin\left[\omega_c t + \phi(t)\right] \qquad (B.1)$$

where $\phi(t)$ is given by Equation (322), repeated here for convenience,

$$\phi(t) = \Delta\omega t + Me^{-\alpha t} \sin(\beta t + \theta) - \phi_s \quad . \qquad (B.2)$$

Equation (B.2) corresponds to a frequency shift that is symmetrical about the natural frequency of the VCO, or

$$\phi(t) = \begin{cases} -\Delta\omega, & \text{for} \quad t < 0 \\ \Delta\omega, & \text{as} \quad t \to \infty \end{cases} \quad .$$

Employing the trignometric identity for the sum of two angles, Equation (B.1) becomes

$$v(t) = \sin(\omega_2 t - \phi_s) \cos\left[Me^{-\alpha t} \sin(\beta t + \theta)\right] + \cos(\omega_2 t - \phi_s) \sin\left[Me^{-\alpha t} \sin(\beta t + \theta)\right] \quad , \qquad (B.3)$$

and the final frequency ω_2 is given by

$$\omega_2 = \omega_c + \Delta\omega \quad .$$

Consider the following exponential function:

$$f(t) = \exp\left[jMe^{-\alpha t} \sin(\beta t + \theta)\right] \quad . \qquad (B.4)$$

This function can be expanded in a McLaurin series and truncated to provide an approximate representation,

$$f(t) = 1 + jMe^{-\alpha t}\sin(\beta t + \theta) - \frac{M^2}{2}e^{-2\alpha t}\sin^2(\beta t + \theta)$$

$$-j\frac{M^3}{6}e^{-3\alpha t}\sin^3(\beta t + \theta) + \frac{M^4}{24}e^{-4\alpha t}\sin^4(\beta t + \theta)$$

$$-j\frac{M^5}{120}e^{-5\alpha t}\sin^5(\beta t + \theta) + \cdots\cdots\cdots \quad . \qquad (8.5)$$

The sinusoidal factors which are raised to powers greater than unity can be written in terms of sines and cosines of multiple angles by means of trignometric identities or Euler's formula for the sine function. This result is separated into real and imaginary terms;

$$\mathrm{Re}\left[f(t)\right] = 1 - \frac{M^2}{4}e^{-2\alpha t}\left[1 - \cos(2\beta t + 2\theta)\right]$$

$$+\frac{M^4}{192}e^{-4\alpha t}\left[\cos(4\beta t + 4\theta) - 4\cos(2\beta t + 2\theta) + 3\right]$$

$$+ \cdots\cdots\cdots \quad , \qquad (8.6)$$

and

$$\text{Im}\left[f(t)\right] = Me^{-\alpha t}\sin(\beta t + \theta)$$

$$+ \frac{M^3}{24} e^{-3\alpha t}\left[\sin(3\beta t + 3\theta) - 3\sin(\beta t + \theta)\right]$$

$$+ \frac{M^5}{1920} e^{-5\alpha t}\left[\sin(5\beta t + 5\theta) - 5\sin(3\beta t + 3\theta) + 10\sin(\beta t + \theta)\right]$$

$$+ \cdots\cdots\cdots \quad ; \tag{B.7}$$

where

$$\text{Re}\left[f(t)\right] = \cos\left[Me^{-\alpha t}\sin(\beta t + \theta)\right]$$

and

$$\text{Im}\left[f(t)\right] = \sin\left[Me^{-\alpha t}\sin(\beta t + \theta)\right] \quad .$$

Substituting (B.6) and (B.7) into (B.3) and using the trignometric identity for the product of a sine and cosine, the series expansion becomes

$$\begin{aligned} v(t) = {} & G_o \sin(\omega_2 t - \phi_s) \\ & + G_1\left(\sin\left[(\omega_2 + \beta)t - \phi_s + \theta\right] - \sin\left[(\omega_2 - \beta)t - \phi_s - \theta\right]\right) \\ & + G_2\left(\sin\left[(\omega_2 + 2\beta)t - \phi_s + 2\theta\right] + \sin\left[(\omega_2 - 2\beta)t - \phi_s - 2\theta\right]\right) \\ & + G_3\left(\sin\left[(\omega_2 + 3\beta)t - \phi_s + 3\theta\right] - \sin\left[(\omega_2 - 3\beta)t - \phi_s - 3\theta\right]\right) \\ & + \cdots\cdots\cdots \\ & + G_p\left(\sin\left[(\omega_2 + p\beta)t - \phi_2 + p\theta\right]\right. \\ & \qquad \left. + (-1)^p \sin\left[(\omega_2 - p\beta)t - \phi_s - p\theta\right]\right), \end{aligned} \tag{B.8}$$

$$G_p = G_p(M,\alpha t) = \sum_{k=0}^{\infty} \frac{(-1)^k M^{2k+p} e^{-(2k+p)\alpha t}}{2^p 4^k k! (k+p)!}$$

and

$$p = 0,1,2, \ldots\ldots\ldots .$$

The first term in the infinite series G_0 is unity, giving rise to the steady state sinusoidal component of the PLL output signal. With this one exception, the infinite series G_p consists of time decaying exponential terms.

APPENDIX C

Determination of Fourier Coefficients

The Fourier coefficients associated with the frequency-shifted phase-locked-loop (FS-PLL), periodically keyed at a frequency of f, are obtained by means of

$$C_n = \frac{2}{T}\int_0^T v(t)e^{-jn\omega t}\,dt \quad . \tag{C.1}$$

Equations (4.12) and (4.13) define the time function v(t), and the prescribed keying conditions are presented in Section 4.1. Because of the difficulties encountered in carrying out the indicated integration of (C.1), the series of damped sinusoids which represents v(t) is used for term by term evaluation of C_n.

Substituting from (3.29) into (C.1) gives

$$\begin{aligned} C_n = {} & \frac{2}{T}\int_0^{T/2} e^{-jn\omega t}\sum_{P=0}^{\infty}\left(\sum_{k=0}^{\infty}\frac{(-1)^k\, M^{2k+p}\, e^{-(2k+p)\alpha t}}{2^p\, 4^k\, k!\,(k+p)!}\right) \\ & \times\left(\sin\left[\,(\omega_2+p\beta)t-\phi_s+p\theta\,\right] + (-1)^p\, u_p\, \sin\left[\,(\omega_2-p\beta)t-\phi_s-p\theta\right]\right)dt \\ & + \frac{2}{T}\int_{T/2}^{T} e^{-jn\omega t}\sum_{P=0}^{\infty}\left(\sum_{k=0}^{\infty}\frac{(-1)^k\, M^{2k+p}\, e^{-(2k+p)(t-T/2)\alpha}}{2^p\, 4^k\, k!\quad (k+p)!}\right) \\ & \times\left(\sin\left[(\omega_1+p\beta)(t-T/2)-\phi_s+p\theta\right] + (-1)^p\, u_p\, \sin\left[(\omega_1-p\beta)(t-T/2)\right.\right. \\ & \left.\left. - \phi_s-p\theta\right]\right)dt \quad . \end{aligned} \tag{C.2}$$

The function u_p is defined as

$$u_p = \begin{cases} 0, & \text{for } p = 0 \\ 1, & \text{for } p > 0 \end{cases} .$$

The first integral represents a frequency shift from f_1 to f_2, where $f_1 < f_2$; therefore, the second integral represents a shift from f_2 to f_1. Recalling that the series employed here represents a frequency step, it is important to recognize that the value of $\Delta\omega$ involved in M and ϕ_s is positive under the first integral and negative under the second integral. The expression for the Fourier coefficients of (C.2) can be written symbolically as

$$C_n = \sum_{p=0}^{\infty} \sum_{k=0}^{\infty} c_{n,p,k} \qquad (C.3)$$

where $c_{n,p,k}$ represents the term by term contribution of (C.2) to the total spectrum. The contribution of $c_{n,0,0}$ results from the undamped sinusoidal component of (3.28), where the remaining $c_{n,p,k}$ result from the damped sinusoids. It is therefore necessary to evaluate (C.1) for two relatively elementary functions, a sinusoidal function and a damped sinusoidal function.

First, the sinusoidal function is considered. That is, p=k=0, and (C.2) reduces to

$$c_{n,0,0} = \frac{2}{T}\int_0^{T/2} \sin(\omega_2 t+\phi_s)e^{-jn\omega t}\, dt + \frac{2}{T}\int_{T/2}^{T} \sin[\omega_1(t-T/2)+\phi_s]\, e^{-jn\omega t}\, dt \quad .$$

Following through the indicated mathematical operations, the spectral contribution due to the undamped sinusoidal component becomes

$$c_{n,o,o} = \frac{1}{2}(-1)^{q_1}\left(\left[\frac{\sin(2q_2-n)\pi/2}{(2q_2-n)\pi/2}\, e^{-j\phi_s} - \frac{\sin(2q_2+n)\pi/2}{(2q_2+n)\pi/2}\, e^{j\phi_s}\right]\right.$$

$$\left. + (-1)^n\left[\frac{\sin(2q_1+n)\pi/2}{(2q_1+n)\pi/2}\, e^{-j\phi_s} - \frac{\sin(2q_1-n)\pi/2}{(2q_1-n)\pi/2}\, e^{j\phi_s}\right]\right) e^{-j(n-1)\pi/2} \quad , \tag{C.4}$$

where $2q_1 = f_1/f_k$ and $2q_2 = f_2/f_k$.

Secondly, the damped sinusoidal function is considered. This includes all values of p and k greater than zero. It is assumed that a frequency transition is completed before a subsequent frequency shift is initiated. Therefore, the upper limit of the integrals in (C.2) results in a zero value, since the large negative exponentials approach zero. That is to say that the exponentially damped sinusoids have decayed to an insignificant value before the time variable equals the upper limit placed on its respective integral. The order of summation and integration in (C.2) can be reversed, since the series involved is absolutely convergent. Carrying out the indicated integration, the contributions of the damped sinusoidal components become

$$c_{n,p,k} = \left(\frac{e^{-j(\phi_s - p\theta)}}{(2q_2 + p\beta/\omega - n) + j\alpha(2k+p)/\omega} + \frac{e^{j(\phi_s - p\theta)}}{(2q_2 + p\beta/\omega + n) - j\alpha(2k+p)/\omega} \right.$$

$$+ (-1)^n u_p \left[\frac{e^{-j(\phi_s + p\theta)}}{(2q_2 - p\beta/\omega - n) + j\alpha(2k+p)/\omega} + \frac{e^{j(\phi_s + p\theta)}}{(2q_2 - p\beta/\omega + n) - j\alpha(2k+p)/\omega} \right]$$

$$+ (-1)^p \left\{ \frac{e^{j(\phi_s + p\theta)}}{(2q_1 + p\beta/\omega - n) + 2j\alpha(2k+p)/\omega} + \frac{e^{-j(\phi_s + p\theta)}}{(2q_1 + p\beta/\omega + n) - j\alpha(2k+p)/\omega} \right.$$

$$\left. \left. + (-1)^n u_p \left[\frac{e^{j(\phi_s - p\theta)}}{(2q_1 - p\beta/\omega - n) + j\alpha(2k+p)\omega} + \frac{e^{-j(\phi_s - p\theta)}}{(2q_1 - p\beta/\omega + n) - j\alpha(2k+p)/\omega} \right] \right\} \right)$$

$$\times \frac{(-1)^k M^{2k+p}}{2\pi \, 2^p \, 4^k \, k! \, (k+p)!} \quad , \qquad (C.5)$$

where

$$k = 1, 2, 3, \ldots\ldots\ldots$$

and

$$p = 1, 2, 3, \ldots\ldots\ldots$$

In equations (C.4) and (C.5) the sign associated with $\Delta\omega$ has been taken into account; thus, the values of M and ϕ_s are given directly by (3.24) and (3.27) upon substituting a positive value for $\Delta\omega$.

APPENDIX D

Initial Conditions on the Tuned Circuit

The initial conditions are determined from the steady state response at time zero. At time, t=0, it is assumed that the circuit excitation has been

$$v(t) = V \sin(\omega_1 t + \phi_s) \qquad (D.1)$$

for all $t<0$. The steady state current response of the circuit of Figure 5.1 to this excitation is

$$i_s(t) = \frac{\omega_1 \omega_r}{RQ\sqrt{(\omega_1\omega_r/Q)^2 + (\omega_1^2 - \omega_r^2)^2}} \sin(\omega_1 t + \phi_s - \phi_o) \ , \qquad (D.2)$$

where

$$\phi_o = \arctan\left[\frac{\omega_1^2 - \omega_r^2}{\omega_1\omega_r/Q}\right]$$

and

$$Q = \omega_r L/R \ .$$

The initial current in the inductor becomes

$$I_o = i_s(0) = \frac{\omega_1\omega_r \sin(\phi_s - \phi_o)}{RQ\sqrt{(\omega_1\omega_r/Q)^2 + (\omega_1^2 - \omega_r^2)^2}} \qquad (D.3)$$

and the initial capacitor voltage is

$$V_o = \frac{-\omega_r^2 \cos(\phi_s - \phi_o)}{\sqrt{(\omega_1\omega_r/Q)^2 + (\omega_1^2 - \omega_r^2)^2}} \ . \qquad (D.4)$$

Using Equations (5.5) and (5.6) and employing the definitions of Q and ω_r, the transformed current component resulting from initial conditions can be written as

$$I_{ic} = \frac{SI_o - \omega_r V_o/RQ}{(S + \omega_r/2Q)^2 + \omega_r^2} \qquad (D.5)$$

Tables of Laplace transforms [44] give the inverse transform of (D.5) as

$$i_{ic}(t) = \frac{1}{Q}\sqrt{(I_o/2 + V_o/R)^2 + (QI_o)^2}\ \sin(\omega_r t + \lambda_o) \quad , \qquad (D.6)$$

where

$$\lambda_o = \arctan\left[\frac{QI_o}{-(I_o/2 + V_o/R)}\right] .$$

APPENDIX E

Analysis of a Series Tuned Circuit Excited by the Series Representation of the FS-PLL Output

The narrowband series tuned circuit response, to its source only, is of interest here. From (5.4) the Laplace transformed current response is

$$I_s = \frac{V}{Z} = \frac{\sum\sum F_{p,k}}{Z} , \qquad (E.1)$$

where each quantity above is a function of the Laplace transform variable, S. The transformed voltage source of (3.29) is represented term by term by the summation on $F_{p,k}$. Circuit response to a term of the form

$$f(t) = A\, e^{-at} \sin(bt + \sigma) \quad , \qquad (E.2)$$

is considered. Equation (E.2) represents the form of each term of (3.29), provided the first term is undamped (i.e., a=0).

The response of the circuit to (E.2) is represented by

$$R = \frac{F}{Z} \quad , \qquad (E.3)$$

where F is the transform of f(t), and Z is the series impedance. Applying a trigonometric identity [45] to (E.2), the Laplace transform of f(t) becomes [44]

$$F = \frac{b\cos(\sigma) + (S - a)\sin(\sigma)}{(S - a)^2 + b^2} \quad . \qquad (E.4)$$

The circuit impedance, from (5.5), is

$$Z = \frac{L}{S}\left[(S + c)^2 + d^2\right] \quad , \qquad (E.5)$$

where

$$c = R_c/2L \quad ,$$

$$d \simeq \omega_r \quad , \qquad \text{(for high Q circuits)}$$

and the circuit's natural undamped frequency is

$$\omega_r = \sqrt{1/LC_c} \quad .$$

Combining (E.4) and (E.5) with (E.3), the transformed current response becomes

$$R = \frac{Sb\ \cos(\sigma) + S(S + a)\ \sin(\sigma)}{L\left[(S + a)^2 + b^2\right]\left[(S + c)^2 + d^2\right]} \qquad (E.6)$$

The inverse Laplace transformation of (E.6) produces the current response teme function. Transform tables do not normally include the above function; however, the inverse transformation can be effected by means of a partial fraction expansion. Such an expansion and the subsequent inverse transformation of the resulting elementary functions are straight forward, but tedious. Proceeding in the usual manner of partial fraction expansions gives

$$R = A\left[\frac{K_1}{S + a - jb} + \frac{\bar{K}_1}{S + a + jb} + \frac{K_2}{S + c - jd} + \frac{\bar{K}_2}{S + c + jd}\right] \quad , \qquad (E.7)$$

where the bar on K indicates the complex conjugate. The value of K_1 is found to be

$$K_1 = \frac{1}{2L}\sqrt{\frac{a^2 + b^2}{\left[(c - a)^2 - b^2 + d^2\right]^2 + \left[2b(c - a)\right]^2}}\, e^{j(\lambda_1 - \lambda_2 - \pi/2)} \quad , \quad (E.8)$$

where

$$\lambda_1 = \arctan\left[\frac{b\cos(\sigma) - a\sin(\sigma)}{-a\cos(\sigma) - b\sin(\sigma)}\right]$$

and

$$\lambda_2 = \arctan\left[\frac{2b(c - a)}{(c - a)^2 - b^2 + d^2}\right] \quad .$$

Likewise,

$$K_2 = \frac{1}{2Ld}\sqrt{\frac{\left[(c^2 - d^2 - ac)\sin(\sigma) - bc\cos(\sigma)\right]^2 + \left[(ad - 2cd)\sin(\sigma) + bd\cos(\sigma)\right]^2}{\left[(a-c)^2 - d^2 + b^2\right]^2 + \left[2d(a-c)\right]^2}}$$

$$\times\, e^{j(\lambda_3 - \lambda_4 - \pi/2)} \quad , \quad (E.9)$$

where

$$\lambda_3 = \arctan\left[\frac{(ad - 2cd)\sin(\sigma) + bd\cos(\sigma)}{(c^2 - d^2 - ac)\sin(\sigma) - bc\cos(\sigma)}\right]$$

and

$$\lambda_4 = \arctan\left[\frac{2d(a - c)}{(a - c)^2 - d^2 + b^2}\right] \quad .$$

The inverse transformation of (E.7) can be written as

$$r(t) = 2A\left[K_1 e^{-at}\cos(bt) + K_2 e^{-ct}\cos(dt)\right] \quad . \quad (E.10)$$

Equation (E.10) gives the time function representing the current response of a series tuned circuit to the voltage excitation given by

(E.2), which has the form of each term of the excitation series (3.29). In order to determine the response to the general term of (3.29), the constants in (E.10) are replaced through comparison with (3.29) as follows:

$$a = (2k + p)\alpha \quad , \tag{E.11}$$

$$A = \frac{(-1)^k \, \mu^{2k+p}}{2^p \, 4^k \, k! \, (k+p)!} \quad , \tag{E.12}$$

and depending upon whether the sum or difference frequency term is involved, b becomes either

$$b^+ = \omega_2 + p\beta$$

or

$$b^- = \omega_2 - p\beta \quad ; \tag{E.13}$$

likewise σ is replaced by either

$$\sigma^+ = -\phi_s + p\theta$$

or

$$\sigma^- = -\phi_s - p\theta \quad . \tag{E.14}$$

The quantities α and β are defined in (3.25) and (3.26) respectively. Since K_1 and K_2, and their respective angles, are functions of a, b and σ, it follows that these values are substituted into Equations (E.8) and (E.9) according to the sum and difference frequency notation employed above. That is, K_1 becomes

$$K_1^+ = K_1(a,b^+,\sigma^+)$$

or

$$K_1^- = K_1(a,b^-,\sigma^-) \quad , \tag{E.15}$$

and K_2 becomes

$$K_2^+ = K_2(a,b^+,\sigma^+)$$

or

$$K_2^- = K_2(a,b^-,\sigma^-) \quad . \tag{E.16}$$

Now the response to the general term of (3.29) can be written as

$$r_{p,k}(t) = 2A\left\{K_1^+ e^{-at}\cos(b^+t) + K_2^+ e^{-ct}\cos(dt)\right.$$

$$\left. + (-1)^p u_p \left[K_1^- e^{-at}\cos(b^-t) + K_2^- e^{-ct}\cos(dt)\right]\right\}, \tag{E.17}$$

where

$$p = 0,1,2,3, \quad \cdots\cdot$$

and

$$k = 0,1,2,3, \quad \cdots\cdot \quad .$$

Finally the total current response due to the source becomes

$$i_s(t) = \sum_{p=0}^{\infty}\sum_{k=0}^{\infty} r_{p,k}(t) \quad . \tag{E.18}$$

This expression states that the response of the series tuned circuit is the superposition of the response to each term of the series excitation. The individual responses are obtained from (E.18) by making the appropriate substitutions from (E.12) through (E.17).

The vita has been removed from the scanned document

AN ANALYTICAL AND EXPERIMENTAL INVESTIGATION OF A FREQUENCY-SHIFT-KEYED SIGNAL GENERATED BY A PHASE-LOCKED-LOOP WITH APPLICATION TO NARROWBAND FSK

by

Thomas Hunter Gee

ABSTRACT

Narrowband communications systems employing frequency-shift-keyed (FSK) carrier modulation demand careful consideration of system transient responses. Discontinuous waveforms or their derivatives, such as produced by frequency modulation, can result in the generation of large transient currents and voltages. These transient conditions produce distortion which interferes with demodulation processes, and may be in excess of the physical limitations on continuous operation of the transmitting terminal.

It has been suggested that a phase-locked-loop (PLL), whose reference signal is instantaneously switched between two discrete frequency sources, be employed as the modulated source of an FSK carrier. The characteristics of the PLL provide signal coherence and a means of "shaping" the modulation waveform, both of which are required in certain FSK transmissions. The investigation undertaken here is primarily concerned with the characterization of such a PLL output signal (exhibiting a finite frequency transition interval). Expressions are obtained for the output signal and the resulting modulation waveform for the case of a single frequency shift. Graphical evidence of

the dependence of the modulation waveform on the loop parameters, gain and bandwidth, is presented. In order to facilitate the analysis of linear networks excited by the FS-PLL, an infinite series of damped sinusoidal terms, representing the PLL output signal is developed. This series is also utilized to determine the coefficients of the Fourier series representation of a periodically keyed PLL. Using this result, the signal bandwidth is shown to vary directly as the loop bandwidth. Application of the FS-PLL as a voltage source is made in the case of the equivalent circuit (a high Q series tuned circuit) of a VLF transmitting antenna. Representative curves are provided which show that the series tuned circuit transient response is in general the superposition of a transient component, resulting from a change in frequency, and a quasi-stationary component.

Finally, an experiment is devised which provides an additional investigative tool. A unique method for achieving demodulation of narrowband signals, while maintaining wideband demodulator response characteristics, is used to experimentally substantiate the predicted modulation waveforms. Experimental data is also obtained, and graphically compared with the theory, to verify the frequency domain analysis of the FS-PLL output as well as the tuned circuit time domain analysis.